LAWRENCE
LIVERMORE
NATIONAL
LABORATORY

LLNL-TR-491099

Investigations on Repository Near-Field Thermal Modeling - Repository Science/Thermal Load Management & Design Concepts (M41UF033302)

M. Sutton, J. A. Blink, M. Fratoni, H. R. Greenberg, A. D. Ross

July 19, 2011

Disclaimer

This document was prepared as an account of work sponsored by an agency of the United States government. Neither the United States government nor Lawrence Livermore National Security, LLC, nor any of their employees makes any warranty, expressed or implied, or assumes any legal liability or responsibility for the accuracy, completeness, or usefulness of any information, apparatus, product, or process disclosed, or represents that its use would not infringe privately owned rights. Reference herein to any specific commercial product, process, or service by trade name, trademark, manufacturer, or otherwise does not necessarily constitute or imply its endorsement, recommendation, or favoring by the United States government or Lawrence Livermore National Security, LLC. The views and opinions of authors expressed herein do not necessarily state or reflect those of the United States government or Lawrence Livermore National Security, LLC, and shall not be used for advertising or product endorsement purposes.

This work performed under the auspices of the U.S. Department of Energy by Lawrence Livermore National Laboratory under Contract DE-AC52-07NA27344.

Used Fuel Disposition Campaign

Repository Science/Thermal Load Management & Design Concepts
(Work Package FTLL11UF0333)

Level 4 Milestone (M4): M41UF033302
(LLNL input to SNL L3 Milestone)

INVESTIGATIONS ON REPOSITORY NEAR-FIELD THERMAL MODELING

Lawrence Livermore National Laboratory

Mark Sutton, James A. Blink, Massimiliano Fratoni,
Harris R. Greenberg and Amber D. Ross

JULY 22ND 2011

LLNL-TR-491099

This document was prepared as an account of work sponsored by an agency of the United States government. Neither the United States government nor Lawrence Livermore National Security, LLC, nor any of their employees makes any warranty, expressed or implied, or assumes any legal liability or responsibility for the accuracy, completeness, or usefulness of any information, apparatus, product, or process disclosed, or represents that its use would not infringe privately owned rights. Reference herein to any specific commercial product, process, or service by trade name, trademark, manufacturer, or otherwise does not necessarily constitute or imply its endorsement, recommendation, or favoring by the United States government or Lawrence Livermore National Security, LLC. The views and opinions of authors expressed herein do not necessarily state or reflect those of the United States government or Lawrence Livermore National Security, LLC, and shall not be used for advertising or product endorsement purposes.

This work performed under the auspices of the U.S. Department of Energy by Lawrence Livermore National Laboratory under Contract DE-AC52-07NA27344.

TABLE OF CONTENTS

Tables v

Figures vi

Acronyms xii

Nomenclature and Symbols xiv

1. Introduction 1

2. Inventory 1

3. Geologic Setting and Geologic Host Media 1

4. Concept of Operations 1

5. Thermal Analyses 2

5.1 Conceptual Model 2

5.1.1 Geometry 3

5.1.2 Approach 8

5.1.3 Input Data and Assumptions 9

5.2 Results 14

5.2.1 Host Rock Temperature 14

5.2.2 Waste Package and EBS Peak Temperature 18

5.2.3 Waste Package Surface Peak Temperature for Salt 22

5.2.4 Peak Temperature at Compliance Locations as a Function of Storage Time and Waste Package Capacity 24

6. Summary and Recommendations 26

6.1 Summary 26

6.2 Future Work 27

7 References 29

Appendix G G-1

G.1 Introduction G-1

G.2 Variables Used in the Analytical Models G-2

G.2.1 Host Rock Property Data G-2

G.2.2 Repository Reference Design Data G-2

G.2.3 Waste Form Count G-4

G.2.4 The Effects of Surface Storage G-5

G.2.5 Heat Source Calculation G-5

G.3 Host Rock Transient Temperature Analytical Model G-6

G.4 Waste Package and EBS Quasi-Steady-State Temperature Analytical Model G-7

G.5 Model Limitations and Potential Future Model Improvements G-9

Appendix H H-1

H.1 Introduction H-1

H.2 Contributions to Total System Heat from the Central Waste Package, and Adjacent Axial and Lateral Heat Sources H-2

H.3 Transient temperature in the Host Rock H-27

H.4 Waste Package Surface Temperature H-51
H.5 Waste Package Peak Temperature as a Function of Storage Time and Number of Assemblies H-76
H.6 Trade-off of Storage Time and Waste Package Capacity H-82

TABLES

Table 5.1-1 Repository layout axial (center to center waste package) and lateral spacing (meters) used in thermal analysis models 4
Table 5.2-1: Host rock peak temperature (at the "calculation radius") and corresponding time of the peak for four geologic media, six waste forms and four aging times 18
Table 5.2-2: Waste package surface temperature at time of peak host rock temperature occurs in the host rock 20
Table 5.2-3: Temperature at the interface between EBS components in a clay - MOX/UOX case at the time the peak temperature occurs in the host rock at the calculation radius 21
Table 5.2-4: Temperature at interface between EBS components in a deep borehole repository at the time the peak temperature occurs in the host rock 21
Table 5.2-5: Waste package peak surface temperature in a salt repository with the temperature based on a steady-state calculation inward from the 4 m rock calculation radius at each time step of the homogeneous transient calculation 23

FIGURES

Figure 5.1-1 Illustration defining the terminology used for the potential layers of the near-field Engineered Barriers System (EBS) from waste form to host rock 3
Figure 5.1-2 Conceptual layout of a central waste package of interest and both axial and lateral emplacement lines (plan and elevation view) 4
Figure 5.1-3 Graphical representation of a granite design for SNFA (left) and HLW (right), including material properties and dimensions 5
Figure 5.1-4 Graphical representation of a clay design for SNFA (left) and HLW (right), including material properties and dimensions 6
Figure 5.1-5 Graphical representation of a salt design for SNFA (left) and HLW (right), including material properties and dimensions 7
Figure 5.1-6 Graphical representation of a deep borehole design for SNFA (left) and HLW (right), including material properties and dimensions 8
Figure 5.1-7 Decay heat curves for 1 assembly or 1 canister per waste package for UOX, MOX, co-extraction, new extraction, EC-ceramic, and EC-metal 10
Figure 5.1-8 Decay heat curves for 1 UOX or MOX assembly and 0.291 co-extraction, new extraction, EC-ceramic or EC-metal canister per waste package (deep borehole design) 11
Figure 5.1-9 Decay heat curves for 1, 2, 3, 4 and 12 UOX or MOX assemblies per waste package 12
Figure 5.2-1 Transient host rock temperature at the "calculation radius" after storage times of 10, 50 and 100 years for a waste package containing 1, 2, 3, 4 and 12 MOX assemblies per waste package in granite 15
Figure 5.2-2 Contributions to the transient rock temperature at the "calculation radius" from the central package, adjacent point sources and adjacent line sources for 4 MOX assemblies per waste package in granite after 10 years storage 15
Figure 5.2-3 Transient host rock temperature at the "calculation radius" after storage times of 10, 50 and 100 years for a waste package containing 1, 2, 3, 4 and 12 UOX assemblies per waste package in clay 16
Figure 5.2-4 Contributions to the transient rock temperature at the "calculation radius" from the central package, adjacent point sources and adjacent line sources for 4 UOX assemblies per waste package in clay after 10 years storage 16
Figure 5.2-5 Calculated waste package temperature after storage times of 10, 50 and 100 years for 4 MOX assemblies per canister in granite 19
Figure 5.2-4 Calculated waste package temperature after 10 years storage time for 4 MOX assemblies per canister in salt assuming the waste package is in contact with crushed salt or intact salt, either fully or for 75% of its area 23
Figure 5.2-7 Minimum surface storage time necessary to comply with waste package surface temperature limit as function of UOX assemblies per waste package in a granite, clay, and salt repository (with 75% of the waste package surface contacting intact salt) 25
Figure 5.2-8 Minimum surface storage time necessary to comply with waste package surface temperature limit as function of MOX assemblies per waste package in a granite, clay, and salt repository (with 75% of the waste package surface contacting intact salt) 25

Figure G.4-1 Normalized thermal resistance of each EBS layer G9
Figure G.5-1 Effects of porosity and temperature on thermal conductivity of crushed salt G10
Figure G.5-2 Effects of porosity and temperature on thermal diffusivity of crushed salt G11
Figure H.2-1 Contributions to the transient rock temperature at the calculation radius from the central package, adjacent point sources and adjacent line sources for 4 UOX assemblies per waste package (UOX-4) in granite H3
Figure H.2-2 Contributions to the transient rock temperature at the calculation radius from the central package, adjacent point sources and adjacent line sources for 4 MOX assemblies per waste package (MOX-4) in granite H4
Figure H.2-3 Contributions to the transient rock temperature at the calculation radius from the central package, adjacent point sources and adjacent line sources for one co-extraction HLW (co-extraction-1) canister per waste package in granite H5
Figure H.2-4 Contributions to the transient rock temperature at the calculation radius from the central package, adjacent point sources and adjacent line sources for one new extraction HLW (new extraction-1) canister per waste package in granite H6
Figure H.2-5 Contributions to the transient rock temperature at the calculation radius from the central package, adjacent point sources and adjacent line sources for one EC-Ceramic HLW (ECC-1) canister per waste package in granite H7
Figure H.2-6 Contributions to the transient rock temperature at the calculation radius from the central package, adjacent point sources and adjacent line sources for one EC-Metal HLW (ECM-1) canister per waste package in granite H8
Figure H.2-7 Contributions to the transient rock temperature at the calculation radius from the central package, adjacent point sources and adjacent line sources for UOX-4 in clay H9
Figure H.2-8 Contributions to the transient rock temperature at the calculation radius from the central package, adjacent point sources and adjacent line sources for MOX-4 in clay H10
Figure H.2-9 Contributions to the transient rock temperature at the calculation radius from the central package, adjacent point sources and adjacent line sources for co-extraction-1 in clay H11
Figure H.2-10 Contributions to the transient rock temperature at the calculation radius from the central package, adjacent point sources and adjacent line sources for new extraction-1 in clay H12
Figure H.2-11 Contributions to the transient rock temperature at the calculation radius from the central package, adjacent point sources and adjacent line sources for ECC-1 in clay H13
Figure H.2-12 Contributions to the transient rock temperature at the calculation radius from the central package, adjacent point sources and adjacent line sources for ECM-1 in clay H14
Figure H.2-13 Contributions to the transient rock temperature at the calculation radius from the central package, adjacent point sources and adjacent line sources for UOX-4 in salt H15

Figure H.2-14 Contributions to the transient rock temperature at the calculation radius from the central package, adjacent point sources and adjacent line sources for MOX-4 in salt H16
Figure H.2-15 Contributions to the transient rock temperature at the calculation radius from the central package, adjacent point sources and adjacent line sources for co-extraction-1 in salt H17
Figure H.2-16 Contributions to the transient rock temperature at the calculation radius from the central package, adjacent point sources and adjacent line sources for new extraction-1 in salt H18
Figure H.2-17 Contributions to the transient rock temperature at the calculation radius from the central package, adjacent point sources and adjacent line sources for ECC-1 salt H19
Figure H.2-18 Contributions to the transient rock temperature at the calculation radius from the central package, adjacent point sources and adjacent line sources for ECM-1 in salt H20
Figure H.2-19 Contributions to the transient rock temperature at the calculation radius from the central package, adjacent point sources and adjacent line sources for UOX-1 in a deep borehole H21
Figure H.2-20 Contributions to the transient rock temperature at the calculation radius from the central package, adjacent point sources and adjacent line sources for MOX-1 in a deep borehole H22
Figure H.2-21 Contributions to the transient rock temperature at the calculation radius from the central package, adjacent point sources and adjacent line sources for one narrow co-extraction (co-extraction-0.291) HLW canister per waste package in a deep borehole. The narrow canister contains 0.291 times the waste in a standard canister H23
Figure H.2-22 Contributions to the transient rock temperature at the calculation radius from the central package, adjacent point sources and adjacent line sources for one narrow new extraction (new extraction-0.291) HLW canister per waste package in a deep borehole. The narrow canister contains 0.291 times the waste in a standard canister H24
Figure H.2-23 Contributions to the transient rock temperature at the calculation radius from the central package, adjacent point sources and adjacent line sources for one narrow EC-Ceramic (ECC-0.291) HLW canister per waste package in a deep borehole. The narrow canister contains 0.291 times the waste in a standard canister H25
Figure H.2-24 Contributions to the transient rock temperature at the calculation radius from the central package, adjacent point sources and adjacent line sources for one narrow EC-Metal (ECM-0.291) HLW canister per waste package in a deep borehole. The narrow canister contains 0.291 times the waste in a standard canister H26
Figure H.3-1 Transient host rock temperature at the calculation radius after storage times of 10, 50 and 100 years for a waste package containing 1, 2, 3, 4 and 12 UOX assemblies in granite H27

Figure H.3-2 Transient host rock temperature at the calculation radius after storage times of 10, 50 and 100 years for a waste package containing 1, 2, 3, 4 and 12 MOX assemblies in granite H28
Figure H.3-3 Transient host rock temperature at the calculation radius after storage times of 10, 50 and 100 years for co-extraction-1 in granite H29
Figure H.3-4 Transient host rock temperature at the calculation radius after storage times of 10, 50 and 100 years for new extraction-1 in granite H30
Figure H.3-5 Transient host rock temperature at the calculation radius after storage times of 10, 50 and 100 years for ECC-1 in granite H31
Figure H.3-6 Transient host rock temperature at the calculation radius after storage times of 10, 50 and 100 years for ECM-1 in granite H32
Figure H.3-7 Transient host rock temperature at the calculation radius after storage times of 10, 50 and 100 years for a waste package containing 1, 2, 3, 4 and 12 UOX assemblies in clay H33
Figure H.3-8 Transient host rock temperature at the calculation radius after storage times of 10, 50 and 100 years for a waste package containing 1, 2, 3, 4 and 12 MOX assemblies in clay H34
Figure H.3-9 Transient host rock temperature at the calculation radius after storage times of 10, 50 and 100 years for co-extraction-1 in clay H35
Figure H.3-10 Transient host rock temperature at the calculation radius after storage times of 10, 50 and 100 years for new extraction-1 in clay H36
Figure H.3-11 Transient host rock temperature at the calculation radius after storage times of 10, 50 and 100 years for ECC-1 in clay H37
Figure H.3-12 Transient host rock temperature at the calculation radius after storage times of 10, 50 and 100 years for ECM-1 in clay H38
Figure H.3-13 Transient host rock temperature at the calculation radius after storage times of 10, 50 and 100 years for a waste package containing 1, 2, 3, 4 and 12 UOX assemblies in salt H39
Figure H.3-14 Transient host rock temperature at the calculation radius after storage times of 10, 50 and 100 years for a waste package containing 1, 2, 3, 4 and 12 MOX assemblies in salt H40
Figure H.3-15 Transient host rock temperature at the calculation radius after storage times of 10, 50 and 100 years for co-extraction-1 in salt H41
Figure H.3-16 Transient host rock temperature at the calculation radius after storage times of 10, 50 and 100 years for new extraction-1 in salt H42
Figure H.3-17 Transient host rock temperature at the calculation radius after storage times of 10, 50 and 100 years for ECC-1 in salt H43
Figure H.3-18 Transient host rock temperature at the calculation radius after storage times of 10, 50 and 100 years for ECM-1 in salt H44
Figure H.3-19 Transient host rock temperature at the calculation radius after storage times of 10, 50 and 100 years for UOX-1 in a deep borehole H45
Figure H.3-20 Transient host rock temperature at the calculation radius after storage times of 10, 50 and 100 years for MOX-1 in a deep borehole H46
Figure H.3-21 Transient host rock temperature at the calculation radius after storage times of 10, 50 and 100 years for co-extraction-0.291 in a deep borehole H47

Figure H.3-22 Transient host rock temperature at the calculation radius after storage times of 10, 50 and 100 years for new extraction-0.291 in a deep boreholeH 48
Figure H.3-23 Transient host rock temperature at the calculation radius after storage times of 10, 50 and 100 years for ECC-0.291 in a deep borehole.....H49
Figure H.3-24 Transient host rock temperature at the calculation radius after storage times of 10, 50 and 100 years for ECM-0.291 in a deep borehole H50
Figure H.4-1 Calculated waste package temperature after storage times of 10, 50 and 100 years for UOX-4 in granite.....H52
Figure H.4-2 Calculated waste package temperature after storage times of 10, 50 and 100 years for MOX-4 in granite.....H53
Figure H.4-3 Calculated waste package temperature after storage times of 10, 50 and 100 years for co-extraction-1 in granite H54
Figure H.4-4 Calculated waste package temperature after storage times of 10, 50 and 100 years for new extraction-1 in granite.....H55
Figure H.4-5 Calculated waste package temperature after storage times of 10, 50 and 100 years for ECC-1 in granite H56
Figure H.4-6 Calculated waste package temperature after storage times of 10, 50 and 100 years for ECM-1 in granite H57
Figure H.4-7 Calculated waste package temperature after storage times of 10, 50 and 100 years for UOX-4 in clay H58
Figure H.4-8 Calculated waste package temperature after storage times of 10, 50 and 100 years for MOX-4 in clay H59
Figure H.4-9 Calculated waste package temperature after storage times of 10, 50 and 100 years for co-extraction-1 in clay.....H60
Figure H.4-10 Calculated waste package temperature after storage times of 10, 50 and 100 years for new extraction-1 in clay H61
Figure H.4-11 Calculated waste package temperature after storage times of 10, 50 and 100 years for ECC-1 in clay H62
Figure H.4-12 Calculated waste package temperature after storage times of 10, 50 and 100 years for ECM-1 in clay.....H63
Figure H.4-13 Calculated waste package temperature after storage times of 10, 50 and 100 years for UOX-4 in salt, with 75% of the waste package surface contacting intact salt H64
Figure H.4-14 Calculated waste package temperature after storage times of 10, 50 and 100 years for MOX-4 in salt, with 75% of the waste package surface contacting intact salt H65
Figure H.4-15 Calculated waste package temperature after storage times of 10, 50 and 100 years for co-extraction-1 in salt, with 75% of the waste package surface contacting intact salt.....H66
Figure H.4-16 Calculated waste package temperature after storage times of 10, 50 and 100 years for new extraction-1in salt, with 75% of the waste package surface contacting intact salt.....H67
Figure H.4-17 Calculated waste package temperature after storage times of 10, 50 and 100 years for ECC-1 in salt, with 75% of the waste package surface contacting intact salt H68

Figure H.4-18 Calculated waste package temperature after storage times of 10, 50 and 100 years for ECM-1 in salt, with 75% of the waste package surface contacting intact salt H69
Figure H.4-19 Calculated waste package temperature after storage times of 10, 50 and 100 years for UOX-1 in a deep borehole H70
Figure H.4-20 Calculated waste package temperature after storage times of 10, 50 and 100 years for MOX-1 in a deep borehole H71
Figure H.4-21 Calculated waste package temperature after storage times of 10, 50 and 100 years for co-extraction-0.291 in a deep borehole H72
Figure H.4-22 Calculated waste package temperature after storage times of 10, 50 and 100 years for new extraction-0.291in a deep borehole H73
Figure H.4-23 Calculated waste package temperature after storage times of 10, 50 and 100 years for ECC-0.291 in a deep borehole H74
Figure H.4-24 Calculated waste package temperature after storage times of 10, 50 and 100 years for ECM-0.291 in a deep borehole H75
Figure H.5-1 Waste package surface peak temperature as a function of surface storage time for UOX in a granite repository H76
Figure H.5-2 Waste package surface peak temperature as a function of surface storage time for MOX in a granite repository H77
Figure H.5-3 Waste package surface peak temperature as a function of surface storage time for UOX in a clay repository H78
Figure H.5-4 Waste package surface peak temperature as a function of surface storage time for MOX in a clay repository H79
Figure H.5-5 Waste package surface peak temperature as a function of surface storage time for UOX in a salt repository with 75% of the waste package surface contacting intact salt H80
Figure H.5-6 Waste package surface peak temperature as a function of surface storage time for MOX in a salt repository with 75% of the waste package surface contacting intact salt H81
Figure H.6-1 Minimum surface storage time necessary to comply with waste package surface temperature limit as function of UOX assemblies per waste package in a granite, clay, and salt (with 75% of the waste package surface contacting intact salt) repository H82
Figure H.6-2 Minimum surface storage time necessary to comply with waste package surface temperature limit as function of MOX assemblies per waste package in a granite, clay, and salt (with 75% of the waste package surface contacting intact salt) repository H83

ACRONYMS

ABR	Advanced Breeder Reactor
ANL	Argonne National Laboratory
BSC	Bechtel SAIC
BWR	Boiling Water Reactor
DOE	U.S. Department of Energy
EBS	Engineered Barriers System
EC, E-Chem	Electro-Chemical (with –C or –M indicates ceramic or metal respectively) HLW waste form
FEPs	Features, Events and Processes
FY	Fiscal Year
GTCC	Greater Than Class C
GWd	Gigawatt days
GWd/MT	Gigawatt (thermal) - days per Metric Ton
GWe	Gigawatts electric
GWt	Gigawatts thermal
HLW	High-Level nuclear Waste
LLNL	Lawrence Livermore National Laboratory
LLW	Low Level Waste
LTHLW	Lower Than High-Level nuclear Waste
LWR	Light Water Reactor
MWd	Megawatt days
MOX	Mixed Oxide fuel
MT	Metric Ton
MTHM	Metric Tons of Heavy Metal
MTIHM	Metric Tons of Initial Heavy Metal
MTU	Metric Tons of Uranium
NE	DOE-Nuclear Energy
ORNL	Oak Ridge National Laboratory
PWR	Pressurized Water Reactor
SFR	Sodium Fast Reactor
SNFA	Spent Nuclear Fuel Assembly

SNL	Sandia National Laboratories
SRNL	Savannah River National Laboratory
TBD	To Be Determined
UFD	Used Fuel Disposition
UNF	Used Nuclear Fuel
UOX	Uranium Oxide Fuel
WF	Waste Form
WP	Waste Package
YMP	Yucca Mountain Project

NOMENCLATURE AND SYMBOLS

α	thermal diffusivity, $m^2/s = k/(\rho \cdot C_p)$
A	area, m^2
h	convection coefficient, $W/(m^2\text{-}K)$
i.d.	internal diameter
k, k_{th}	thermal conductivity, J/(m-K)
q_A	heat per unit area, W/m^2
q_L	heat per unit length, W/m
Q	heat, W
r	radius
R	thermal resistance, $(m^2\text{-}K)/W$
t	time, s
T	temperature, °C
T_{store}	surface storage time, yr
U	conductance $W/m^2\text{-}K$
V_{dur}	ventilation duration
V_{eff}	ventilation efficiency

~

The authors gratefully acknowledge the input of Ernie Hardin, Bill Spezialetti, Rob Howard, Joe Carter, Mark Dupont and Steve Sheets in the development of this work.

~

1. INTRODUCTION

This section will be written by a partnering National Laboratory.

2. INVENTORY

This section will be written by a partnering National Laboratory.

3. GEOLOGIC SETTING AND GEOLOGIC HOST MEDIA

This section will be written by a partnering National Laboratory.

4. CONCEPT OF OPERATIONS

This section will be written by a partnering National Laboratory.

5. THERMAL ANALYSES

The modeling tools generated in MathCAD, Excel, and MatLab were used to calculate the temperature evolution for combinations of waste form and geologic medium, assuming a particular emplacement layout for each concept (Sutton et al. 2011). Two types of spent nuclear fuel assemblies (SNFA) were considered, namely UOX from an open fuel cycle and MOX from a modified-open fuel cycle. Four types of high level waste (HLW) canisters were considered, namely "co-extraction" glass from a modified-open fuel cycle and "new extraction" glass, electrochemical ceramic (EC-C) and electrochemical metal (EC-M) from a closed fuel cycle. While the "co-extraction" process is similar in function to the industrial Co-Extraction™ (COEX) process deployed by AREVA, the two processes assume different processing methods and steps and so the product and waste streams cannot be directly compared. Similar is true for the "new extraction" process documented in this report and the NUEX industrial process proposed by Energy Solutions, which also cannot be directly compared.

The modified open fuel cycle has PWRs and MOX PWRs, and the closed fuel cycle has PWRs and sodium fast reactors with a 0.75 conversion ratio (SFRs, a type of Advanced Burner Reactor, ABR). In the closed fuel cycle, the new extraction glass is produced by reprocessing the PWR SNFAs, and the other three waste forms are produced by reprocessing the SFR metallic fuel. These waste forms have been investigated in four different geologic media (granite, clay, salt and deep borehole). In addition, the number of assemblies per waste package (WP) has been varied to provide information to the future evaluation on the trade-off between pre-emplacement storage time and repository footprint.

The reference design concepts used in this report, and shown in Figures 5.1-1 to 5.1-4, were developed in a working group session hosted by LLNL on June 8 to 9, 2011. The Thermal Design and Analysis team selected representative international design concepts for the repositories in granite, clay, salt, and deep borehole (Andra 2005, Ondraf-Niras 2010, SNL 2009 and SRNL 2011 respectively).

5.1 CONCEPTUAL MODEL

The conceptual models presented in this report calculate (a) the temperature history at or near the interface between the Engineered Barrier System (EBS) and the geologic medium and (b) the temperature history at selected locations within the EBS. In the former, the model assumes a homogeneous medium with the EBS simply replaced by the geologic media, and with the heat source being a combination of a finite line for the central WP in the calculation, point sources for nearby WPs, and infinite lines for more distant WPs. In the latter, a steady state calculation is performed at each point in time, using the heat source and interface temperature as boundary conditions, and using appropriate thermal properties for each component of the EBS.

5.1.1 GEOMETRY

Figure 5.1-1 shows a generic EBS, with standard names adopted for this report, to describe the various components. These names may be somewhat different from those published from design to design.

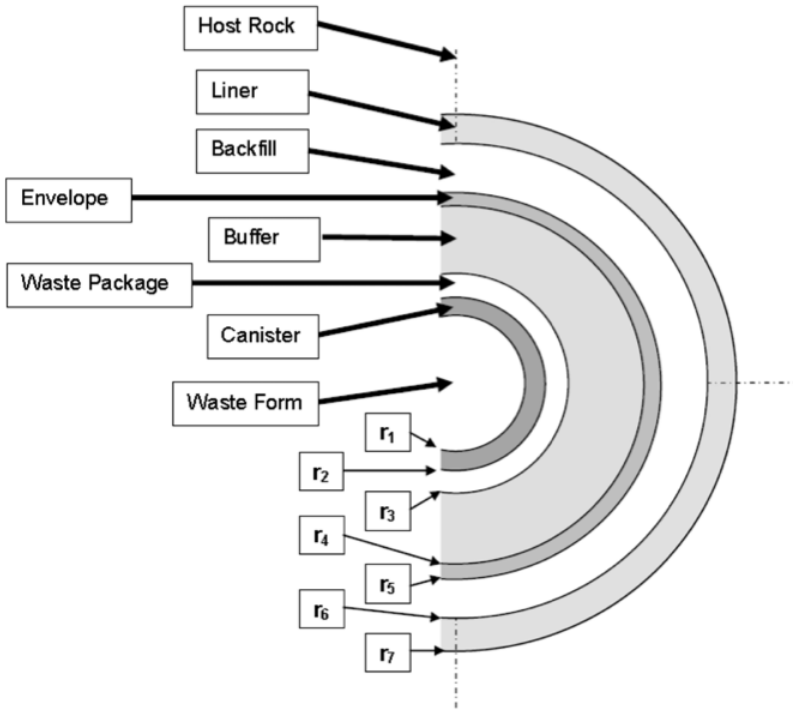

Figure 5.1-1 Illustration defining the terminology used for the potential layers of the near-field Engineered Barriers System (EBS) from waste form to host rock

For each geologic medium, a WP layout was selected for initial calculations by the multi-lab team (LLNL, ORNL, SNL, SRNL, and also the DOE sponsor). These repository layouts constitute a base case, from which variations will be explored in late FY11 and FY12. For this report the repository layout was fixed for each geologic medium based on previous published international designs. Figure 5.1-2 shows a generic repository layout that defines the spacing of waste packages. The design for each geologic medium can be interpreted using this figure. In some cases, the waste package axis is horizontal, and in others, it is vertical. In one case, the axial direction is a line of alcoves, and in others, it is an emplacement borehole or line of boreholes. The lateral direction is the separation of boreholes or of emplacement drifts, depending on the geologic medium.

Table 5.1-1 Repository layout axial (center to center waste package) and lateral spacing (meters) used in thermal analysis models

Geology	SNF		HLW	
	Axial	Lateral	Axial	Lateral
Granite	10	20	10	20
Clay	10	30	6	30
Salt	20	20	20	20
Deep Borehole	6	200	6	200

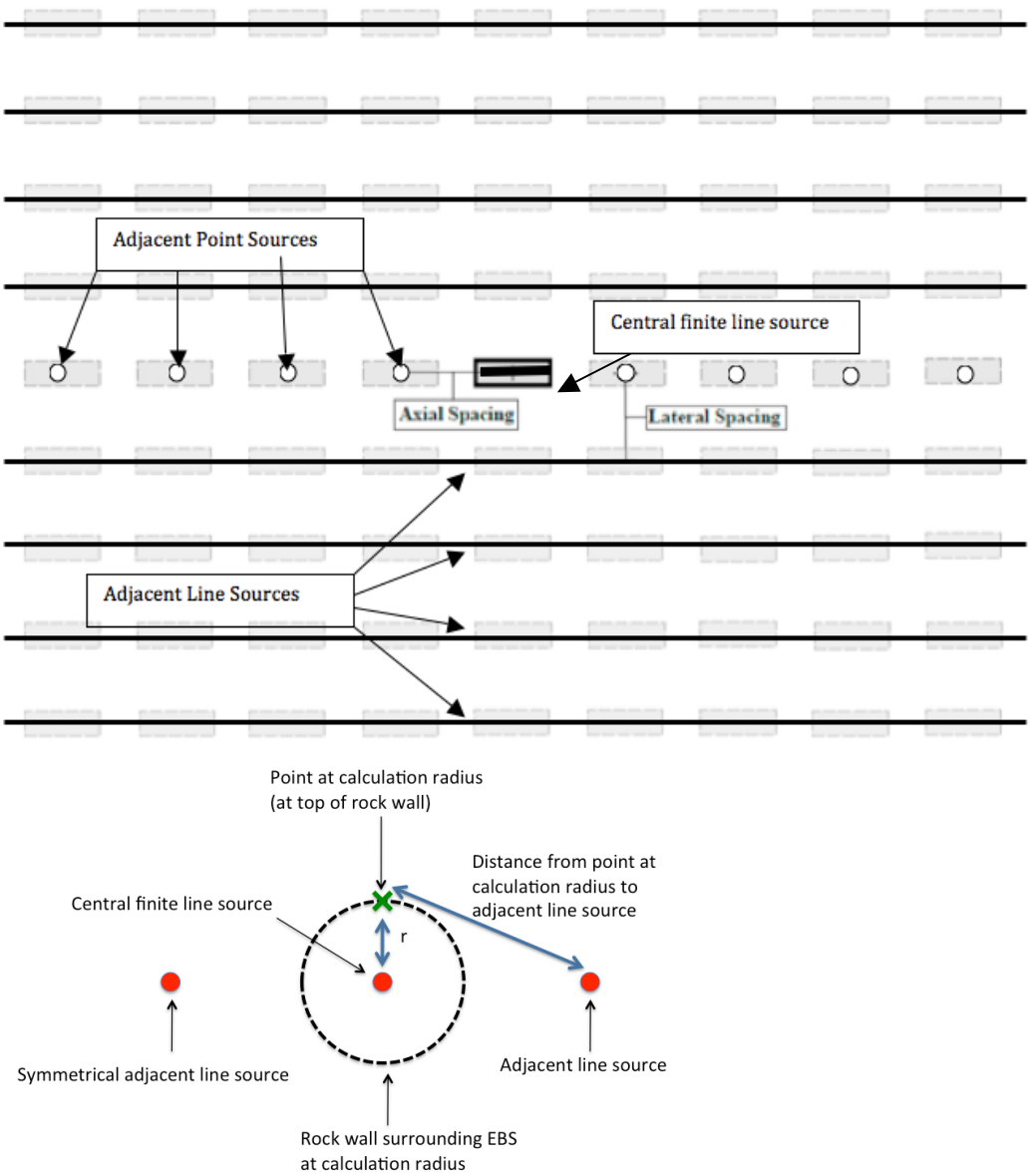

Figure 5.1-2 Conceptual layout of a central waste package of interest and both axial and lateral emplacement lines (plan and elevation view)

The components and dimensions of the EBS are tailored to each geologic medium. Figures 5.1-3 through 5.1-6 show the EBS for each of the four media, including differences due to the different sizes of the waste form.

Figure 5.1-3 shows the EBS cross-section for the granite design. The waste packages are based on Andra 2005 and are assumed to include four SNFAs or one canister (i.e., six calculations for the two SNFA types and four canister types). The waste packages are surrounded by a bentonite buffer for both WF-types. A single waste package is emplaced in an emplacement borehole in the floor of an emplacement drift. The drifts can be filled with lower than HLW (LTHLW) waste prior to repository closure; however, that does not significantly affect the thermal calculation. Four neighboring waste packages on either side of the central borehole are modeled as point sources 10 meters apart (axial spacing). The central package is modeled as a finite line that is horizontal, rather than vertical, to conform to model restrictions. This rotation of the WP in the homogeneous calculation is not expected to significantly influence the resulting temperatures. The reason for selecting a finite line source is to avoid unrealistic computational smearing of the heat between the emplacement boreholes. Finally, four adjacent emplacement drifts, on either side of the central drift, are modeled as infinite lines separated by 20 meters (lateral spacing).

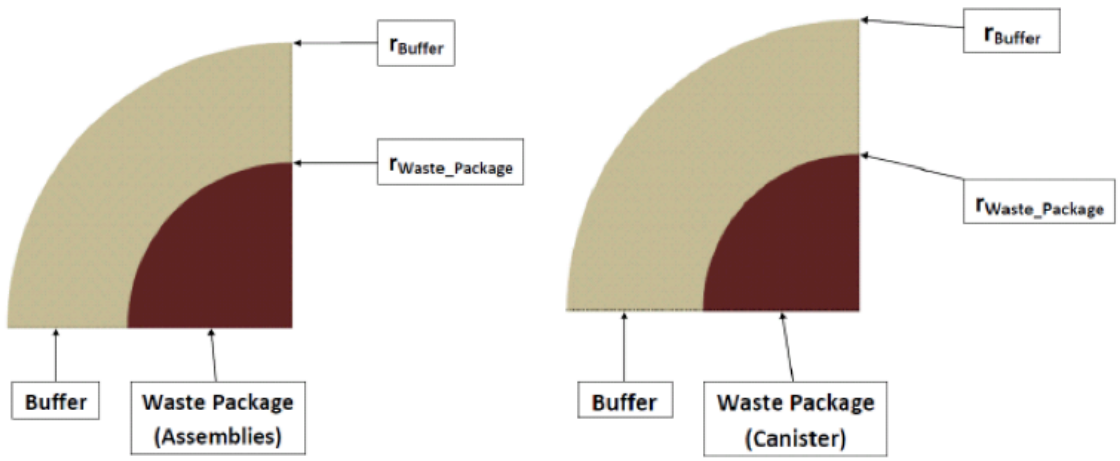

Key	Region	Material		Thermal Conductivity (W/m-K)	Radius (m)
	Waste Package	4-PWR Waste Package	Copper	366.9	0.48
			Steel	46	
	Buffer	Bentonite	Wet	0.85	0.83
			Dry	0.60	

Key	Region	Material		Thermal Conductivity (W/m-K)	Radius (m)
	Waste Package	Carbon Steel		53	0.41
	Buffer	Bentonite	Wet	0.85	0.76
			Dry	0.60	

Figure 5.1-3 Graphical representation of a granite design for SNFA (left) and HLW (right), including material properties and dimensions

Figure 5.1-4 shows the EBS cross-section for the clay design. As in the granite design, it is assumed that the waste package will include either four SNFAs or one

canister. Based on the French design, the SNFA WPs are surrounded by a bentonite buffer, but the HLW canister waste packages are not. The *supercontainer* comprises the stainless steel envelope, the concrete buffer and the carbon steel overpack. The waste packages are assumed to be emplaced in horizontal boreholes drilled from the emplacement drift, with nine WPs per drift (this number is somewhat different than published designs, but is not expected to significantly affect the temperature calculation). For SNF, the central WP is modeled as a finite line, and the eight neighboring WPs are modeled as point sources 10 meters apart (axial). Finally, four adjacent emplacement boreholes, on either side of the central borehole, are modeled as infinite lines 30 meters apart (lateral spacing). For HLW, the axial spacing is 6 m (center to center, with a 4.57 m waste package) and the lateral spacing is 30 m.

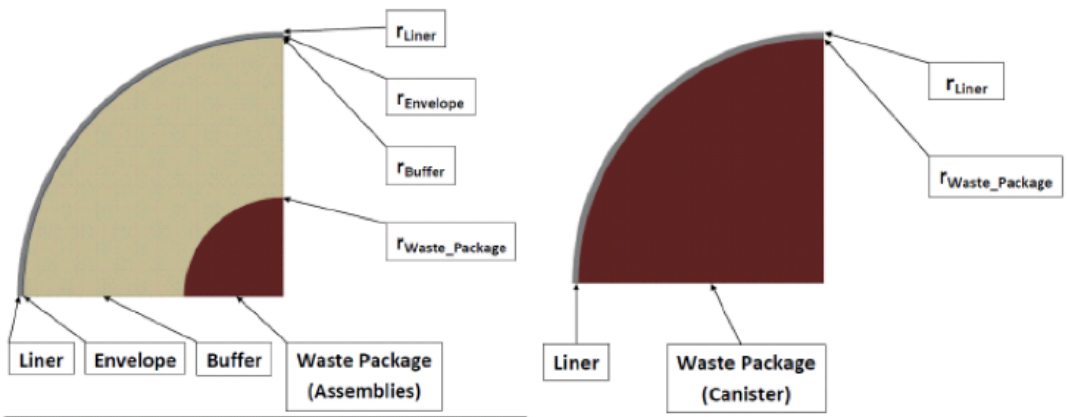

Key	Region	Material		Thermal Conductivity (W/m-K)	Radius (m)
	Waste Package	4-PWR Waste Package, Carbon Steel		53	0.49
	Buffer	Bentonite	Wet	0.85	1.29
			Dry	0.60	
	Envelope	Carbon Steel		53	1.296
	Liner	Steel		46	1.321

Key	Region	Material	Thermal Conductivity (W/m-K)	Radius (m)
	Waste Package	Carbon Steel	53	0.36
	Liner	Steel	46	0.37

Figure 5.1-4 Graphical representation of a clay design for SNFA (left) and HLW (right), including material properties and dimensions

Figure 5.1-5 shows the EBS cross-section for the salt design. As in the granite and clay designs, it is assumed that the waste package will include either four SNFAs or one canister. The waste packages are assumed to be emplaced at the bottom-back of a mined alcove, and covered with a sloping surface of crushed salt. The axis of the waste package is parallel to the emplacement drift axis. The central WP is modeled as a finite line, and eight neighboring WPs (four on either end, as adjacent alcoves) are modeled as point sources with an axial spacing of 20 m. Finally, four adjacent emplacement drifts, on either side of the central drift, are modeled as infinite lines

with lateral spacing of 20 m. The backfill of crushed salt is expected to consolidate into intact salt in a relatively short time (perhaps five years). Because the thermal conductivity of crushed salt is more than seven times lower than intact salt, the calculation radius for the homogeneous calculation was set at 4 m, somewhat farther than the 3.048 m radius if the backfill is converted, volumetrically, to a cylindrical geometry. Then, the EBS temperatures were calculated with intact salt inward to 3.048 m, and either intact or crushed salt inward from that point (two cases to investigate sensitivity). Also, it was recognized that about ¾ of the waste package circumference is in good contact with virgin intact salt; therefore, an additional sensitivity calculation was done using intact salt from 4 m inward to the waste package, but with only 75% of the periphery available to transfer heat.

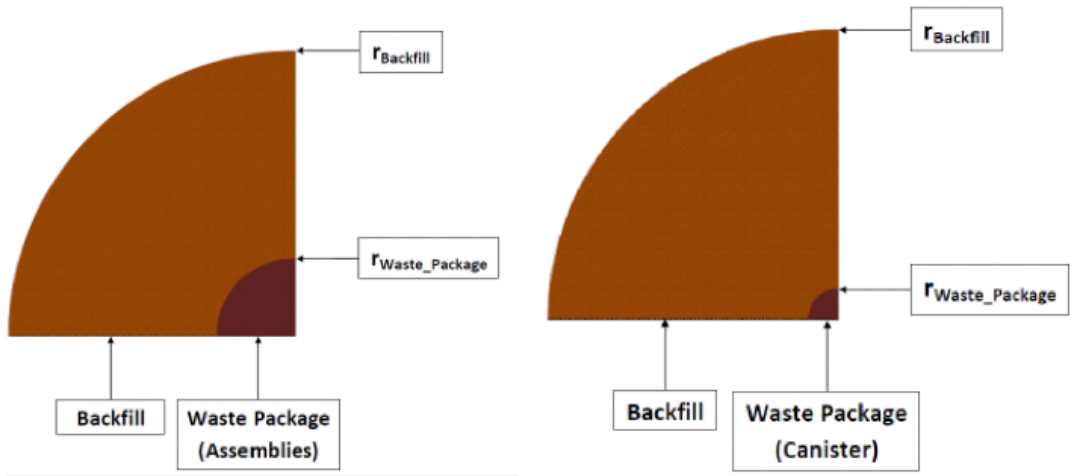

Key	Region	Material	Thermal Conductivity (W/m-K)	Radius (m)
	Waste Package	4-PWR Waste Package, Carbon Steel	53	0.41
	Backfill	Crushed Salt	0.57	3.048

Key	Region	Material	Thermal Conductivity (W/m-K)	Radius (m)
	Waste Package	Steel	46	0.305
	Backfill	Crushed Salt (10 ft. high excavation)	0.57	3.048

Figure 5.1-5 Graphical representation of a salt design for SNFA (left) and HLW (right), including material properties and dimensions

Figure 5.1-6 shows the EBS cross-section for the deep borehole design. This design is limited by the maximum feasible size of the borehole, from a drilling perspective. The SNFA WP is assumed to have one assembly, but with rod consolidation to reduce the diameter. The canister WPs are limited by the borehole diameter, and will only contain 0.291 times the volume of waste as the standard canister used for the other four media. The waste packages are assumed to be emplaced in deep vertical boreholes drilled from the surface, with nine WPs per drift (this number is somewhat much lower than published designs, but is not expected to significantly affect the temperature calculation at the central WP). The central WP is modeled as a finite line, and the eight neighboring WPs are modeled as point sources with axial spacing of 6 meters. Finally, four adjacent emplacement boreholes, on two sides of the central borehole, are modeled as infinite lines (this is fewer neighbors than the

published designs with lateral spacing of 200 meters, but the large borehole spacing means that there will be little effect on the central WP temperature history).

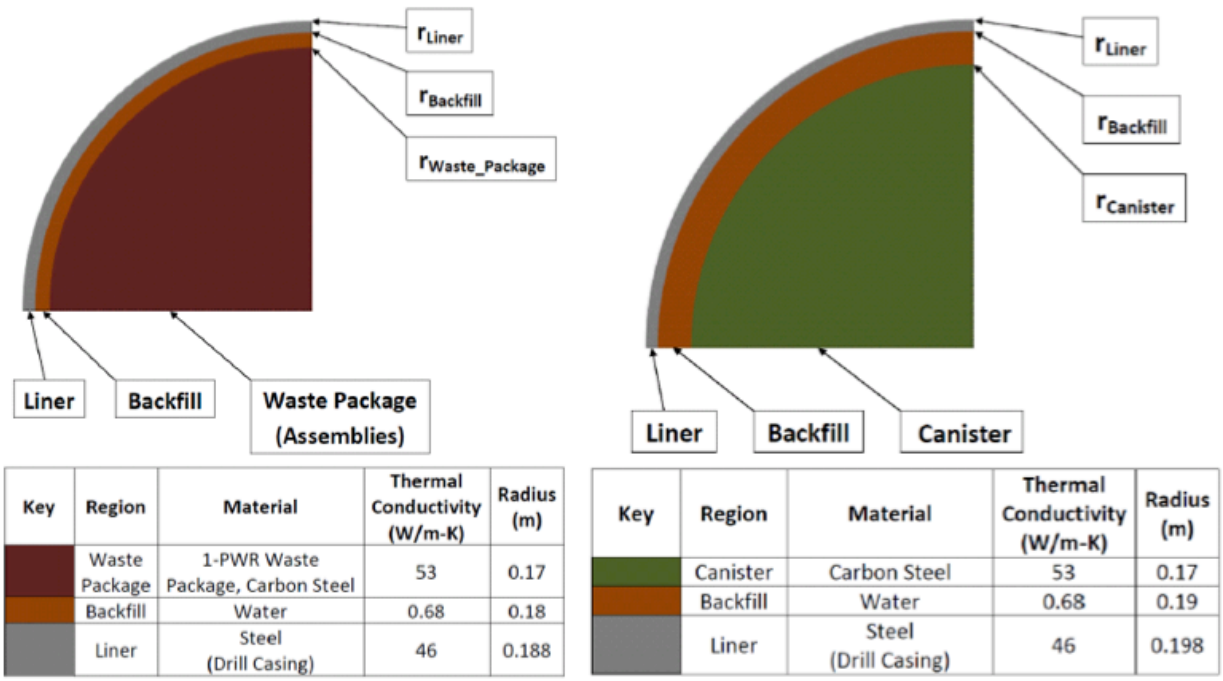

Key	Region	Material	Thermal Conductivity (W/m-K)	Radius (m)
	Waste Package	1-PWR Waste Package, Carbon Steel	53	0.17
	Backfill	Water	0.68	0.18
	Liner	Steel (Drill Casing)	46	0.188

Key	Region	Material	Thermal Conductivity (W/m-K)	Radius (m)
	Canister	Carbon Steel	53	0.17
	Backfill	Water	0.68	0.19
	Liner	Steel (Drill Casing)	46	0.198

Figure 5.1-6 Graphical representation of a deep borehole design for SNFA (left) and HLW (right), including material properties and dimensions

5.1.2 APPROACH

For each case, time-dependent temperature calculations were performed for the interface of the EBS and the geological medium and (ii) within the EBS. To better understand the application of potential analytical solutions for various line sources, point sources, and heat loads, 4 examples were examined:

- Approach A: The central <u>infinite</u> emplacement line assumes end-to-end WPs with a line load equal to the waste package heat load divided by the waste package length (i.e., equal to the local radial heat load along the WP, which in practice adds energy to the calculation by using this same heat load in the gaps between the WPs). The calculation also includes eight neighbor emplacement lines (four on either side of the central line separated by an assumed spacing), modeled as infinite line sources, with an average heat load based on the WP heat load divided by the axial WP spacing (i.e., the neighbor emplacement lines contain the correct amount of heat). This approach leads to a temperature model that overestimates the temperature for designs with a significant gap between WPs.

- Approach B: Similar to Approach A, except that the central drift line load is the WP heat divided by the axial spacing (i.e., the correct amount of energy, but with energy not being concentrated at the actual waste packages). This leads to an underestimate of temperature.

- Approach C: Similar to Approach A, except that the central drift has only one finite waste package. The heat load at the central WP is thus correct, but the axial neighbor WPs are not included in the calculation. This results in an underestimate of temperature.

- Approach D: The central drift consists of one finite line source and eight point sources, and represents a finite waste package with four axial neighboring waste packages on each side modeled as point sources with the nominal waste package center-to-center spacing. As in the other approaches, there are four neighboring emplacement lines on each side of the central waste package line represented by infinite line sources. This model has the correct local heat flux for the central package and also includes, separately, the axial neighbors and the lateral neighbors.

These approaches were applied to several test cases, and the differences in calculated peak temperatures were significant. Because Approach D combines the correct local heat flux and considers the effects of neighboring WPs and neighboring lines of WPs, it is expected to be the most accurate of the four approaches; and therefore, it was selected for use in this study. Further, it was realized that the relative contributions to peak temperature from the central WP, the axial neighbors, and the lateral neighbors can provide insight into the effects of increasing or decreasing the WP spacing; hence, it was decided that those three contributions to the temperature would be tracked individually.

5.1.3 Input Data and Assumptions

The decay heat curves for the six waste forms of interest are shown in Figures 5.1-7 to 5.1-9. In Figure 5.1-7, the curves represent one assembly or canister per waste package from storage times from 5 to 100 years (longer times were considered in the parametric calculations to determine the sensitivity of temperature to a wide range of storage times).

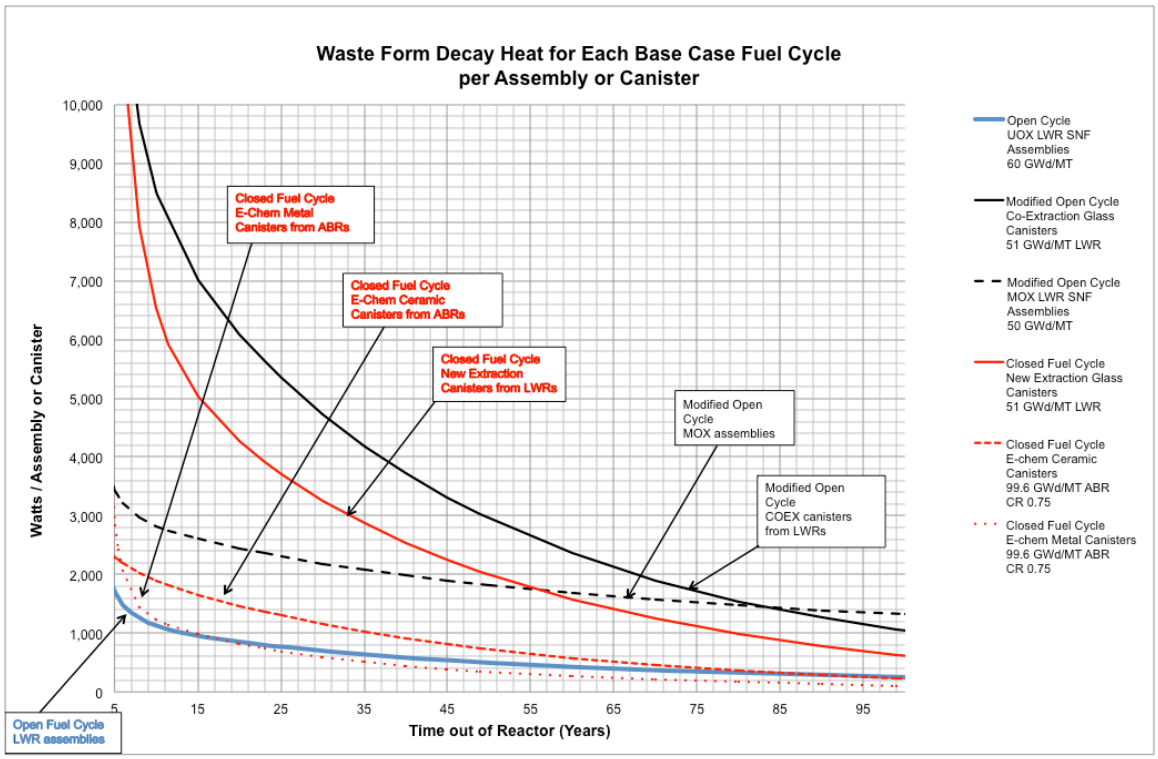

Figure 5.1-7 Decay heat curves for 1 assembly or 1 canister per waste package for UOX, MOX, co-extraction, new extraction, EC-ceramic, and EC-metal

The curves shown in Figure 5.1-8 represent the deep borehole design, in which a single UOX or MOX assembly can be placed in a WP using rod consolidation. For HLW, however, the limited borehole diameter prohibits use of the standard (2 foot diameter) canisters used in the other designs. Using the available diameter, each narrow canister will contain the same waste as 0.291 standard canisters of the same length.

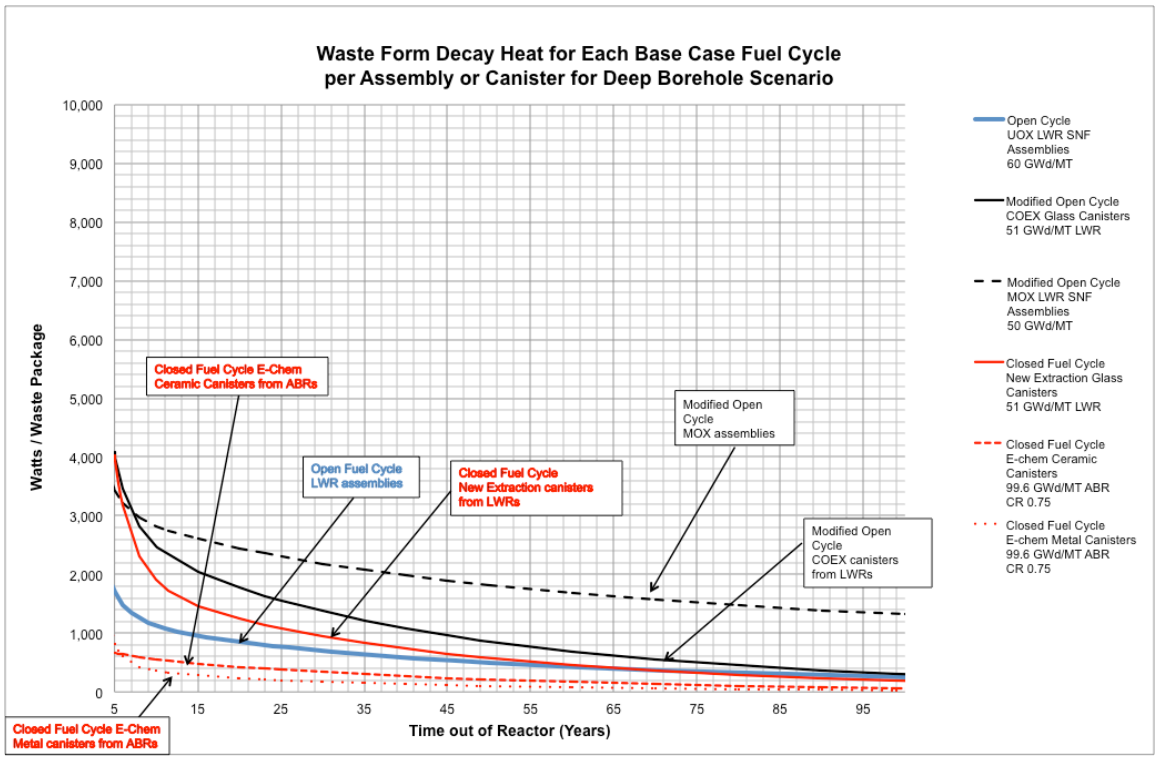

Figure 5.1-8 Decay heat curves for 1 UOX or MOX assembly and 0.291 co-extraction, new extraction, EC-ceramic or EC-metal canister per waste package (deep borehole design)

Some geologic media, depending on storage time, can accommodate WPs with multiple UOX or MOX assemblies. Figure 5.1-9 shows the heat per waste package for 1, 2, 3, 4 and 12 SNFAs per WP.

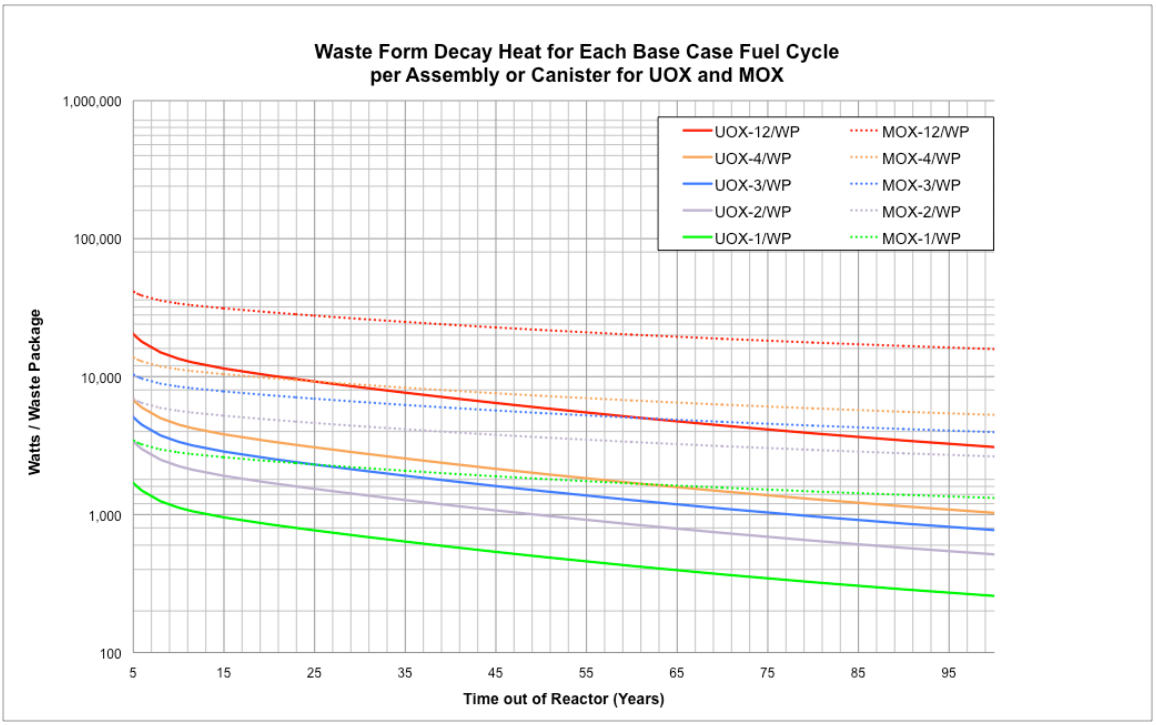

Figure 5.1-9 Decay heat curves for 1, 2, 3, 4 and 12 UOX or MOX assemblies per waste package

The following assumptions were based team consensus developed at the June 8 to 9, 2011 working group meeting:

- An ambient average ground surface temperature of 15°C was assumed for all reference repository designs
- The rock properties were evaluated at an assumed host rock temperature of 100°C to be more representative of post-emplacement heat transfer conditions.

The host rock property data (see Section 5.2.2.1) for thermal conductivity (W/m-K) and thermal diffusivity (m^2/s) were developed by literature search and comparison to the rock thermal properties from Andra 2005, Jia et al 2009, SRNL 2011, and SNL 2009, which served as the basis of the chosen reference repository design concepts. It is assumed that at any given point at time, the relatively low thermal mass of the EBS components, compared to the infinite host rock medium, implies that the thermal gradient between the waste package surface, the other EBS components, and the host rock surface can be considered to be at a quasi-steady state condition.

The calculation radius, associated with the radius of the host rock wall, was developed for each design concept by the team at the June 8 to 9, 2011 working group meeting by referring to the reference design concept reports (Andra 2005, Ondraf-Niras 2010, SRNL 2011, and SNL 2009). It was recognized that the waste package dimensions for UOX and MOX SNF waste packages would both have the same dimensions, and that all of the HLW canisters had the same outer dimension, so two distinct EBS configurations were assumed for each host rock type. One

configuration was assumed for SNF assemblies and another one applicable to HLW canisters. Using the reference design concepts and group discussion for each of the two EBS constructs, the inner radius and thickness of each engineered barrier component was tabulated, eventually summing to the rock wall radius. This "calculation radius" was determined in this manner for all media except salt. The calculation radius for salt was based on the height of the excavation alcove for a generic salt repository from SNL 2009, with some additional margin to approximate a circular enveloping shape filled with crushed salt. The calculation radius selected was 4 m, where the maximum extent of the crushed salt layer was assumed to be 10 ft (3.048 m).

The design of the 4-PWR waste package was taken from NAGRA 2003 (Figure 7). This same design diameter and wall thickness was assumed for waste packages containing 2, 3, and 4 assemblies. In the sensitivity studies a 1-PWR assembly waste package was assumed with half the diameter of the 4-PWR waste package, having the same wall thickness as the 4-PWR package. A 12-PWR waste package was also modeled, which assumed an inner diameter of the 12-PWR long waste package design (OCRWM 2001, Table 2) with the same wall material and thickness as the 4-PWR waste package.

5.2 RESULTS

The results of the homogeneous analytic solution model and the quasi-steady-state heterogeneous concentric cylinder model are presented in this section.

5.2.1 HOST ROCK TEMPERATURE

Using the analytic model, the host rock temperature was determined for all combination of the four geologic media and the six waste forms considered in this study. In addition, for UOX and MOX, the host rock temperature was evaluated as a function of the number of assemblies per waste package (namely 1, 2, 3, 4 and 12 per package). The waste package length and thermal output, the rock properties, and the axial and lateral spacing of the waste packages are shown in Section 5.1.1.

This analytic model assumes that the EBS volume has the properties of the bulk rock. More information on the thermal resistance is given in Appendix G, Section 4. Future work will validate the results presented in this report using a finite element model that explicitly calculates temperatures in the heterogeneous geometry.

Figure 5.2-1 illustrates the temperature transient of the host rock after surface storage times of 10, 50, and 100 years for a waste package containing 1, 2, 3, 4 and 12 MOX and UOX assemblies in a granite repository. A full set of illustrations for all media and waste forms is provided in Appendix H, Section 3. The temperature rise results from the combination of three contributions (Section H.2): central waste package (finite line source), axially adjacent waste packages (point sources), and laterally adjacent emplacement arrays (infinite line sources). Waste package spacing (axial) and adjacent line spacing (lateral) is detailed in Section 5.1.1. Figure 5.2-2 shows these three temperature components in granite for a waste package containing four MOX assemblies after 10 years cooling. Examples of UOX in clay are shown in Figures 5.2-3 and 5.2-4. Similar figures for other media and waste forms are provided in Appendix H, Section 2.

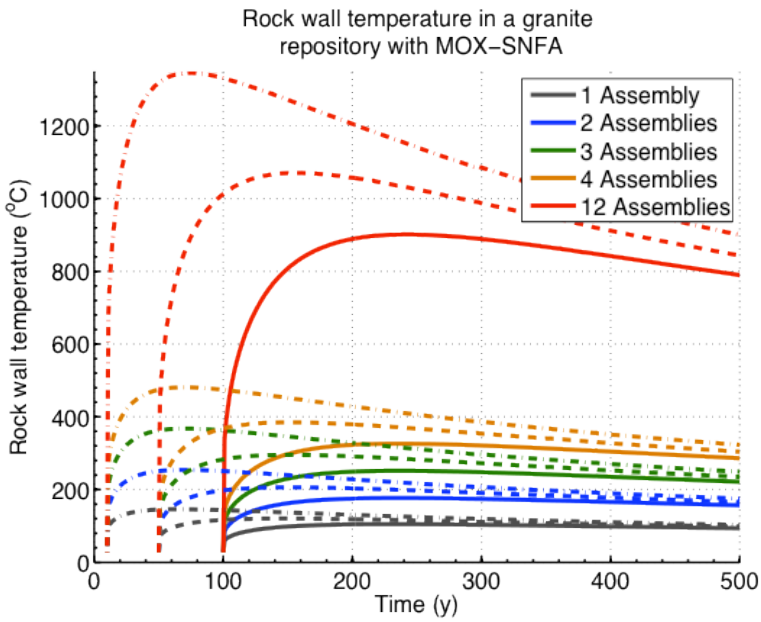

Figure 5.2-1 Transient host rock temperature at the "calculation radius" after storage times of 10, 50 and 100 years for a waste package containing 1, 2, 3, 4 and 12 MOX assemblies per waste package in granite

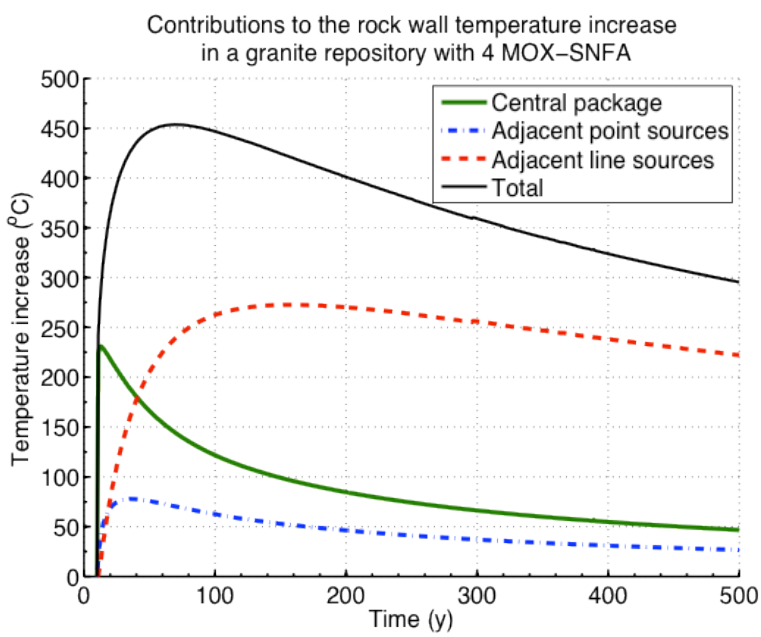

Figure 5.2-2 Contributions to the transient rock temperature at the "calculation radius" from the central package, adjacent point sources and adjacent line sources for 4 MOX assemblies per waste package in granite after 10 years storage

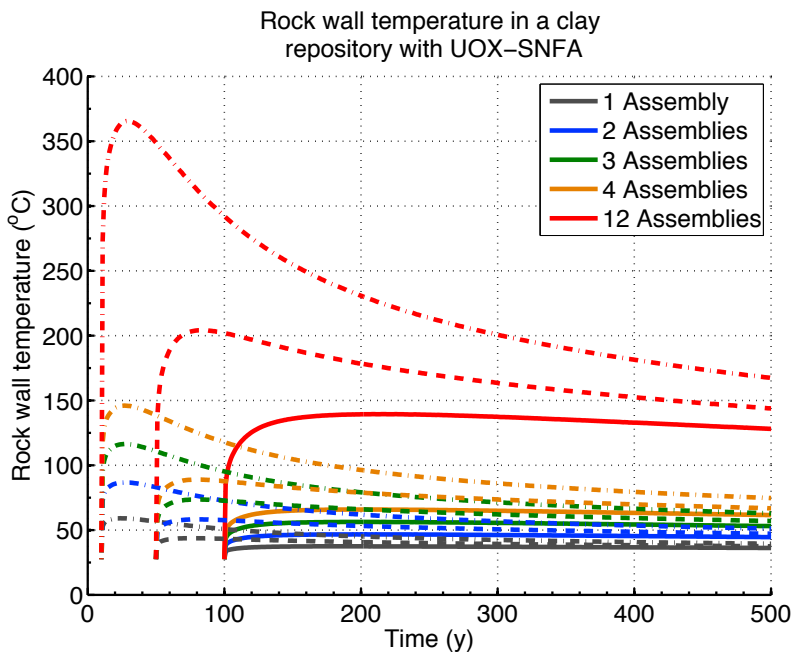

Figure 5.2-3 Transient host rock temperature at the "calculation radius" after storage times of 10, 50 and 100 years for a waste package containing 1, 2, 3, 4 and 12 UOX assemblies per waste package in clay

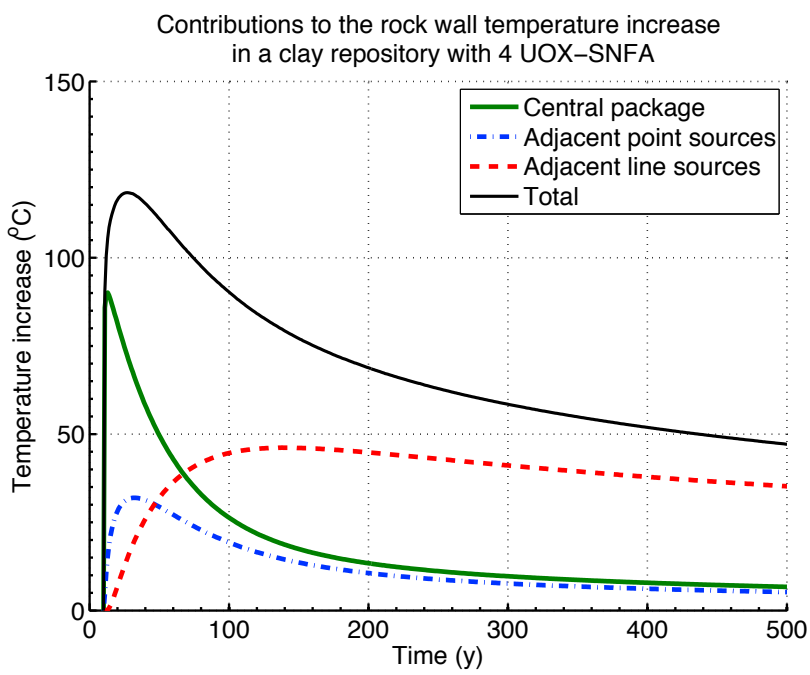

Figure 5.2-4 Contributions to the transient rock temperature at the "calculation radius" from the central package, adjacent point sources and adjacent line sources for 4 UOX assemblies per waste package in clay after 10 years storage

Table 5.2-1 summarizes the host rock peak temperature and the corresponding time out-of-reactor when the peak occurs. In deep borehole media, where the adjacent lines are widely spaced at 200 m, the temperature reaches its peak shortly after emplacement (10 years or less) and the time of the peak is not very sensitive to the waste package heat load. In clay, the peak temperature is reached quickly for HLW. In granite, clay and salt, the adjacent waste package lines are closer, namely 20 m, 30 m and 20 m respectively, the temperature peaks after only a few decades or more, and the time necessary to reach the peak increases as the waste package heat load decreases. In clay the peak temperature is first driven by the central package, then by the adjacent waste package line (e.g. Figure 5.2-4). In deep borehole media, the peak temperature is driven by the central package; whereas, in granite and salt, the contribution to the temperature rise by adjacent waste package lines is dominant at the time of the peak temperature (e.g. Figure 5.2-2).

The thermal constraints considered in this study depend on the geologic medium (e.g., the bulk rock) or the engineered components (e.g., the bentonite buffer). By comparing the host rock temperature at the calculation radius with the compliance limits for a set of repository designs (see Section 5.2.2, below), the following conclusions can be drawn:

- A waste package containing four UOX assemblies requires surface storage of approximately 50 years before emplacement in granite or clay, and less than 10 years in salt
- A waste package containing four MOX assemblies requires surface storage for more than 200 years before emplacement in granite or clay
- In granite even a single MOX assembly package requires more than 100 years storage, whereas a single UOX assembly package may be emplaced in granite, clay or salt media within 10 years out of the reactor
- Co-extraction glass, the hottest of the HLW forms, requires more than 50 years storage in before emplacement in granite or clay.

Table 5.2-1: Host rock peak temperature (at the "calculation radius") and corresponding time of the peak for four geologic media, six waste forms and four aging times

Geology	Waste Form	Assemblies / WP	Calculation Radius, m	Peak Temp, °C	Time of Peak, Yr	Peak Temp, °C	Time of Peak, Yr	Peak Temp, °C	Time of Peak, Yr	Peak Temp, °C	Time of Peak, Yr
Granite	UOX4-SNFA	4	0.83	165.8	35	100.7	87	73.0	172	58.7	389
	UOX1-SNFA	1	0.64	64.2	31	46.8	83	39.4	166	35.6	351
	MOX4-SNFA	4	0.83	481.2	69	384.9	154	326.5	229	263.4	389
	MOX1-SNFA	1	0.64	146.0	63	120.3	146	104.9	229	88.2	372
	Co-Extraction	1	0.76	279.9	26	126.0	69	64.9	126	43.4	372
	New Extraction	1	0.76	205.2	24	92.7	67	47.9	118	29.6	217
	EC-Ceramic	1	0.76	88.3	28	51.4	67	34.9	117	28.2	217
	EC-Metal	1	0.76	65.5	17	39.7	64	31.2	115	27.9	215
Clay	UOX4-SNFA	4	1.32	146.0	27	88.9	80	65.8	201	55.5	477
	UOX1-SNFA	1	1.13	59.1	24	43.7	76	37.4	186	34.7	452
	MOX4-SNFA	4	1.32	406.5	76	335.8	211	291.0	299	239.7	477
	MOX1-SNFA	1	1.13	126.2	69	106.9	201	95.2	299	81.9	461
	Co-Extraction	1	0.37	477.9	15	197.3	59	89.5	111	52.3	447
	New Extraction	1	0.37	354.9	13	141.1	57	62.9	108	31.1	208
	EC-Ceramic	1	0.37	133.5	17	69.0	57	40.4	108	28.8	208
	EC-Metal	1	0.37	105.0	13	50.8	55	34.6	106	28.2	206
Salt	UOX4-SNFA	4	4.00	69.8	44	50.3	95	41.9	176	37.3	351
	UOX1-SNFA	1	4.00	38.1	44	33.2	95	31.1	176	30.0	403
	MOX4-SNFA	4	4.00	170.3	79	140.3	161	121.8	240	101.5	390
	MOX1-SNFA	1	4.00	63.2	79	55.7	161	51.1	240	46.0	390
	Co-Extraction	1	4.00	99.6	36	56.1	80	38.6	139	32.4	405
	New Extraction	1	4.00	77.9	35	46.2	76	33.4	128	28.1	230
	EC-Ceramic	1	4.00	45.0	38	34.4	76	29.6	128	27.7	229
	EC-Metal	1	4.00	36.9	32	30.7	77	28.5	127	27.6	229
Deep Borehole	UOX-SNFA	1	0.19	183.7	13	160.7	55	151.1	107	145.9	214
	MOX-SNFA	1	0.19	257.6	16	219.5	59	199.5	113	182.3	218
	Co-Extraction	0.291	0.20	238.2	13	176.0	54	152.9	105	143.8	210
	New Extraction	0.291	0.20	212.5	12	164.2	54	147.5	104	140.8	204
	EC-Ceramic	0.291	0.20	162.7	14	148.9	54	142.8	104	140.3	204
	EC-Metal	0.291	0.20	157.6	12	145.2	53	141.6	103	140.2	204

Notes:

(1) The heat source is a waste package with 4 neighboring waste packages on each end of the finite line (WP) with 4 neighboring lines on each side of the WP line.

(2) Deep borehole canisters (co-extraction, new extraction, EC-Ceramic, EC-Metal) are narrower (and thus have less heat) than the standard canisters used for the other three media.

(3) All times are years out of reactor (rather than time after reprocessing or time after emplacement).

5.2.2 WASTE PACKAGE AND EBS PEAK TEMPERATURE

The waste package surface and EBS transient temperatures were calculated using the quasi steady-state approach. At each point in time, the steady-state heterogeneous model, described in Section G.4, was used to calculate the waste package surface temperature, assuming the rock temperature at the calculation radius and the package heat load as boundary conditions. Figure 5.2-5 (example) and Appendix H, Section 4, document the waste package surface transient temperature for the different host rocks and waste forms.

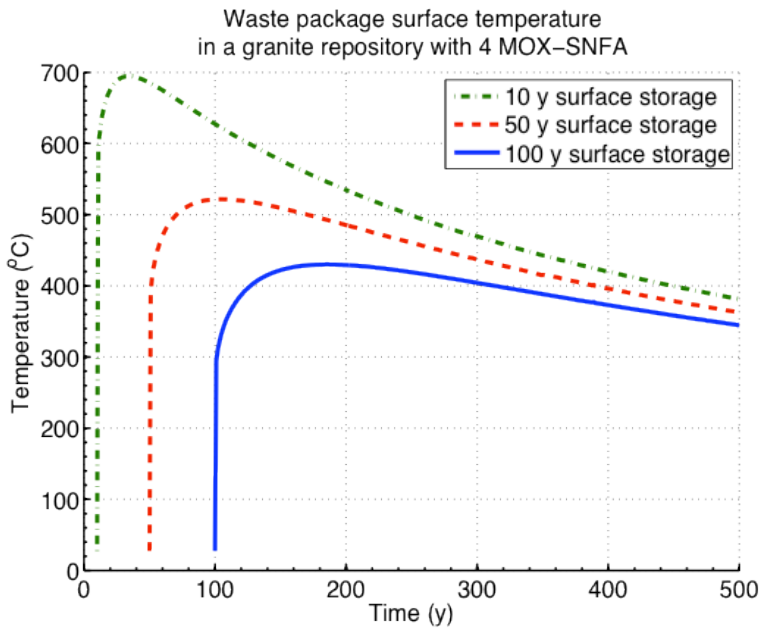

Figure 5.2-5 Calculated waste package temperature after storage times of 10, 50 and 100 years for 4 MOX assemblies per canister in granite

The following temperature limits were applied at the interface between the waste package surface and the EBS (or rock wall, depending on design):

- Granite: 100°C. This is based on a bentonite layer near the waste package surface
- Clay: 100°C. This is based on the host rock for the HLW cases, and on a bentonite layer for the UOX and MOX cases
- Salt: 200°C. This is based on the bulk salt
- A limit for deep borehole remains to be determined.

These temperature limits are not final, and may be lower than the limits that will eventually be set after site investigations and in license applications. Table 5.2-2 shows the peak temperature at the package surface for granite, clay, and deep borehole (salt is presented in Section 5.2.3).

For this granite repository design a bentonite buffer results in the waste package temperature peak being much hotter than the granite wall peak temperature. Key results from the Table 5.2-2, for granite, include:

- Waste packages loaded with a single MOX assembly require more than 200 years surface storage in order to comply with the thermal limits
- Four-assembly UOX waste packages require about 100 years of surface storage
- One-assembly UOX waste packages require somewhat more than 10 years of surface storage
- Co-extraction and new extraction require between 50 and 100 years of surface storage

- EC-C and EC-M require less than 50 years of surface storage.

Table 5.2-2: Waste package surface temperature at time of peak host rock temperature occurs in the host rock

Disposal Scenarios			Storage Time, Yr							
			10		50		100		200	
Geology	Waste Form	Assemblies / WP	Peak Temp, °C	Peak Time, yr	Peak Temp, °C	Peak Time, yr	Peak Temp, °C	Peak Time, yr	Peak Temp, oC	Peak Time, yr
Granite	UOX4-SNFA	4	256.9	17	141.2	65	92.8	134	68.9	299
	UOX1-SNFA	1	100.5	17	62.6	59	47.0	122	39.4	273
	MOX4-SNFA	4	694.6	35	521.7	104	430.1	186	337.1	324
	MOX1-SNFA	1	229.8	25	172.9	88	144.0	166	116.2	299
	Co-Extraction	1	521.2	12	209.9	56	93.6	108	49.8	273
	New Extraction	1	396.6	11	149.9	55	65.6	105	31.3	206
	EC-Ceramic	1	142.0	15	72.2	55	41.4	105	28.9	206
	EC-Metal	1	124.8	11	55.7	53	36.0	103	28.3	203
Clay	UOX4-SNFA	4	341.9	12	174.0	55	106.4	111	72.9	273
	UOX1-SNFA	1	127.1	11	73.5	53	52.0	107	41.0	241
	MOX4-SNFA	4	860.7	16	600.1	67	474.2	148	366.1	299
	MOX1-SNFA	1	288.6	13	203.4	64	161.8	130	126.8	273
	Co-Extraction	1	478.0	15	197.3	59	89.5	111	52.4	447
	New Extraction	1	355.0	13	141.1	57	62.9	108	31.1	208
	EC-Ceramic	1	133.6	17	69.1	57	40.4	108	28.8	208
	EC-Metal	1	105.0	13	50.8	55	34.6	106	28.2	206
Deep Borehole	UOX-SNFA	1	186.4	13	161.9	55	151.7	107	146.3	214
	MOX-SNFA	1	264.5	16	224.1	59	202.9	112	184.7	217
	Co-Extraction	0.291	250.8	12	180.5	54	154.5	104	144.2	209
	New Extraction	0.291	222.1	12	167.2	54	148.5	104	140.9	204
	EC-Ceramic	0.291	165.6	13	150.0	54	143.1	104	140.3	203
	EC-Metal	0.291	160.4	12	146.0	53	141.8	103	140.2	203

Notes:

(1) Derived from steady state calculation of EBS components between waste package and host rock.

(2) See Notes 2 and 3 of Table 5.2-1.

For the UOX and MOX waste forms, the clay repository design has a thick bentonite buffer that results in the waste package temperature peak being much hotter than the rock wall peak temperature. For HLW, the clay repository design does not use a bentonite buffer. Key results from the Table 5.2-2, for clay, include:

- Waste packages loaded with a single MOX assembly require more than 200 years surface storage in order to comply with the thermal limits.
- Four-assembly UOX waste packages require just over 100 years of surface storage
- One-assembly UOX waste packages require between 10 and 50 years of surface storage
- Co-extraction and new extraction require between 50 and 100 years of surface storage
- EC-ceramic requires between 10 and 50 years, and EC-M requires approximately 10 years, of surface storage.

For the deep borehole repository design, water will fill the space between the borehole casing and the waste package. The borehole size, rather than a potential thermal limit, will likely drive the repository design. Also, no temperature limit has been set for components of the deep borehole design, at this time. The borehole size limits the UOX and MOX waste forms to one assembly per waste package, with rod consolidation. For HLW canisters, the borehole diameter limits the canister cross-

sectional area to 29.1% of that of a standard (2 ft diameter) canister. Key results from the Table 5.2-2, for deep boreholes, include:

- For a 300°C temperature limit, all the waste types could be emplaced with less than 10 years of surface storage.
- For a 200°C temperature limit, all the waste types except MOX could be emplaced with less than 50 years of surface storage. MOX would require between 100 and 200 years of surface storage.

UOX and MOX packages in a clay repository are surrounded by a carbon steel envelope placed outside the bentonite buffer zone (Figure 5.1-4). Table 5.2-3 shows the temperature at this interface. With four assemblies, MOX does not meet the constraint within 200 years, and UOX requires between 10 and 50 years.

Table 5.2-3: Temperature at the interface between EBS components in a clay - MOX/UOX case at the time the peak temperature occurs in the host rock at the calculation radius

Disposal Scenario: Clay UOX/MOX			Storage Time, Yr			
			10	50	100	200
EBS Components	**Waste Form**	**Assemblies / WP**	**Peak Temp, °C**	**Peak Temp, °C**	**Peak Temp, °C**	**Peak Temp, °C**
T @ carbon steel envelope (outside the buffer)	UOX4-SNFA	4	146.0	88.9	65.8	55.5
	UOX1-SNFA	1	59.1	43.7	37.4	34.7
	MOX4-SNFA	4	406.6	335.8	291.0	239.7
	MOX1-SNFA	1	126.3	106.9	95.2	82.0

Notes:

(1) Host rock temperature and waste package temperature shown in Table 5.2-1 and 5.2-2 respectively.

(2) See notes 1 and 2 under Table 5.2-2.

A liner is utilized in case of deep boreholes (Figure 5.1-6). The peak temperature at the interface with the water inside the liner is documented in Table 5.2-4. These temperatures are within several degrees of the waste package surface temperatures shown in Table 5.2-2.

Table 5.2-4: Temperature at interface between EBS components in a deep borehole repository at the time the peak temperature occurs in the host rock

Disposal Scenario: Deep Borehole			Storage Time, Yr			
			10	50	100	200
EBS Component	**Waste Form**	**Assemblies / WP**	**Peak Temp, °C**	**Peak Temp, °C**	**Peak Temp, °C**	**Peak Temp, °C**
T @ buffer (water) / liner (steel) interface	UOX-SNFA	1	183.7	160.7	151.1	145.9
	MOX-SNFA	1	257.7	219.6	199.6	182.3
	Co-Extraction	0.291	238.2	176.0	152.9	143.8
	New Extraction	0.291	212.6	164.2	147.6	140.8
	EC-Ceramic	0.291	162.7	148.9	142.8	140.3
	EC-Metal	0.291	157.6	145.2	141.6	140.5

Notes:

(1) Host rock temperature and waste package temperature shown in Table 5.2-1 and 5.2-2.

(2) See notes 1 and 2 under Table 5.2-2.

5.2.3 WASTE PACKAGE SURFACE PEAK TEMPERATURE FOR SALT

The analytic heterogeneous model calculates the temperature distribution from the calculation radius in the rock (4 m in salt) inward to the outer radius of the waste package. At the time of emplacement, part of the salt around the package is crushed and has properties, in particular thermal conductivity, significantly different from intact salt. Consequently, three different assumptions have been evaluated for the properties of the salt in this region:

(1) all intact salt;
(2) crushed salt from the package surface out to 3.05 m radius (totally surrounding the waste package in the calculation) and intact salt to 4 m radius. No credit is taken for consolidation of the crushed salt after emplacement, which is conservative;
(3) all intact salt, but with the package-salt contact limited to 75% of the available surface. This 75% of the area contacts the back wall and floor of the emplacement alcove, with contact resistance reduced by shaping that back edge of the repository to conform to a waste package cylinder. The other 25% of the surface area is within the alcove, and has crushed salt. No heat transfer credit is taken in this quadrant, which is conservative because the alcove will slowly collapse onto the backfill (over 5-10 years) and then the backfill will consolidate and its thermal conductivity will evolve toward that of intact salt.

Because crushed salt thermal conductivity (0.57 W/m-K) is much lower than that of intact salt (4.2 W/m-K), the temperature rise for the second model is very large, resulting in results so conservative that they are not of much use (note the log scale on the Figure 5.2-6). The third model limits heat transfer to three quadrants of the circumference of the waste package; the result is a temperature rise of less than 50°C above the non-conservative intact salt case (the first model) are therefore useful. For the third model (75% contact), the 200°C thermal limit at the WP surface contact with the salt is met for all waste forms (including 4 MOX assemblies) considered, within 100 years of storage time (Table 5.2-5).

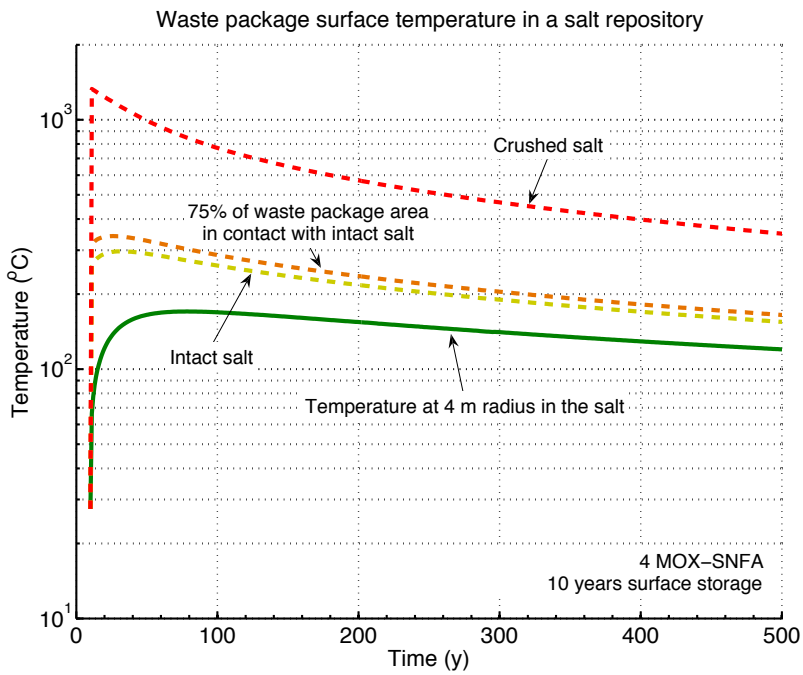

Figure 5.2-4 Calculated waste package temperature after 10 years storage time for 4 MOX assemblies per canister in salt assuming the waste package is in contact with crushed salt or intact salt, either fully or for 75% of its area

Table 5.2-5: Waste package peak surface temperature in a salt repository with the temperature based on a steady-state calculation inward from the 4 m rock calculation radius at each time step of the homogeneous transient calculation

Disposal Scenario: Salt, WP temperature			Storage Time, Yr							
			10		50		100		200	
Model	**Waste Form**	**Assemblies / WP**	**Peak Temp, °C**	**Peak Time, yr**	**Peak Temp, °C**	**Peak Time, yr**	**Peak Temp, °C**	**Peak Time, yr**	**Peak Temp, °C**	**Peak Time, yr**
Intact salt	UOX4-SNFA	4	120.4	17	73.5	65	53.8	129	43.6	277
	UOX1-SNFA	1	55.3	13	40.9	61	35.0	123	32.0	266
	MOX4-SNFA	4	296.9	32	224.3	93	185.8	165	147.6	299
	MOX1-SNFA	1	105.3	27	83.3	84	71.9	156	60.9	288
	Co-Extraction	1	230	12	102.2	56	54.5	108	36.4	252
	New Extraction	1	179.6	11	77.7	55	43.1	105	29.1	205
	EC-Ceramic	1	74.4	15	45.8	55	33.2	105	28.1	204
	EC-Metal	1	69.2	11	39.5	52	31.1	103	27.9	202
Crushed salt to 3.048 m (all times)	UOX4-SNFA	4	534.4	11	256.4	51	147.2	101	89.3	208
	UOX1-SNFA	1	191.7	11	101.7	51	66.3	101	47.4	204
	MOX4-SNFA	4	1329.7	11	874.7	52	649.9	106	466.6	215
	MOX1-SNFA	1	449.3	11	301.6	51	228.0	103	167.9	210
	Co-Extraction	1	1217.1	11	449.5	51	177.1	101	68.8	202
	New Extraction	1	921.2	11	312.2	51	116.0	101	36.3	201
	EC-Ceramic	1	296.2	11	131.4	51	59.9	101	30.6	201
	EC-Metal	1	281.9	11	100.5	51	49.5	101	29.6	201
75% contact with intact salt, 25% crushed salt	UOX4-SNFA	4	139.9	13	81.8	61	57.9	122	45.7	267
	UOX1-SNFA	1	62.1	11	43.8	57	36.4	117	32.7	255
	MOX4-SNFA	4	341.8	26	252.8	84	206.4	156	162.2	284
	MOX1-SNFA	1	120.8	21	93.1	76	79.0	144	65.9	273
	Co-Extraction	1	281.5	11	119.1	54	60.4	105	37.8	236
	New Extraction	1	218.4	11	89.2	53	46.7	103	29.4	204
	EC-Ceramic	1	85.3	13	50.0	53	34.5	103	28.2	204
	EC-Metal	1	80.3	11	42.6	51	32.1	102	27.9	202

Notes:

(1) Salt consolidation at high temperature is expected to change the regions of crushed salt to intact salt on the order of 5-10 years and therefore these temperatures a crushed salt scenario are an overestimate. Actual values will be between this case and that for intact salt.

(2) See notes 1 and 2 under Table 5.2-2.

5.2.4 Peak Temperature at Compliance Locations as a Function of Storage Time and Waste Package Capacity

The temperature at the calculation radius was examined for each geologic media, as described in Section 5.2.2. An additional parametric study was done for UOX and MOX in the selected granite, clay, and salt repository layout design to determine the peak temperature at the "compliance" location as a function of the number of assemblies per waste package and the surface storage time. The compliance locations correspond to the lowest thermal limit of any of the host rock or EBS components. For example, in granite, the host rock can accommodate temperatures well above boiling, but the bentonite buffer placed between the waste package and the rock wall has a thermal limit (in this study) of 100°C. Therefore, the compliance location becomes the bentonite buffer material.

Five options were considered: 1, 2, 3, 4 and 12 assemblies per package. With 2, 3, and 4 assemblies, the package size was kept constant (the size of 4 assemblies, with one or two slots not used for the 3- and 2-assembly packages, see Section 5.1.3). For 1 and 12 assemblies the engineering barrier thicknesses were kept the same as in the reference model, while the waste form radius was appropriately adjusted. The 1-assembly-package inner radius was assumed to be one-half of that of the 4-assembly-package. The 12-assembly-package radius was set as in OCRWM, 2001. The storage time was varied between 10 years and 300 years. Peak temperatures for all media and fuel forms are illustrated in Appendix H, Section 5.

The minimum storage time required to comply with the temperature limits was determined by interpolating the peak temperature data above. The results are shown in Figure 5.2-7 for UOX. In granite and clay, about 100 years of surface storage are sufficient to comply with the thermal limits for up to 4 UOX assemblies per package. In salt, which has higher thermal conductivity, only 5 years (the minimum time considered in this analysis) are needed. For a 12 UOX assembly package, salt meets the constraints in about 50 years; whereas more than 300 years are required for granite and clay. The results for MOX are shown in Figure 5.2-8. In granite and clay, the 1-assembly MOX package complies with the thermal constraints within 300 to 350 years. For salt, four MOX assemblies per package require approximately 100 years of surface storage.

For those geologic medium / waste form combinations with significant contributions to peak temperature from neighboring waste packages, lower the amount of storage time needed or increase the number of assemblies per package by increasing the waste package or drift spacing, therefore increasing repository footprint. Conversely, for combinations with no significant contributions to the peak temperature from the neighboring waste packages, the waste package spacing and drift spacing may be decreased forming a more compact layout. Future studies will include the effect of varying the waste package and drift spacing.

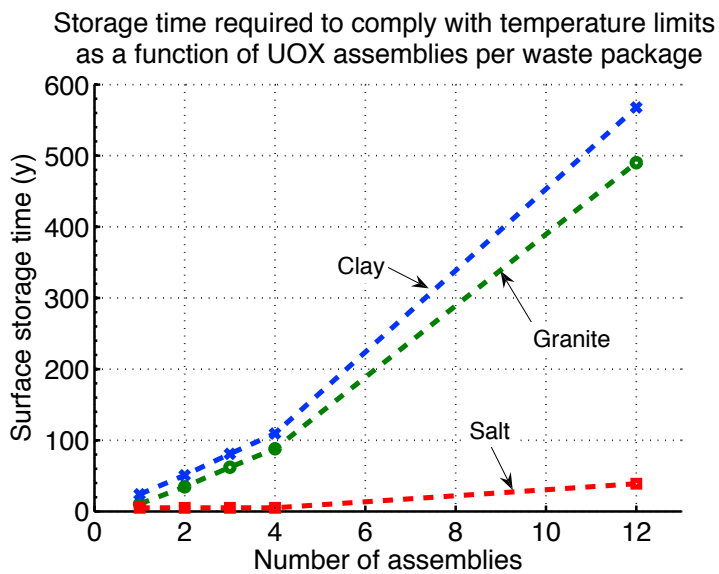

Figure 5.2-7 Minimum surface storage time necessary to comply with waste package surface temperature limit as function of UOX assemblies per waste package in a granite, clay, and salt repository (with 75% of the waste package surface contacting intact salt)

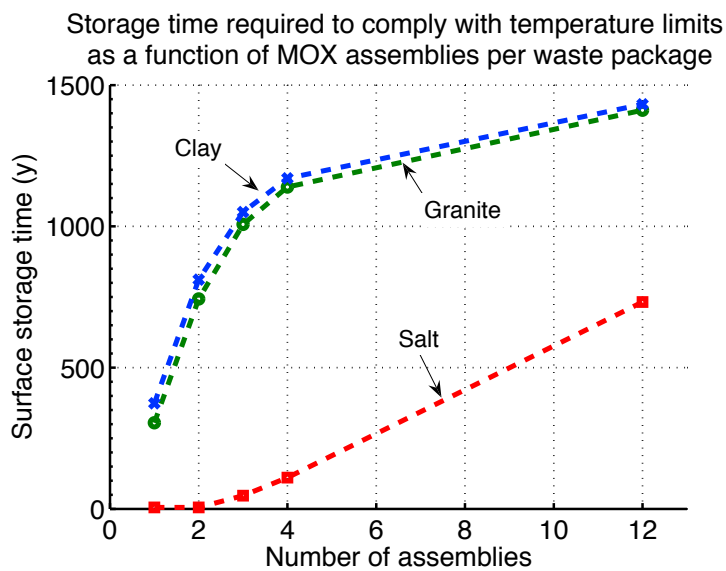

Figure 5.2-8 Minimum surface storage time necessary to comply with waste package surface temperature limit as function of MOX assemblies per waste package in a granite, clay, and salt repository (with 75% of the waste package surface contacting intact salt)

6. SUMMARY AND RECOMMENDATIONS

This section will be written by a partnering National Laboratory.

6.1 SUMMARY

This section will be written by a partnering National Laboratory. The following is the LLNL portion of this section, which summarizes the work in Section 5.

The various layers of material from the waste package (such as components of the engineered barrier system and the host rock surface) to a given distance within the rock wall at a given distance can be described as concentric circles with varying thermal properties (see Figure 5.1-1).

The selected model approach examines the contributions of the waste package, axial waste package neighbors and lateral neighboring emplacement drifts (see Section 5.2.1 and Appendix H, Section 2). In clay and deep borehole media, the peak temperature is driven by the central waste package whereas, in granite and salt, the contribution to the temperature rise by adjacent (lateral) waste packages in drift or emplacement borehole lines is dominant at the time of the peak temperature.

Mathematical models generated using Mathcad software provide insight into the effects of changing waste package spacing for six waste forms, namely UOX, MOX, co-extraction, new extraction, E-Chem ceramic and E-Chem metal in four different geologic media (granite, clay, salt and deep borehole). Each scenario includes thermal conductivity and diffusivity for each layer between the waste package and the host rock, dimensions of representative repository designs (such as waste package spacing, drift or emplacement borehole spacing, waste package dimensions and layer thickness), and decay heat curves generated from knowledge of the contents of a given waste form after 10, 50, 100 and 200 years of surface storage.

Key results generated for each scenario include rock temperature at a given time calculated at a given radius from the central waste package (Section 5.2.1 and Appendix H, Section 3), the corresponding temperature at the interface of the waste package and EBS material, and at each EBS layer in between (Section 5.2.2 and Appendix H, Section 4). This information is vital to understand the implications of repository design (waste package capacity, surface storage time, waste package spacing, and emplacement drift or borehole spacing) by comparing the peak temperature to the thermal limits of the concentric layers surrounding the waste package; specifically 100°C for the bentonite buffer in granite and clay repositories, 100°C for rock wall in a clay repository and 200°C at the rock wall for a salt repository. These thermal limits are both preliminary and approximate, and serve as a means to evaluate design options rather than determining compliance for licensing situations.

The thermal behavior of a salt repository is more difficult to model because it is not a concentric geometry and because the crushed salt backfill initially has a much higher thermal resistance than intact salt. Three models were investigated, namely

a waste package in complete contact with crushed salt, secondly a waste package in contact with intact salt, and thirdly a waste package in contact with 75% intact and 25% crushed salt. The latter model best depicts emplacement of a waste package in the corner of an intact salt alcove and subsequently covered with crushed salt backfill to the angle of repose. The most conservative model (crushed salt) had temperatures much higher than the other models and although bounding, is too conservative to use. The most realistic model (75/25) had only a small temperature difference from the simplest (non-conservative, intact salt) model, and is the one chosen in this report (see Section 5.2.3).

A trade-study investigating three key variables (surface storage time, waste package capacity and waste package spacing) is important to understand and design a repository. Waste package heat can be reduced by storing for longer periods prior to emplacement, or by reducing the number of assemblies or canisters within that waste package. Waste package spacing can be altered to optimize the thermal load without exceeding the thermal limits of the host rock or EBS components. By examining each of these variables, repository footprint (and therefore cost) can be optimized. For this report, the layout was fixed for each geologic medium based on prior published designs in the international community, but it will be varied in future work. Section 5.2.4 summarizes the conclusions based on varying two of the three parameters (storage time and waste package capacity), and the results are shown in Appendix H, Sections 5 and 6).

6.2 FUTURE WORK

Work will continue in FY11 and FY12 on the following improvements and developments to the models for the thermal analysis for disposition of six waste forms in four geologic media:

- Additional mathematical models assessing the storage time and number of assemblies in waste packages will be run, with different repository layouts, to provide insight into the most effective manner of waste disposition. This will provide input to aid designers and decision makers in the assessment of how long each waste form should be stored before emplacement in each medium and balancing that with repository footprint.
- Evaluate additional mathematical models for fully coupled multi-layer transient calculations in place of the current combination of a transient model in the host rock coupled with a quasi-steady state model calculation within the EBS.
- Application of TOPAZ3D modeling for:
    - Validating the analytic model results in this report
    - Exploration of the evolution of salt temperature, considering non-cylindrical geometry, backfill consolidation, and early transient behavior.
    - Comparison of analytic results from this report and generic salt repository study results.

- Benchmark both the analytical models and the TOPAZ3D models against the 2D and 3D salt repository calculations in Clayton and Gable 2009.
- Address variations and uncertainties in the model inputs, including those associated with host rock properties, EBS component properties, and design parameters.

7 REFERENCES

Andra 2005, Dossier 2005 Granite–Safety Analysis of a Geological Repository," Andra Report, December 2005

Brady et al. 2009, Deep Borehole Disposal of High-Level Radioactive Waste, SNL Report, SAND 2009-4401, August 2009

Carslaw H. S. and Jaeger, J.C. Conduction of Heat in Solids, 2nd Edition, Clarendon Press, Oxford, 1959

Clayton and Gable 2009, AFCI-WAST-PMO-MI-DV-2009-000002, D. J. Clayton, and C. W. Gable, 3-D Thermal Analyses of High-Level Waste Emplaced in a Generic Salt Repository, February 2009

Fetter, C.W. Applied Hydrogeology. Third Edition. 1994. Page 281

Jia et al 2009, Y. Jia, H.B. Bian, G. Duveau, K. Su, J.F. Shao, "Numerical modelling of in situ behaviour of the Callovo–Oxfordian argillite subjected to the thermal loading," Engineering Geology, 109 (2009) 262–272

Kreith, F. Principles of Heat Transfer, Second Edition, 1966

OCRWM 2000, YMP analysis Natural Resources Assessment. ANL-NBS-GS-000001 Rev 00. MOL.20010406.0010

OCRWM 2001, Waste Package Outer Barrier Stress Due to Thermal Expansion with Various Barrier Gap Sizes. CAL-EBS-ME-000011 REV 00

Ondraf-Niras 2010, The Joint EC/NEA Engineered Barrier System Project: Synthesis Report (EBSSYN), EUR 24232 EN, 2010

NAGRA 2003, Technical Report 02-11, Canister Options for the Disposal of Spent Fuel, NAGRA Report, April 2003

SNL 2007, MDL-EBS-MD-000001 REV 00 AD 01 - In-Drift Natural Convection and Condensation, YMP Accession Number: DOC.20070907.0004, 2007

SNL 2008, ANL-NBS-HS-000057 REV 00 - Postclosure Analysis of the Range of Design Thermal Loadings, YMP Accession Number: DOC.20080121.0002, January 2008

SNL 2009, "Deep Borehole Disposal of High-Level Radioactive Waste," SAND-2009-4401, 2009

SNRL 2011, A Generic Salt Repository for Disposal of Waste from a Spent Nuclear Fuel Recycle Facility, SRNL-RP-2011-00149 PREDECISIONAL DRAFT Rev 0 January 2011

Sutton, M., Blink, J.A., Greenberg, H.R. and Halsey, W.G. Disposal System Evaluation Framework (DSEF) Version 1.0 - Progress Report, LLNL-TR-484011, May 2011

~

Appendix A through Appendix F will be written by a partnering National Laboratory. Appendix G and Appendix H in this report will be incorporated into the parent document being written by Sandia National Laboratory.

APPENDIX G

MATHEMATICAL MODELS

There are two mathematical/computational modeling methods that can be applied to the geometry described in Section 5.1. The first is based on analytical models, and the second type is a finite element model implemented in a code such as TOPAZ3D. The analysis presented in this report is limited to analytical models implemented in Mathcad 15, Microsoft Excel 2007, and MatLab. Detailed TOPAZ3D models will be run to validate the analytical models in late FY11 and FY12. Additional analytical model calculations will also be conducted, for other axial and lateral WP spacing. In addition, future analytical model calculations will further address variation of material properties (particularly of crushed salt backfill) with time, temperature, and moisture content.

G.1 INTRODUCTION

Section G.2 describes the input variables, Section G.3 describes the transient analytic model in the host rock, and Section G.4 describes the steady state multi-layer analytical model that determines the temperatures at the surface of each of the internal EBS barriers, ending at the surface of the waste package. Section G.5 describes model limitations and potential future considerations.

The transient model described in Section G.3 (referred to here as the "external calculation") is in a homogeneous medium (i.e., the EBS is assumed to have the properties of the geologic medium). The homogeneity permits use of superposed analytic solutions for point, infinite line, and finite line sources that in combination represent the repository layout. The "calculation radius" for the external calculation is generally at the interface between the EBS and the geologic medium, although, for salt, it was placed somewhat further from the WP centerline due to the non-concentric geometry of backfilled salt alcoves.

The temperature histories within the EBS (referred to here as the "internal calculation") are derived from the waste package line load heat source, using the time-dependent results of the external calculation. The internal calculation is steady-state at each point in time, which is equivalent to assuming that the heat flow through the calculation radius at any given time is nearly equal to the heat generation in the waste at that time. This is a reasonable assumption except at the very early times in which the EBS temperatures are changing rapidly due to the change in boundary condition after emplacement. This calculation is conservative in the sense that the steady-state model is a one-dimensional model that effectively assumes an infinite line source with the waste package internal line loading.

G.2 Variables Used in the Analytical Models

The input variables in the analytical models are in the form of several vectors and matrices of data, keyed to two index values. The index WF varies from 1 to 6 and represents the waste forms (UOX, co-extraction, MOX, new extraction, E-Chem ceramic, and E-Chem metal), and the index RT varies from 1 to 4 and represents rock types (granite, clay, salt, and deep borehole) of the repository host rock. As previously stated in Section 5, co-extraction and new-extraction cannot be directly compared to AREVA's COEX and Energy Solutions' NUEX industrial processes, respectively.

For each repository design combination of rock type and waste form, there are specified Engineered Barriers System (EBS) radii, as discussed in Section 5.1. In the transient analytical model in the host rock, only the calculation radius and axial and lateral WP spacing are included from the geometry data. The radial dimensions of the EBS components are used in the internal steady state analytical model that starts at the "calculation radius" and extends to the surface of the waste package.

G.2.1 Host Rock Property Data

The host rock properties consist of a single homogenous set of properties representing an isotropic infinite medium, with the properties assumed at 100°C to approximate the situation after waste emplacement. Ambient rock temperatures at depth differ from this assumption, but variations of rock properties with time and temperature are intended to be addressed later in the TOPAZ3D models as discussed above in Section G.2. The properties given for salt, for example, represent intact salt used in the transient model. The properties of crushed salt backfill are utilized in the quasi-steady-state model of the EBS, and are listed under EBS Material Property Data discussed in Section G.2.2.

The thermal conductivity (W/m-K) is designated K_{th}, and α is the thermal diffusivity (m^2/s):

HOST ROCK PROPERTY DATA

$$Rock_type := \begin{pmatrix} \text{"Granite"} \\ \text{"Clay"} \\ \text{"Salt"} \\ \text{"Deep Borehole"} \end{pmatrix} \qquad Kth := \begin{pmatrix} 2.5 \\ 1.75 \\ 4.2 \\ 3.0 \end{pmatrix} \cdot \frac{W}{m \cdot K} \qquad \alpha := \begin{pmatrix} 1.13 \cdot 10^{-6} \\ 6.45 \cdot 10^{-7} \\ 2.07 \cdot 10^{-6} \\ 1.38 \cdot 10^{-6} \end{pmatrix} \cdot \frac{m^2}{s}$$

G.2.2 Repository Reference Design Data

Figures 5.1-3 through 5.1-6 show the EBS design data. The " calculation radius" is 4.0 m for salt, and is the largest EBS dimension for the other three geologic media. The other variables considered in the analytical model include waste package length, emplacement drift spacing, and waste package spacing within each emplacement drift.

Waste Package Length:

SELECT WASTE FORM INPUT DATA

$$WF_name := \begin{pmatrix} \text{"UOX"} \\ \text{"COEX"} \\ \text{"MOX"} \\ \text{"New_Ext"} \\ \text{"E_CHEM_C"} \\ \text{"E_CHEM_M"} \end{pmatrix} \quad WF_type := \begin{pmatrix} \text{"Assembly"} \\ \text{"Canister"} \\ \text{"Assembly"} \\ \text{"Canister"} \\ \text{"Canister"} \\ \text{"Canister"} \end{pmatrix} \quad WP_length := \begin{pmatrix} 5 \\ 4.572 \\ 5 \\ 4.572 \\ 4.572 \\ 3.048 \end{pmatrix} \cdot m$$

Emplacement Drift Radius ("Calculation Radius"):

The calculation radius is the host rock surface interface with the EBS, and it varies by both waste form (the rows in the matrix below) and rock type (the columns in the matrix). The radius of the deep borehole design is based on the maximum feasible drill casing. The columns of the matrix are the four media (granite, clay, salt, and deep borehole), and the rows are the six waste forms (UOX, co-extraction, MOX, new extraction, EC-C, and EC-M).

The calculation radius also varies with the number of assemblies assumed per waste package. The 4-assembly (UOX or MOX) waste package can also be used with spacers to hold 2, 3 or 4 assemblies, and the calculation radius in the matrix below is consistent with the 4-assembly waste package design. The same model was used with different inputs for the 1-assembly and 12-assembly waste package designs to evaluate sensitivity of the results as a function of the number of assemblies.

$$drift_r := \begin{pmatrix} 0.83 & 1.321 & 4 & 0.188 \\ 0.755 & 0.370 & 4 & 0.198 \\ 0.83 & 1.321 & 4 & 0.188 \\ 0.755 & 0.370 & 4 & 0.198 \\ 0.755 & 0.370 & 4 & 0.198 \\ 0.755 & 0.370 & 4 & 0.198 \end{pmatrix} \cdot m$$

Repository Design – Lateral Spacing, Axial Spacing and Depth:

Lateral spacing (in the "x" direction) is comparable to center-to-center borehole or drift spacing, which is conceptually comparable to the emplacement drift spacing in the Yucca Mountain repository design concept. Axial spacing (in the "y" direction) is comparable to the waste package center-to-center spacing within a given emplacement borehole, series of alcoves, or drift.

Depth is self-explanatory. The depth of the granite, clay, and salt repository reference designs was assumed to be 500 m, and the depth of the deep borehole design was assumed to be 5,000 m. The models assume a geothermal temperature gradient of 25°C per 1,000 m depth (Brady et al 2009 (page 22); Fetter 1994 (page

281); and OCRWM 2000 (page 89)), resulting in different ambient temperatures in the host rock with depth. These input variables are all keyed to the rock type index (granite, clay, salt, and deep borehole).

$$Drift_spacing := \begin{pmatrix} 20 \\ 30 \\ 20 \\ 200 \end{pmatrix} \cdot m \qquad WP_space_SNF := \begin{pmatrix} 10 \\ 10 \\ 20 \\ 6 \end{pmatrix} \cdot m \qquad WP_space_HLW := \begin{pmatrix} 10 \\ 6 \\ 20 \\ 6 \end{pmatrix} \cdot m$$

Repository Design – EBS Component Data:

The selection of the particular reference design configurations is discussed in Section 5.1. In the steady-state internal model calculation, all of the EBS components are assumed to be concentric cylindrical shells, as shown in Figure 5.1-1.

The specific inputs required for the internal calculation are documented in Figures 5.1-3 to 5.1-6, and they include the material type of each EBS component, inner and outer radius of each component, and the thermal conductivity of the material.

G.2.3 Waste Form Count

The time-dependent decay heat data discussed in Section 5.1.3 is per SNF assembly or HLW canister basis, and is multiplied by the waste form count (WF_count) to obtain the heat source per waste package.

The waste form count for the deep borehole reference repository is based on the fixed maximum diameter of the drill casing. For the SNF waste forms, rod consolidation is assumed, enabling a single assembly to fit within the narrow borehole diameter (WF_count = 1). For the HLW waste forms, the length of the canister is assumed to be the same as a single canister (based on manufacturing constraints), but the diameter is limited by the drill casing, which results in less than 30% of the inventory and heat per canister in the deep borehole design, as compared to the other three geologic media (WF_count = dbh_cnt).

The parameter dbh_cnt = 0.291 for the ratio of the small canister internal cross-sectional area divided by the standard HLW canister area. The input matrix below shows the waste form count of 4 assemblies in granite, clay, and salt, and is adjusted accordingly for cases evaluating 1-assembly and 12-assembly waste package in parametric study cases.

$$WF_count := \begin{pmatrix} 4 & 4 & 4 & 1 \\ 1 & 1 & 1 & dbh_cnt \\ 4 & 4 & 4 & 1 \\ 1 & 1 & 1 & dbh_cnt \\ 1 & 1 & 1 & dbh_cnt \\ 1 & 1 & 1 & dbh_cnt \end{pmatrix}$$

G.2.4 The Effects of Surface Storage

Surface storage times of 10, 50, 100, and 200 years were evaluated for all cases analyzed, and input as a vector variable T_{store}. The model used was adapted from a Yucca Mountain model that had a ventilation efficiency during the preclosure period (V_{dur}). In the modified model, the effect of surface storage was the same as the effect of a ventilation system removing the decay heat at 100% efficiency during the surface storage period (T_{store}). This same model can also be used, in the future, to consider potential effects of surface storage followed by some limited ventilation time after emplacement, with a ventilation heat removal efficiency (V_{eff}) of less than 100%.

G.2.5 Heat Source Calculation

The analytic model incorporates three types of heat sources

- Q_{L_wp} - representing a single waste package of interest (as a finite line source), where the line load heat source internal to a single waste package is calculated. The units are W/m.
- Q_{L_avg} - representing an average line load of adjacent emplacement drifts or boreholes (as an infinite line source). The line load heat source represents an average heat load accounting for axial waste package spacing. The units are W/m.
- Q_{wp} - representing a single adjacent waste package (as a point source), where the point source heat load is the total heat source for a waste package. The units are W.

The three heat sources accounting for the effects of surface storage times are calculated as follows:

$Veff := 1.00$ Assume 100% efficiency (equivalent to surface storage), where Vdur = Tstore

$$Q_{L_wp}(t, T_{store}, wf, rt) := \frac{Q(t, wf) \cdot WF_count_{wf, rt}}{WP_length_{wf}} \cdot \left[1 - Veff \cdot (t \le T_{store})\right]$$

$$Q_{L_avg}(t, T_{store}, wf, rt) := \frac{Q(t, wf) \cdot WF_count_{wf, rt}}{WP_spacing_{rt}} \cdot \left[1 - Veff \cdot (t \le T_{store})\right]$$

$$Q_{wp}(t, T_{store}, wf, rt) := Q(t, wf)\, WF_count_{wf, rt} \cdot \left[1 - Veff \cdot (t \le T_{store})\right]$$

Where Q(t, wf) is a continuous decay heat source function for one unit (an assembly or a canister) of waste form. Q(t, wf) is evaluated in Mathcad using a cubic spline interpolation function that is a good fit through the tabular data points which are input to the model. The cubic spline interpolation is stable and provides a good fit for the time period of interest in this calculation. However, when the decay heat values become small in the very long term, the cubic spline can become unstable and result in oscillating values. Those time periods are better addressed using a linear spline interpolation function.

G.3 Host Rock Transient Temperature Analytical Model

This model assumes an infinite medium of a given rock type, where the EBS and WP are modeled as continuous rock to the central line or point source, and the rock temperature at the calculation radius is evaluated based on the rock properties and the time-dependent heat source.

This model consists of three components that sum together to represent the repository design. They include a central finite line source representing the waste package of interest, eight adjacent infinite line sources (four on each side of the central waste package) representing (laterally spaced) adjacent emplacement arrays, and eight adjacent point sources aligned axially with the central waste package finite line source (four on each side of the central waste package) representing adjacent waste packages.

The solution for the finite line source is derived from the point source solution as described in Sutton et al 2011 (Section 8.1.2), and is also documented in SNL 2007. The solution for the infinite line source is presented in Carslaw and Jaeger 1959 (Section 10.3, equation 1), and also described in Sutton et al 2011 (Section 8.1.3). The equation for the temperature transient solution for a point source is based on Carslaw and Jaeger 1959 (Section 10.4, page 261).

The one-dimensional temperature transient is the sum of the contributions from these terms as a function of radial distance and time, and is evaluated at the calculation radius (drift_r). In the current analysis, the number of adjacent lateral line sources (N_{drifts}), and the number of axially adjacent waste packages (N_{adj}) were both set equal to 4. Note that for the second and third terms, the distance is calculated to a location at the crown of the emplacement borehole or drift (see Figure 5.1-2)

$$DW_T_finite_line(t, y, T_{store}, wf, rt) := \left[\int_0^t \frac{Q_{L_wp}(\tau, T_{store}, wf, rt)}{8 \cdot (\pi \cdot Kth_{rt}) \cdot (t-\tau)} \cdot e^{\frac{-\left[(drift_r_{wf,rt})^2\right]}{4 \cdot \alpha_{rt} \cdot (t-\tau)}} \cdot \left[erf\left[\frac{1}{2} \cdot \frac{\left(y + \frac{WP_length_{wf}}{2}\right)}{\sqrt{\alpha_{rt} \cdot (t-\tau)}}\right] - erf\left[\frac{1}{2} \cdot \frac{\left(y - \frac{WP_length_{wf}}{2}\right)}{\sqrt{\alpha_{rt} \cdot (t-\tau)}}\right]\right] d\tau \right]$$

$$DW_T_drifts(t, T_{store}, wf, rt) := 2 \left[\sum_{id=1}^{N_{drifts}} \int_0^t \frac{Q_{L_avg}(\tau, T_{store}, wf, rt)}{4 \cdot (\pi \cdot Kth_{rt}) \cdot (t-\tau)} \cdot e^{\frac{-\left[(drift_r_{wf,rt})^2 + (id \cdot Drift_spacing_{rt})^2\right]}{4 \cdot \alpha_{rt} \cdot (t-\tau)}} d\tau \right]$$

$$DW_T_adjacent_pkgs(t, T_{store}, wf, rt) := 2 \left[\sum_{ip=1}^{N_{adj}} \int_0^t \frac{Q_{wp}(\tau, T_{store}, wf, rt)}{8 \cdot Kth_{rt} \cdot \sqrt{\alpha_{rt}} \cdot \pi^{1.5} \cdot (t-\tau)^{1.5}} \cdot e^{\frac{-\left[(drift_r_{wf,rt})^2 + (ip \cdot WP_spacing_{rt})^2\right]}{4 \alpha_{rt} \cdot (t-\tau)}} d\tau \right]$$

G.4 Waste Package and EBS Quasi-Steady-State Temperature Analytical Model

As described in Section 5.1, it is assumed that at any given point at time, the relatively low thermal mass of the EBS components compared to the essentially infinite geologic medium, can be considered to be at a quasi-steady state condition.

The model for a multi-layer cylindrical steady-state temperature solution is derived from Kreith 1966 (Section 2-2, equation 2-19). In this geometry, the analytical solution is a one-dimensional (radial heat flow) model assuming an infinite line as the heat source. That particular equation is an example of two concentric cylindrical components, such as a steel pipe covered by asbestos insulation with internal convection from a hot fluid (with a convection coefficient h_i), and external convection to air (with a convection coefficient h_o). It includes four thermal resistance components – two conduction only resistances representing the pipe and the insulation, and two convection boundary layer resistances (internal and external).

Total heat transfer is defined as $Q = U * A_{outside} * (T_{inside} - T_{outside})$

Where the conductance, U, is the reciprocal of the sum of the resistances:

$$U = \frac{1}{\frac{r_3}{r_1 \cdot h_i} + \frac{r_3 \ln\left(\frac{r_2}{r_1}\right)}{k_1} + \frac{r_3 \ln\left(\frac{r_3}{r_2}\right)}{k_2} + \frac{1}{h_o}}$$

Where r_3 is the outside surface of the insulation, r_2 is the outside surface of the pipe, and r_1 is the inside surface of the pipe

The heat flux per exterior unit area is defined as $q_A = Q/A_{outside}$

By conservation of energy at steady state, the temperature at the surface of each layer can be calculated as follows:

$$q_A = \frac{(T_i - T_1)}{R_i} = \frac{(T_1 - T_2)}{R_1} = \frac{(T_2 - T_3)}{R_2} = \frac{(T_3 - T_o)}{R_o}$$

Where T_i is the inside fluid temperature, T_1 is the pipe wall internal surface temperature, T_2 is the pipe wall external temperature (and the insulation internal surface temperature), T_3 is the insulation external surface temperature, and T_0 is the air temperature. This equation and the approach were input into MathCad, and validated against Kreith 1966 (example problem 2-7)

Application of this approach to the EBS components drops the convection resistance terms (i.e., $T_i = T_1$ and $T_o = T_3$) and uses a series of thermal resistance values calculated on the basis of the EBS component radii and thermal conductivities. The following equation shows the thermal resistance terms all the way to the surface of the waste form, but the calculation results documented in this report stop at the surface of the waste package.

$$U_{overall} = \frac{1}{R_{canister} + R_{waste_pkg} + R_{buffer} + R_{envelope} + R_{backfill} + R_{liner}}$$

The approach is modified somewhat to be applied to a line load (W/m) instead of an areal heat flux of (W/m^2), by substituting $q_L = q_A * 2\pi r_{outside}$. One example, for the outer surface temperature of the backfill, is the following:

$$T_{BACKFILL} = T_{DW} + \frac{q_L}{2 \cdot \pi \cdot r_{DW}} \cdot R_{LINER} \cdot = T_{DW} + \frac{q_L \cdot r_{DW} \cdot \ln\left(\frac{r_{DW}}{r_{BACKFILL}}\right)}{2 \cdot \pi \cdot r_{DW} k_{LINER}} = T_{DW} + \frac{q_L}{2 \cdot \pi \cdot k_{LINER}} \cdot \ln\left(\frac{r_{DW}}{r_{BACKFILL}}\right)$$

Where k_{LINER} is the liner thermal conductivity.

It is assumed that the EBS (except for the salt case) responds quickly (low thermal mass), and the heat flux at the calculation radius is always the same as the heat source, with a small time delay. The timing of the peak temperature at the calculation radius is more dependent on the rate the heat moves away from that surface into the infinite mass of host rock (and with the rate that heat arrives from

the other adjacent heat sources) with respect to the rate that the decay heat curve is dropping.

This process (the heat flux at the calculation radius feeding the outside calculation) would differ significantly if the EBS possessed a wide range of thermal conductivities (higher for realistic cases, and lower for substituting host rock). In fact, the primary difference is the magnitude of the thermal gradient required to force that same heat flux out of the surface at the calculation radius. The thermal gradient increases with thermal resistance, until the calculated heat flux equals the steady-state heat flux

As the thermal resistance goes up, the thermal gradient gets steeper until the calculated heat flux with the higher resistance matches the required "steady state" heat flux.

The normalized thermal resistance for each layer associated with the calculations for SNF and HLW in the four geologic media are shown in Figure G.4-1, below.

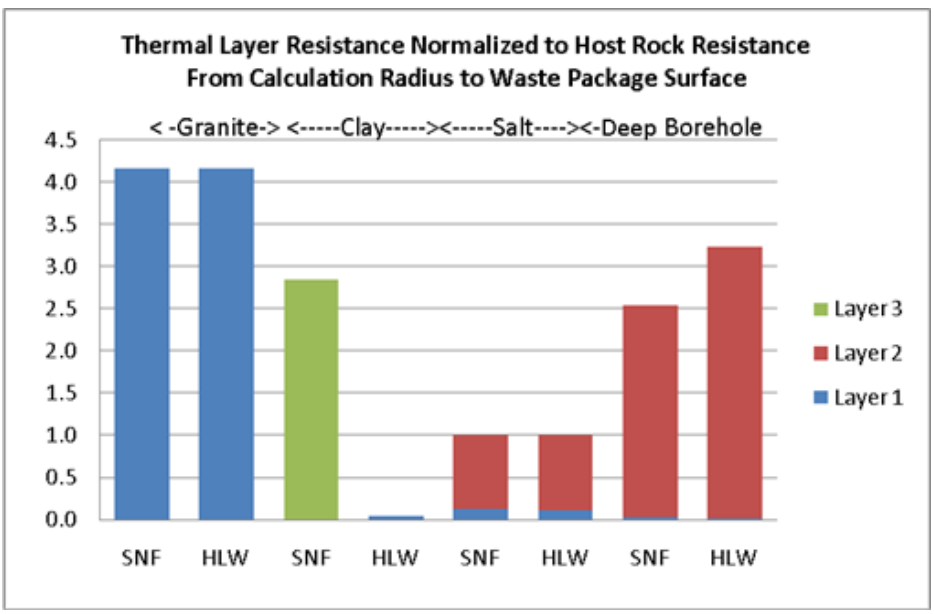

Figure G.4-1 Normalized thermal resistance of each EBS layer

G.5 Model Limitations and Potential Future Model Improvements

The current set of analytical models assumes constant thermal properties for the host rock, and some of the thermal properties, such as thermal conductivity and thermal diffusivity are functions of temperature, porosity, or moisture content that can vary over time. This has not been addressed, except in an effort to bound the variation of salt properties by using crushed and intact salt properties as bounding cases.

Clayton and Gable 2009 (Section 3.1) provides data addressing the thermal conductivity and diffusivity of intact salt with temperature (ibid Equation 3.1), and of crushed salt with porosity and temperature (ibid Equation 3.4). The authors also provide a discussion of the time for reconsolidation of crushed salt to intact salt (ibid Figure 4.18). Figures G.5-1 and G.5-2 are derived from the equations and data in Clayton and Gable 2009 (Section 3.1).

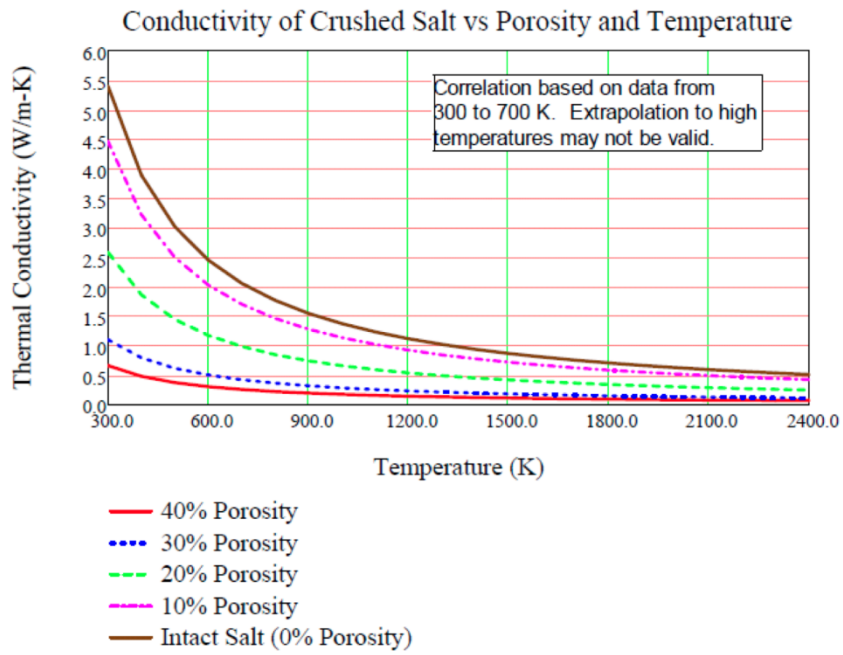

Figure G.5-1 Effects of porosity and temperature on thermal conductivity of crushed salt

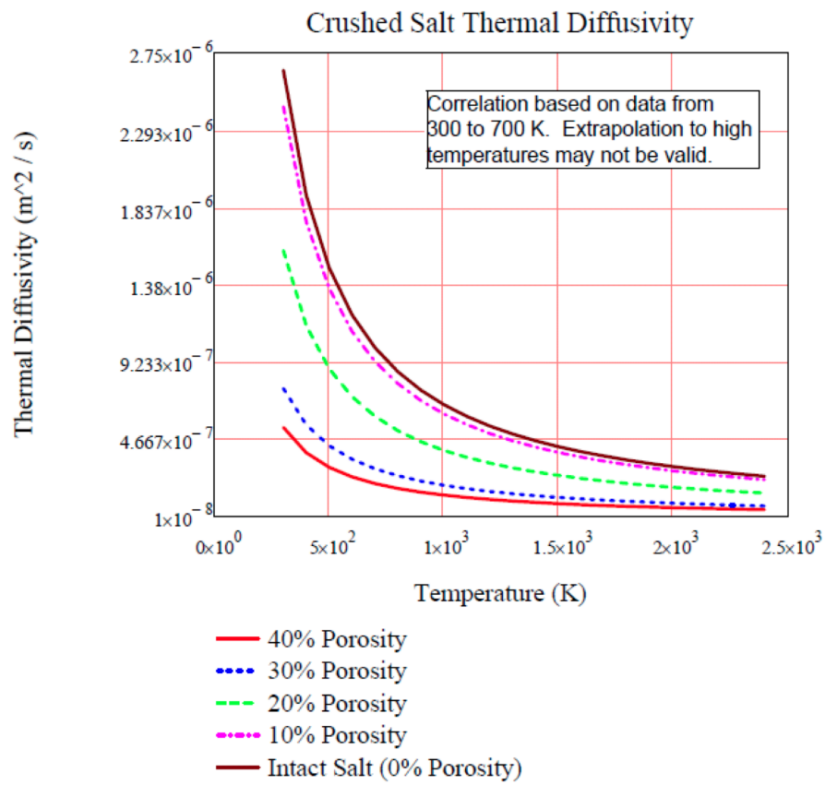

Figure G.5-2 Effects of porosity and temperature on thermal diffusivity of crushed salt

The model assumes zero contact resistance between the various layers of the EBS, and also assumes that there is no settling of buffer or backfill materials, i.e. that there are no air gaps. Both of these potential additional resistances can be addressed.

In a given region, if there is an air gap instead of buffer or backfill material, for example, there will be radiation heat transfer in that region. However, this can be modeled as a linearized "effective" radiation heat transfer coefficient as follows:

$$Q_{radiant} = \sigma \cdot \varepsilon \cdot A \cdot \left(T_1^{\,4} - T_2^{\,4}\right) = \sigma \cdot \varepsilon \cdot A \cdot \left(T_1^{\,2} - T_2^{\,2}\right) \cdot \left(T_1^{\,2} + T_2^{\,2}\right)$$

where σ is the Stefan-Boltzmann constant and ε is the emissivity of the surface.

$$Q_{radiant} = \sigma \cdot \varepsilon \cdot A \cdot \left(T_1 - T_2\right)\left(T_1 + T_2\right) \cdot \left(T_1^{\,2} + T_2^{\,2}\right)$$

We can then define h_{rad} as follows:

$$h_{rad} = \sigma \cdot \varepsilon \cdot \left(T_1 + T_2\right) \cdot \left(T_1^{\,2} + T_2^{\,2}\right) \quad \text{Such that} \quad Q_{radiant} = h_{rad} \cdot A \cdot \left(T_1 - T_2\right) \qquad R_{rad} := \frac{1}{h_{rad}}$$

Then the radiant resistance term can be treated just like an internal or external heat transfer coefficient. However, since h_{rad} is a function of temperature, an initial guess and an iteration process (or a Mathcad Solve Block) are needed to converge on the solution to the temperature distribution.

APPENDIX H

THERMAL ANALYSIS

H.1 INTRODUCTION

The assumptions, inputs, models and solutions for the thermal behavior in clay, granite, salt and deep borehole are documented in Section 5 of this report.

Section H.2 "Contributions to Total System Heat from the Central Waste Package, Axial and Lateral Heat Sources" contains Figures H.2-1 to H.2-24 that show the relative contributions from the central waste package, the axial waste packages along the central emplacement line (4 on either side of the central package) and the lateral emplacement lines (4 on each side of the central line) to the total emplacement temperature.

Section H.3 "Transient Temperature in the Host Rock" contains Figures H.3-1 to H.3-24 that show the overall transient temperature in each host rock media at the calculation radius for 3 storage times, namely 10, 50 and 100 years.

Section H.4 "Waste Package Surface Temperature" contains Figures H.4-1 to H.4-24 that show the waste package surface temperature based on steady state calculations at each point in time through the corresponding layers of the EBS components.

Section H.5 "Waste Package Peak Temperature as a Function of Storage Time and Number of Assemblies" contains Figures H.5-1 to H.5-6 that show the waste package peak temperature as a function of storage time and number of assemblies or canisters within a waste package.

Section H.6 "Trade-off of Storage Time and Waste Package Capacity" contains Figures H.6-1 and H.6-2 that show the trade-off between storage time and waste package capacity.

While the "co-extraction" process is similar in function to the industrial Co-Extraction™ (COEX) process deployed by AREVA, the two processes assume different processing methods and steps and so the product and waste streams cannot be directly compared. Similar is true for the "new extraction" process documented in this report and the NUEX industrial process proposed by Energy Solutions, which also cannot be directly compared.

H.2 Contributions to Total System Heat from the Central Waste Package, and Adjacent Axial and Lateral Heat Sources

This section documents calculation of temperature at a specified calculation radius in a homogeneous medium with a combination of finite line (central package), individual points (adjacent waste packages), and infinite lines (adjacent lines of waste packages).

The calculation radii for the four media are as follows:

- Granite: SNF 0.83 m, HLW 0.76 m
- Clay: SNF 1.32 m, HLW 0.37 m
- Salt: SNF and HLW 4 m
- Deep borehole: SNF 0.19 m, HLW 0.20 m

The number of assemblies or canisters per waste package is indicated in the figure captions that also define shorthand notation that is used in subsequent sections in this appendix.

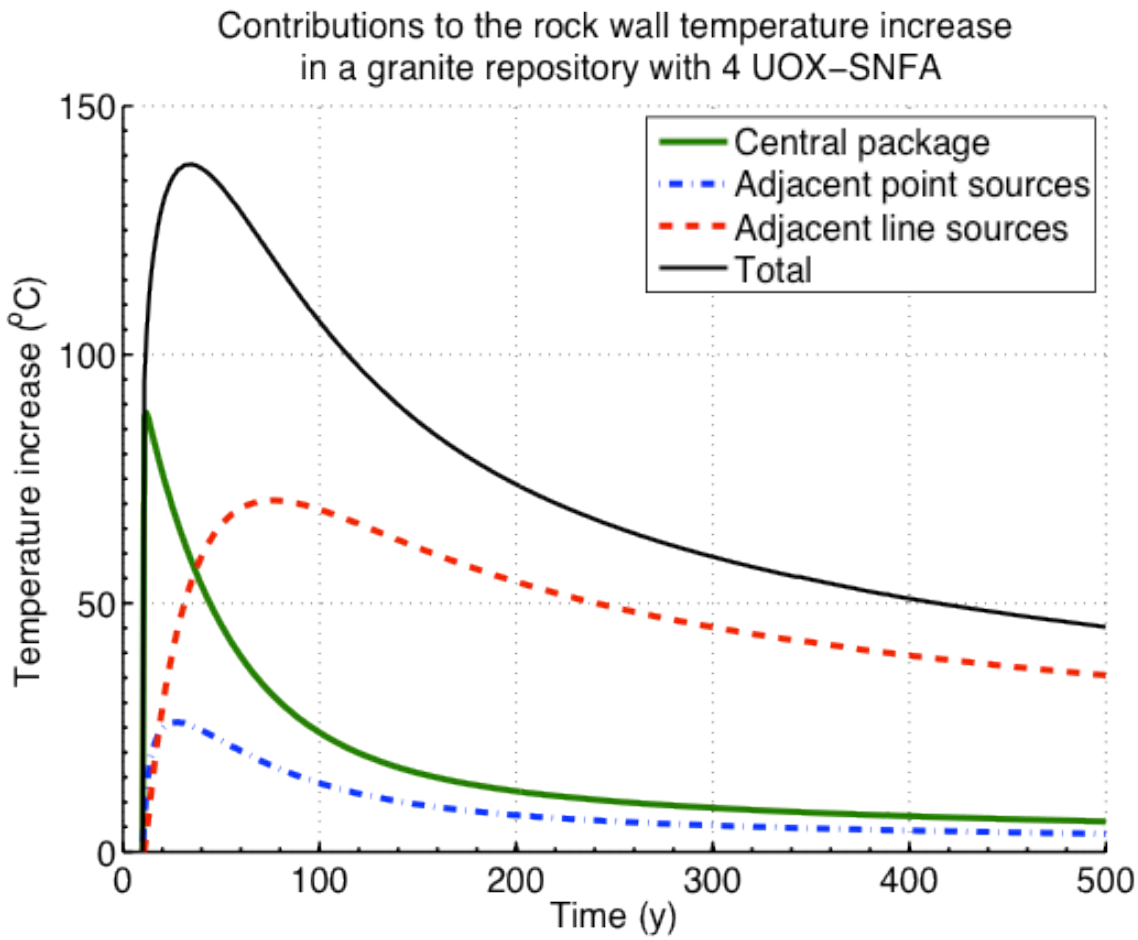

Figure H.2-1 Contributions to the transient rock temperature at the calculation radius from the central package, adjacent point sources and adjacent line sources for 4 UOX assemblies per waste package (UOX-4) in granite

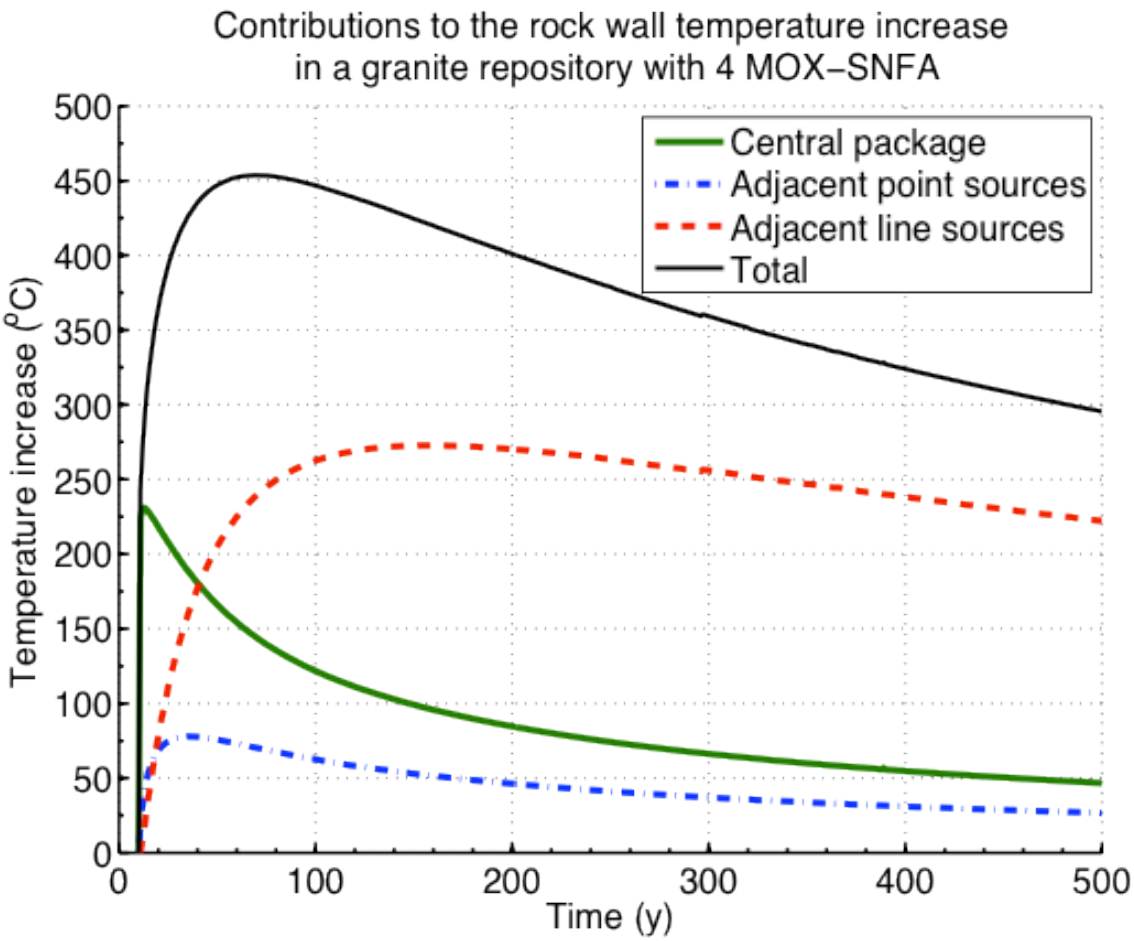

Figure H.2-2 Contributions to the transient rock temperature at the calculation radius from the central package, adjacent point sources and adjacent line sources for 4 MOX assemblies per waste package (MOX-4) in granite

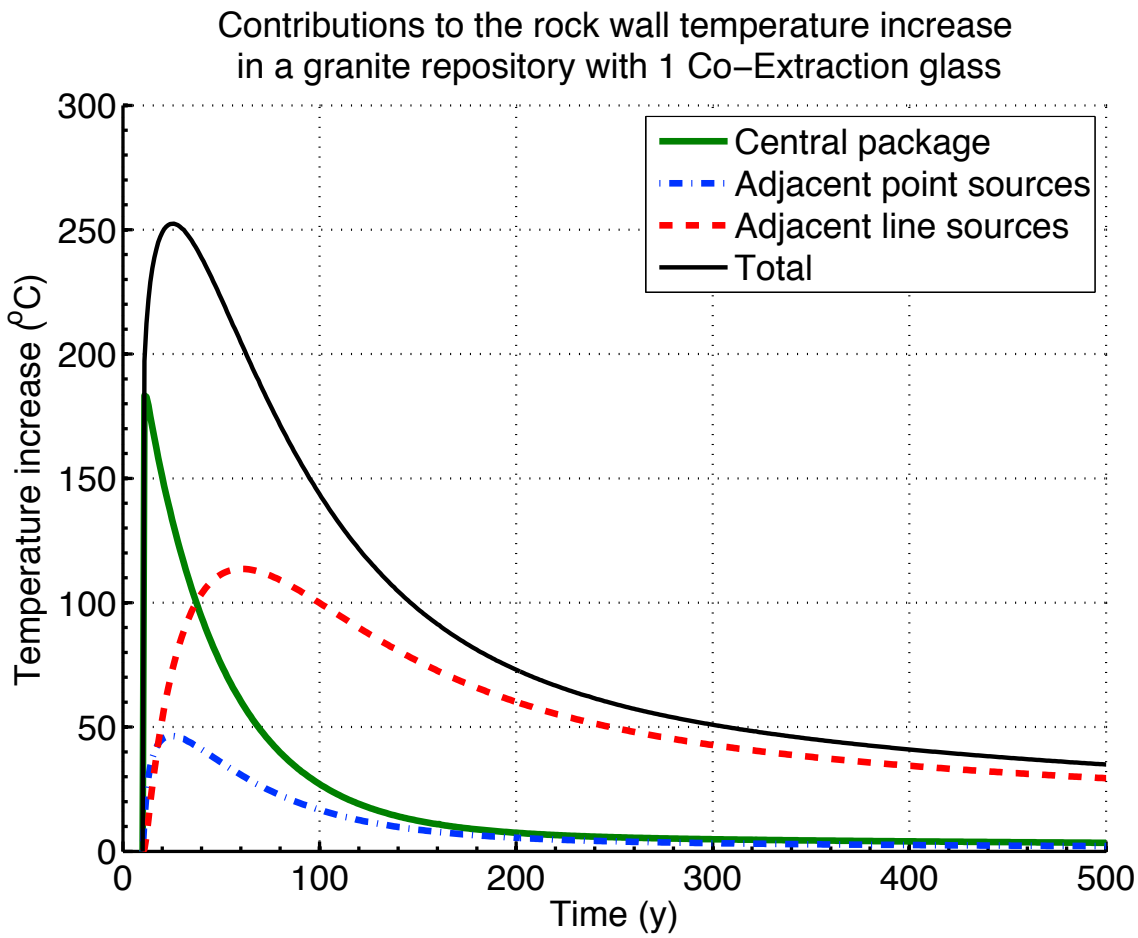

Figure H.2-3 Contributions to the transient rock temperature at the calculation radius from the central package, adjacent point sources and adjacent line sources for one co-extraction HLW (co-extraction-1) canister per waste package in granite

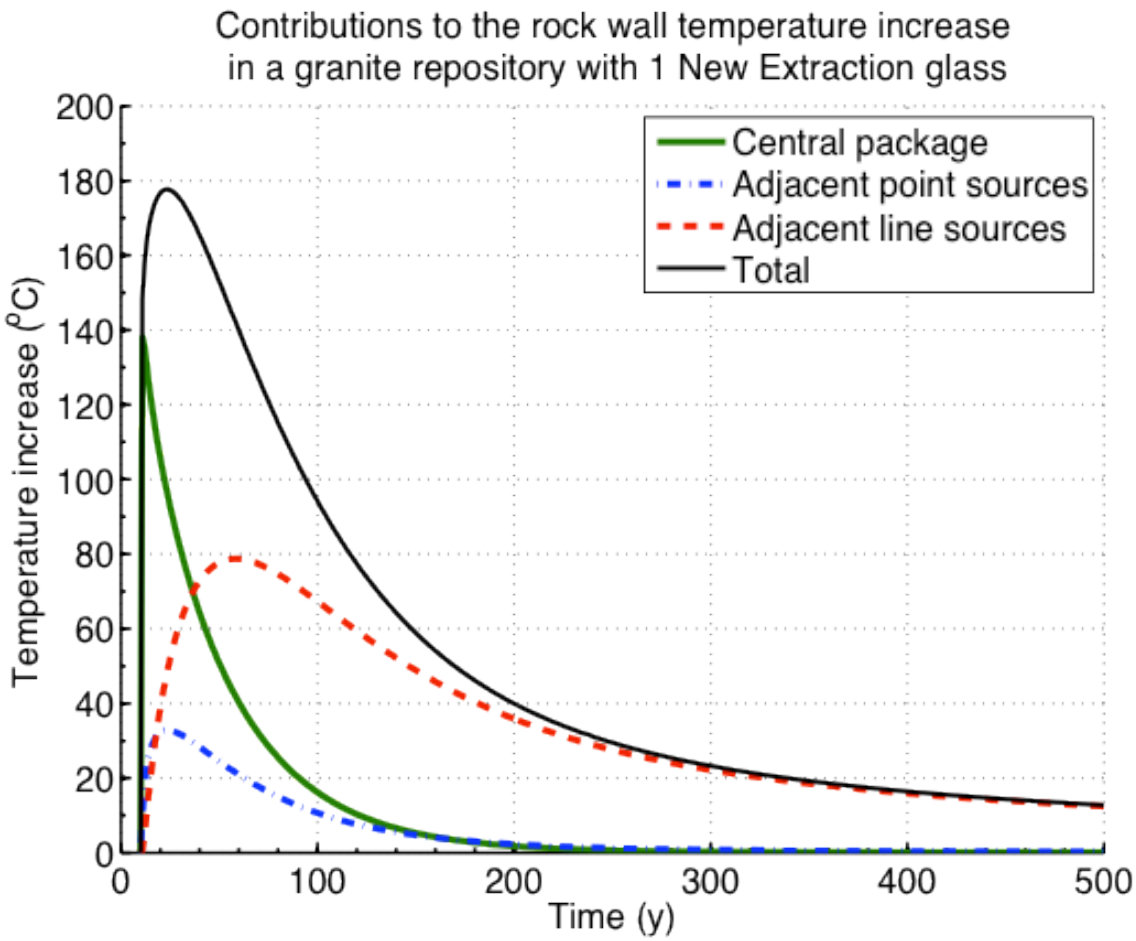

Figure H.2-4 Contributions to the transient rock temperature at the calculation radius from the central package, adjacent point sources and adjacent line sources for one new extraction HLW (new extraction-1) canister per waste package in granite

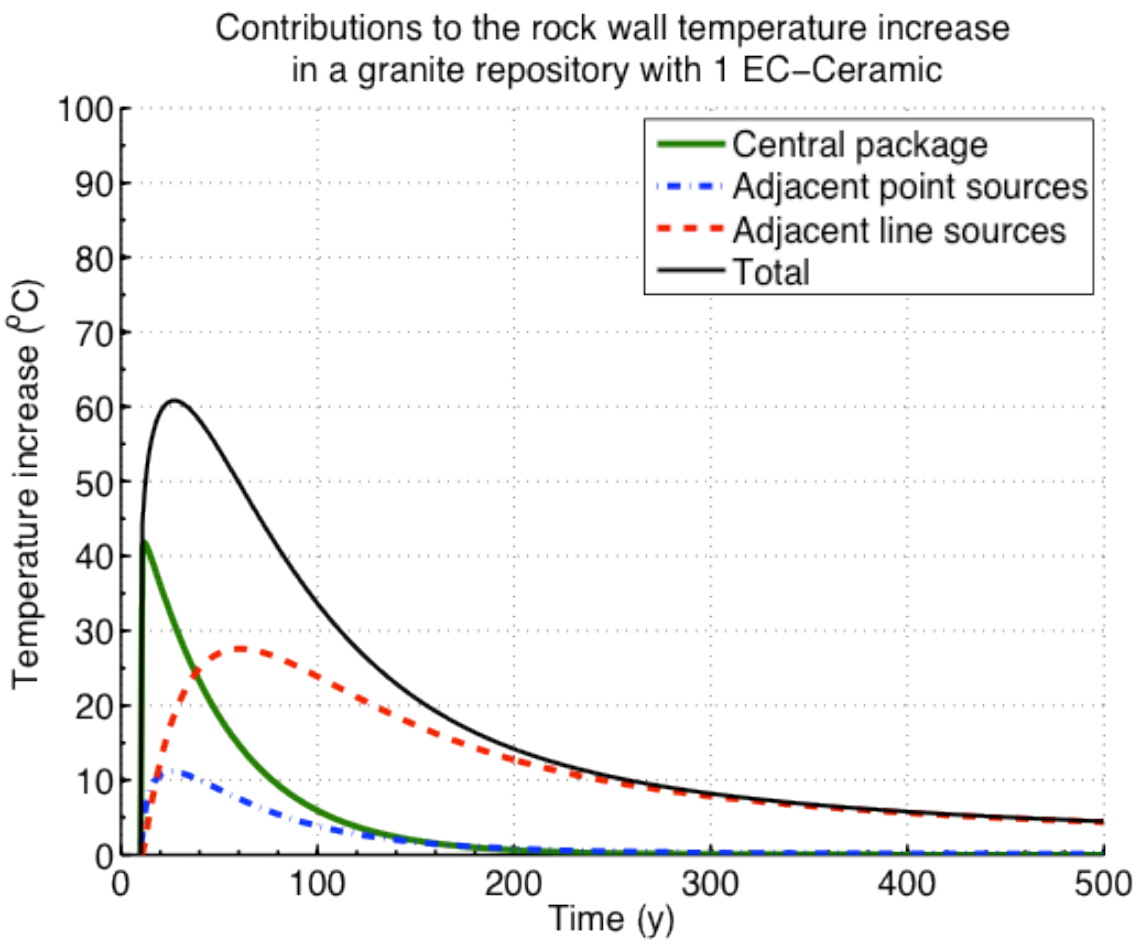

Figure H.2-5 Contributions to the transient rock temperature at the calculation radius from the central package, adjacent point sources and adjacent line sources for one EC-Ceramic HLW (ECC-1) canister per waste package in granite

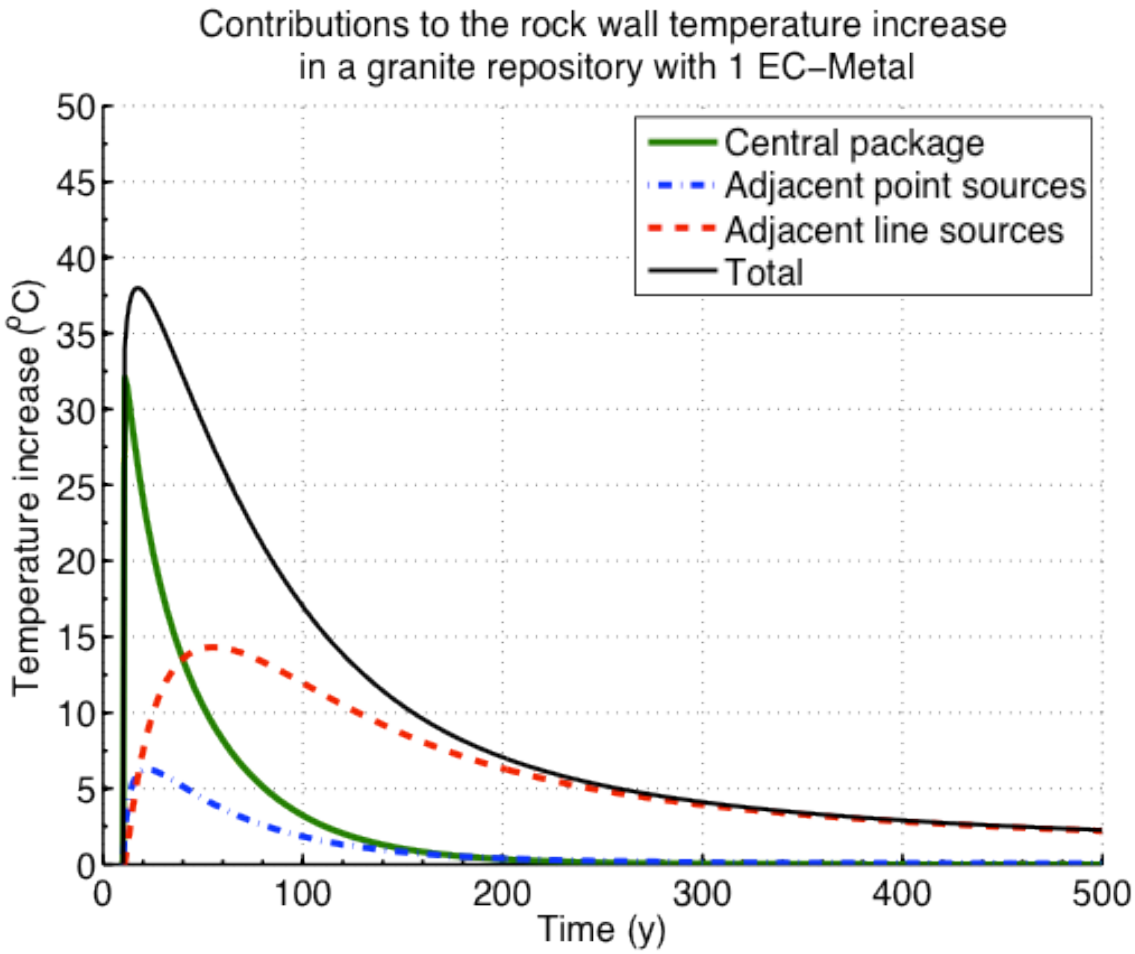

Figure H.2-6 Contributions to the transient rock temperature at the calculation radius from the central package, adjacent point sources and adjacent line sources for one EC-Metal HLW (ECM-1) canister per waste package in granite

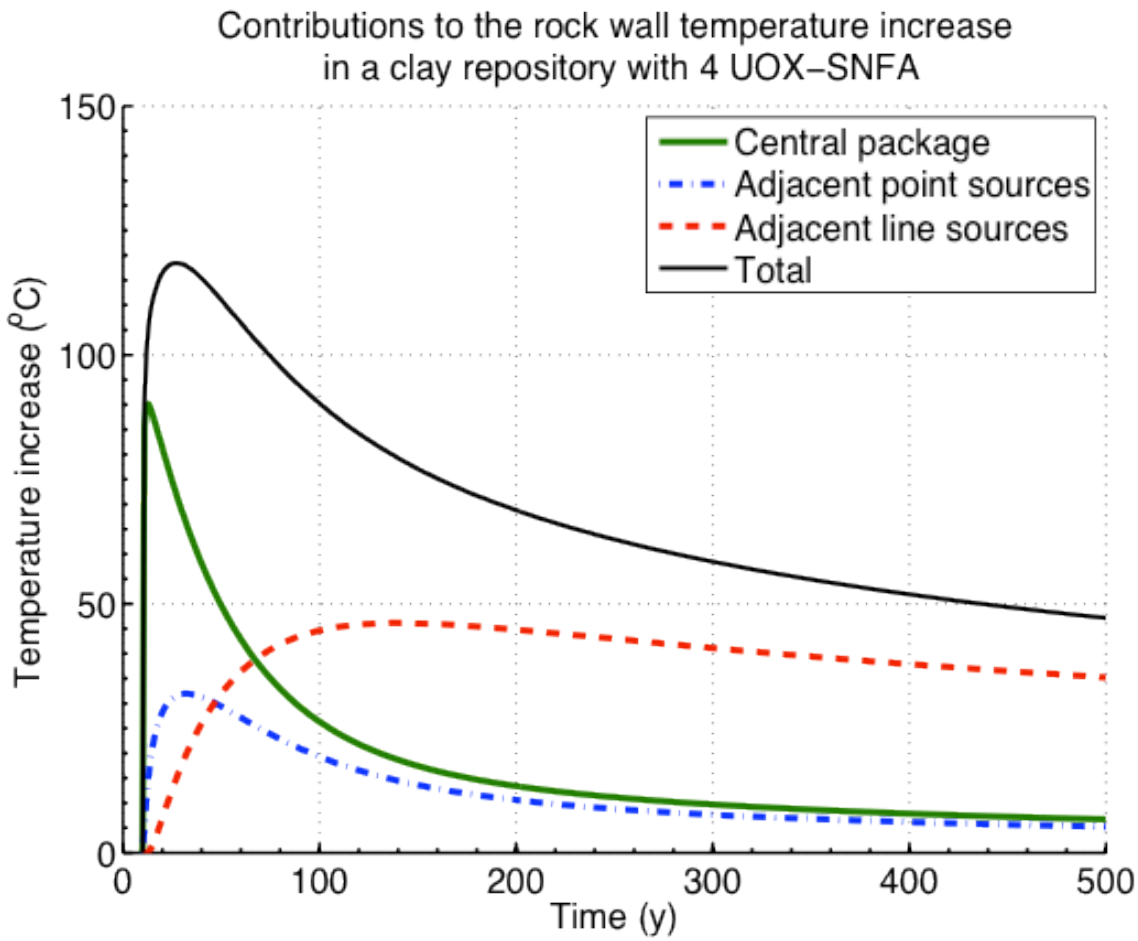

Figure H.2-7 Contributions to the transient rock temperature at the calculation radius from the central package, adjacent point sources and adjacent line sources for UOX-4 in clay

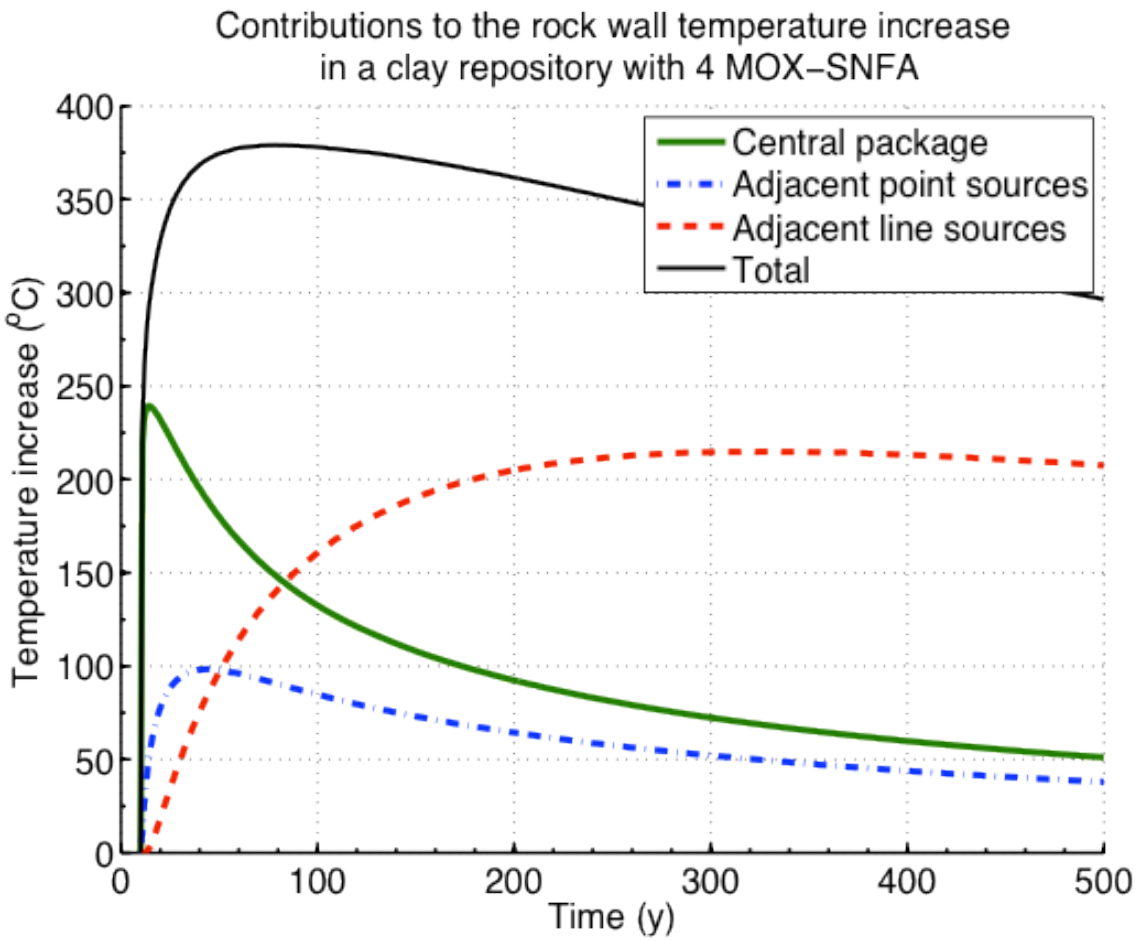

Figure H.2-8 Contributions to the transient rock temperature at the calculation radius from the central package, adjacent point sources and adjacent line sources for MOX-4 in clay

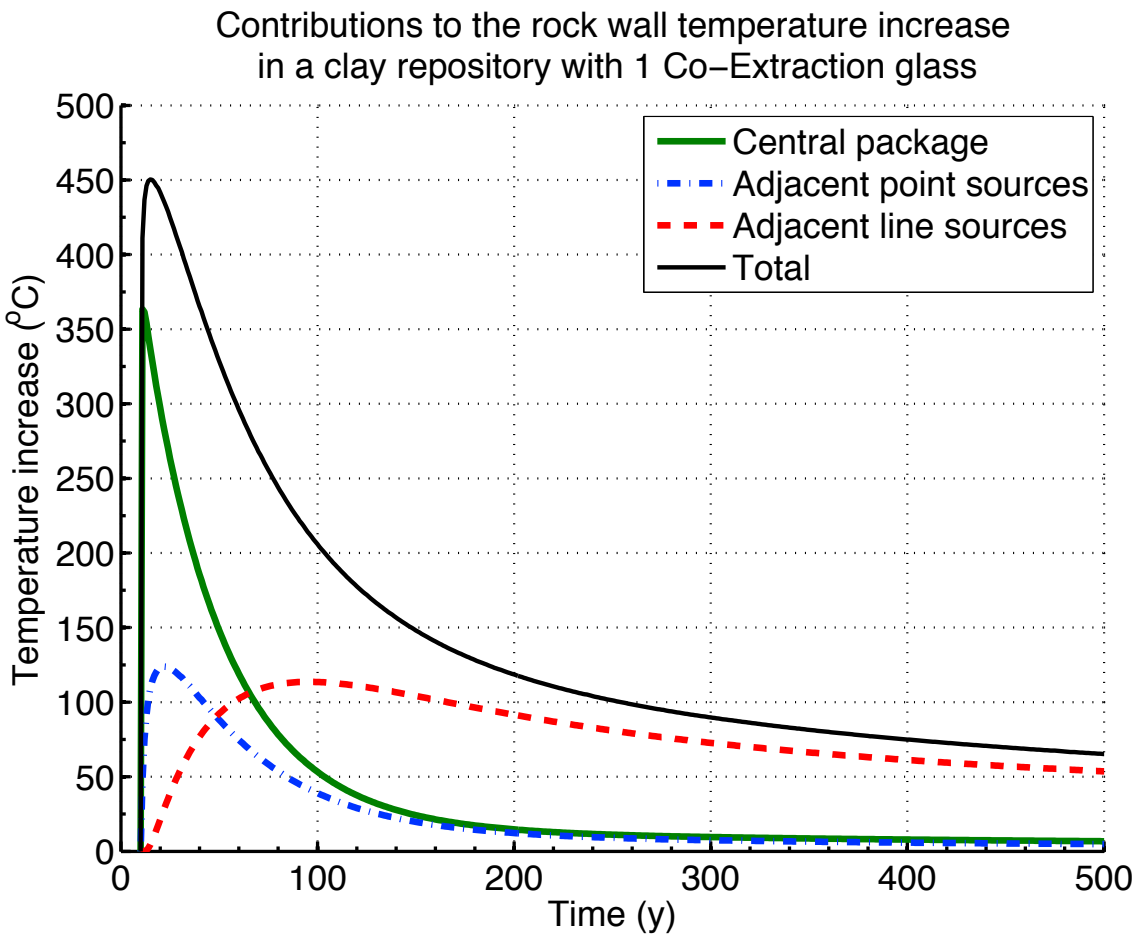

Figure H.2-9 Contributions to the transient rock temperature at the calculation radius from the central package, adjacent point sources and adjacent line sources for co-extraction-1 in clay

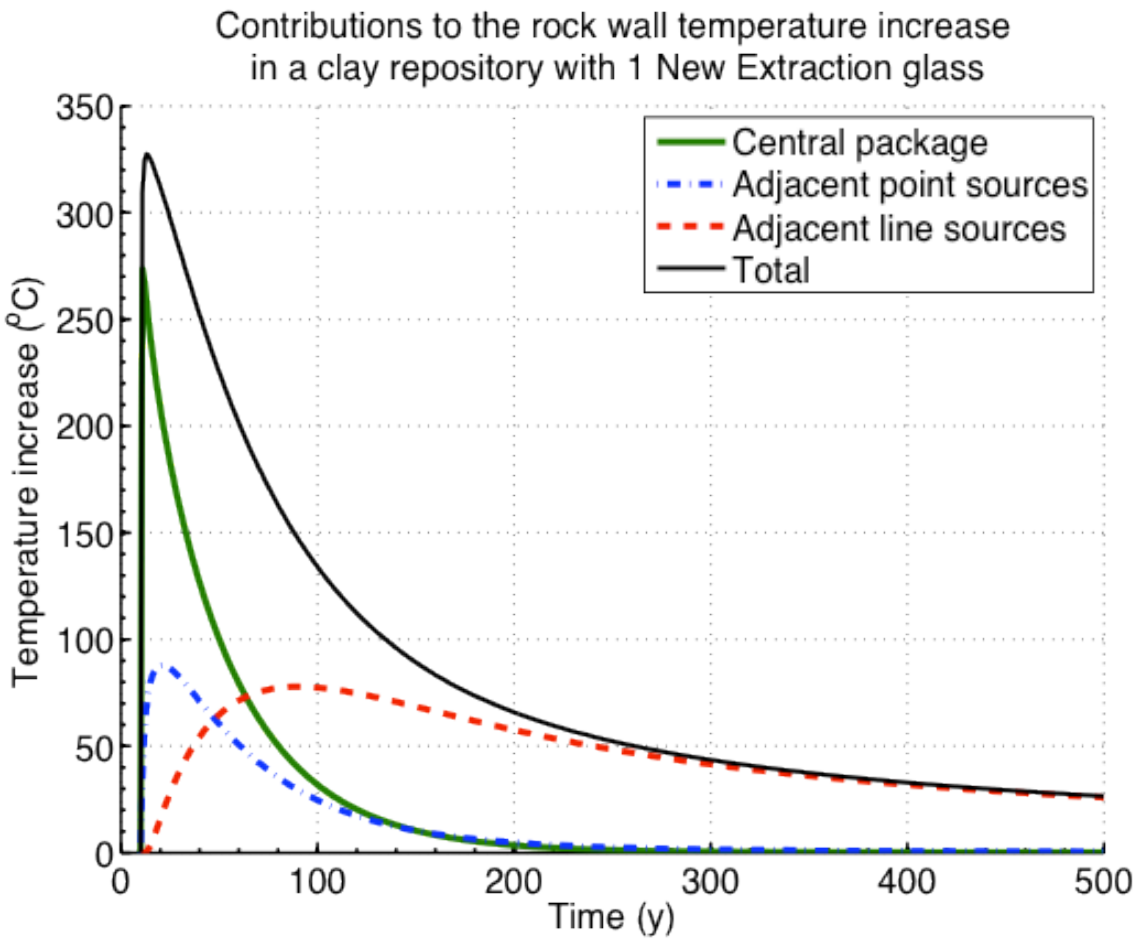

Figure H.2-10 Contributions to the transient rock temperature at the calculation radius from the central package, adjacent point sources and adjacent line sources for new extraction-1 in clay

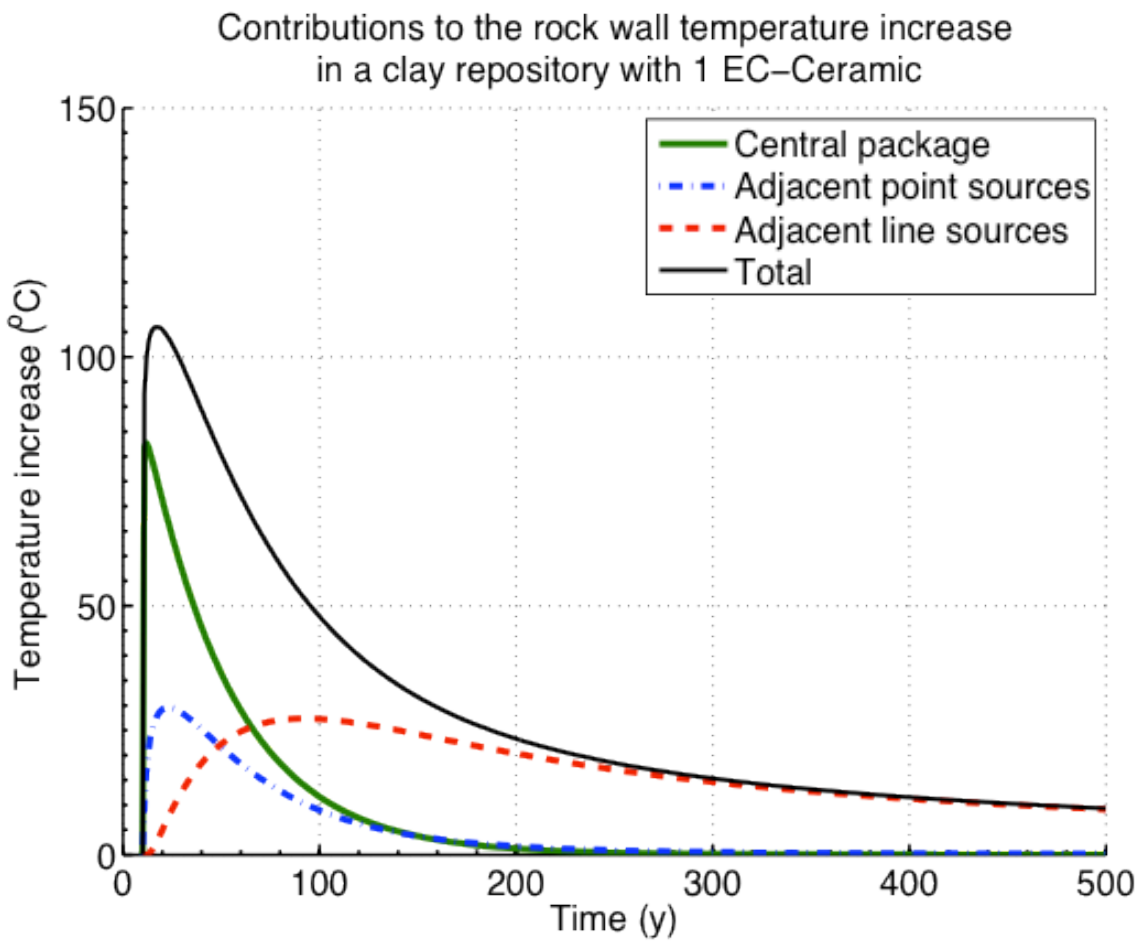

Figure H.2-11 Contributions to the transient rock temperature at the calculation radius from the central package, adjacent point sources and adjacent line sources for ECC-1 in clay

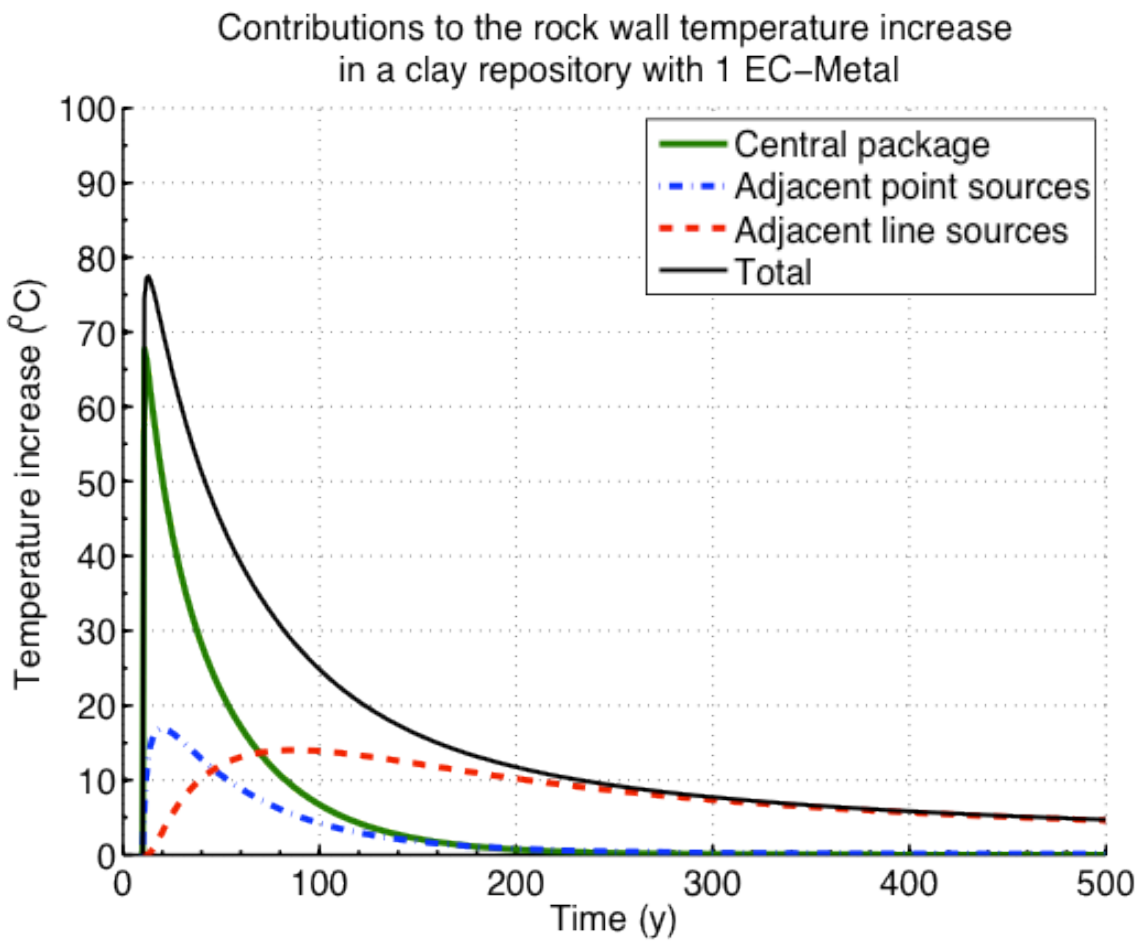

Figure H.2-12 Contributions to the transient rock temperature at the calculation radius from the central package, adjacent point sources and adjacent line sources for ECM-1 in clay

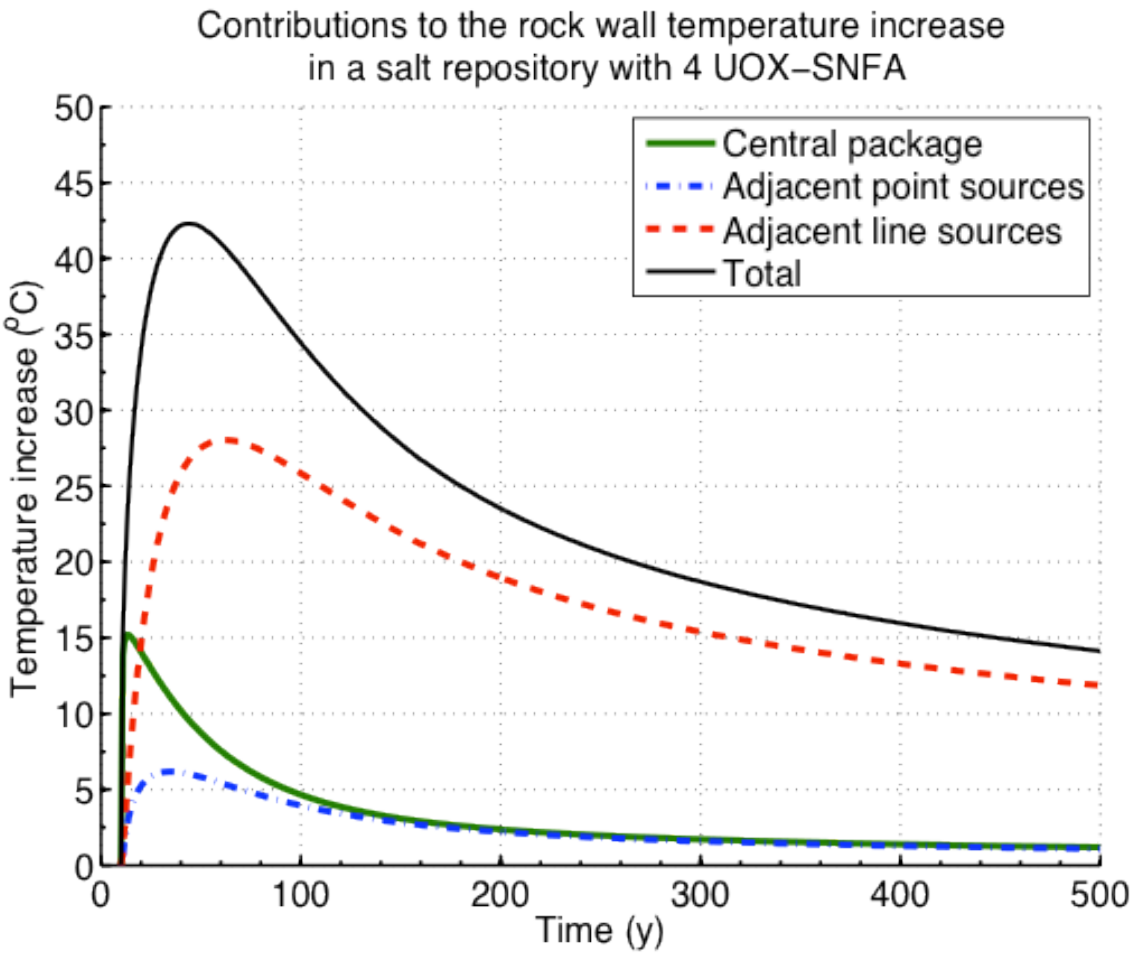

Figure H.2-13 Contributions to the transient rock temperature at the calculation radius from the central package, adjacent point sources and adjacent line sources for UOX-4 in salt

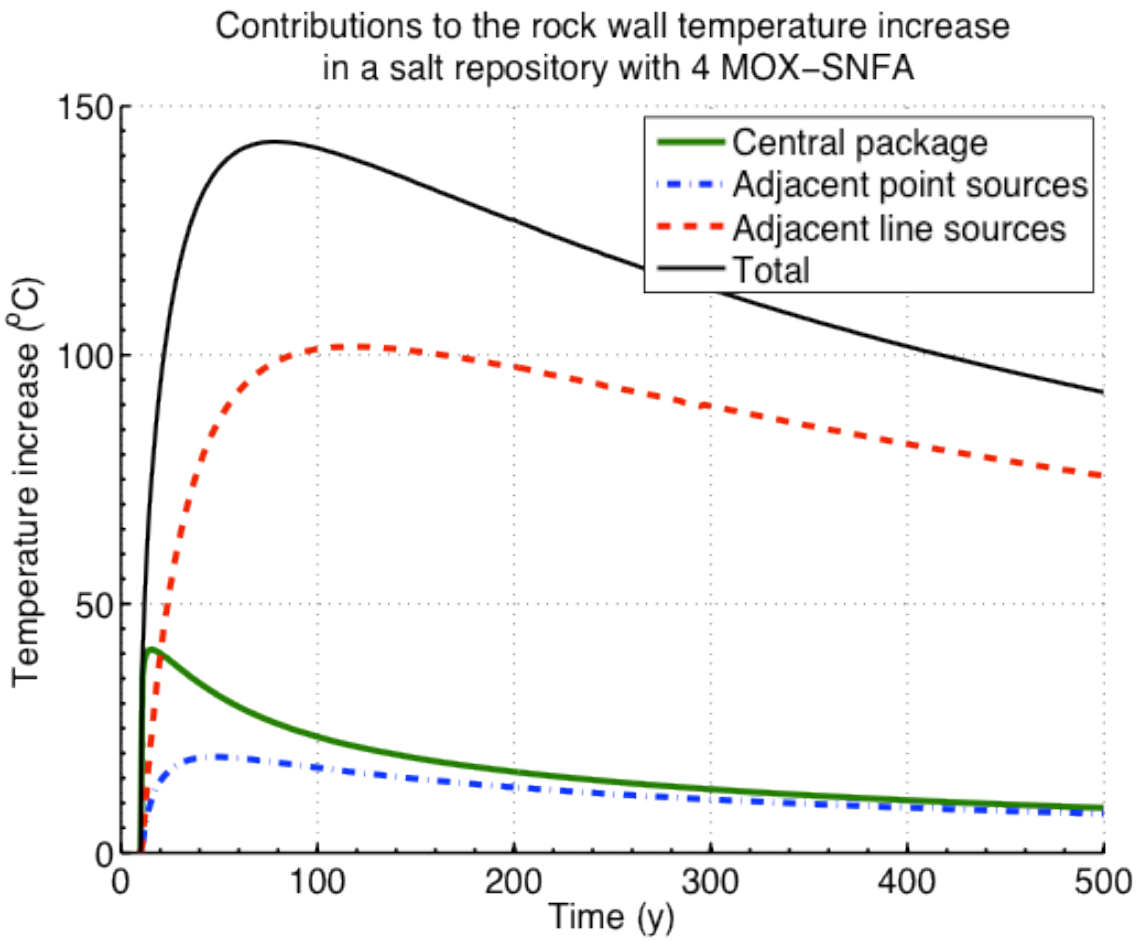

Figure H.2-14 Contributions to the transient rock temperature at the calculation radius from the central package, adjacent point sources and adjacent line sources for MOX-4 in salt

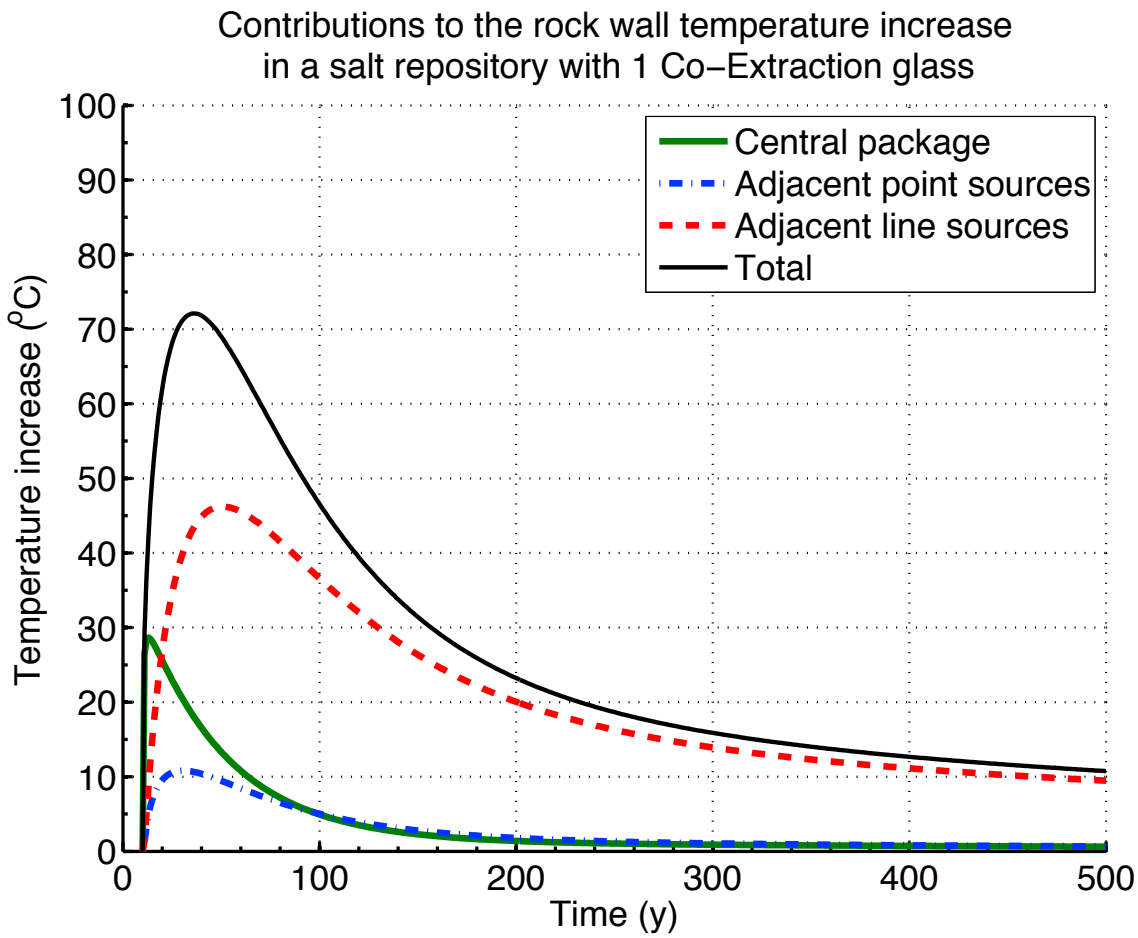

Figure H.2-15 Contributions to the transient rock temperature at the calculation radius from the central package, adjacent point sources and adjacent line sources for co-extraction-1 in salt

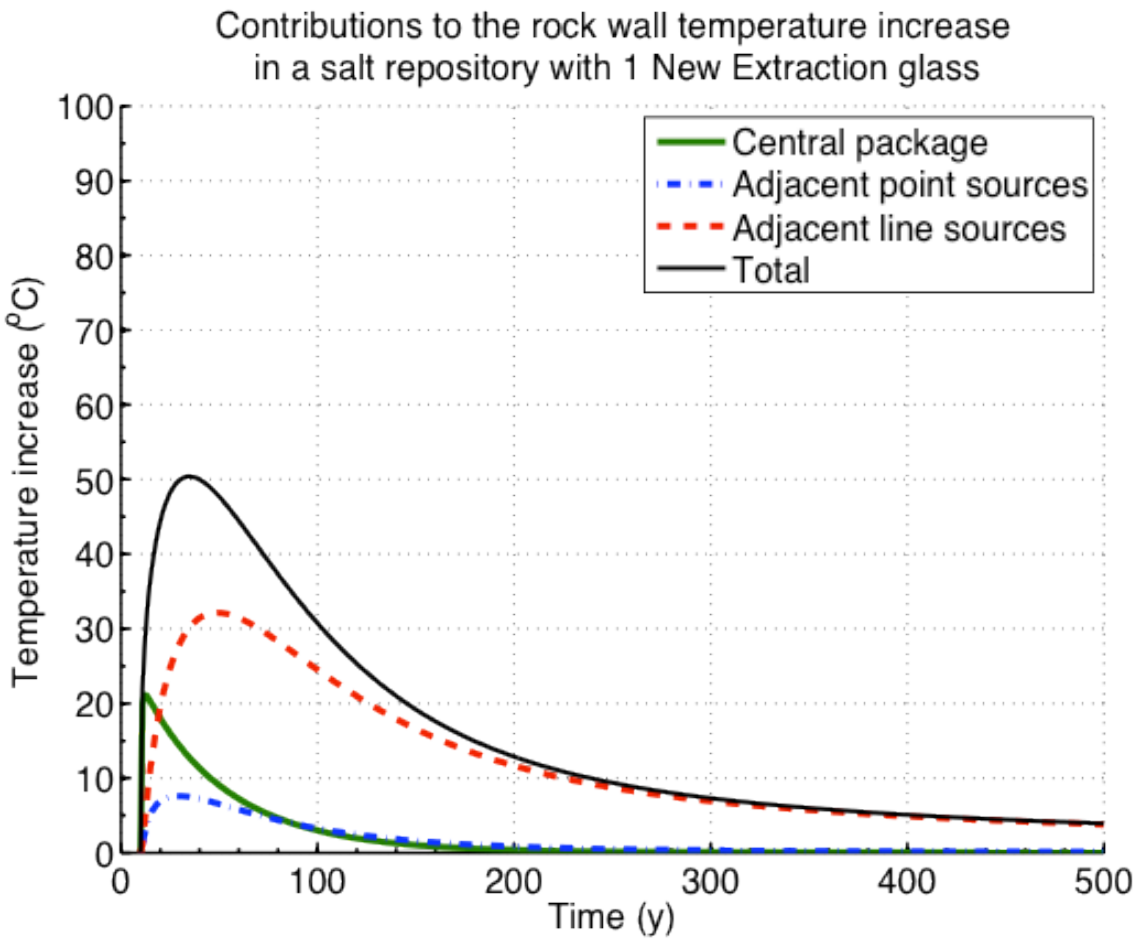

Figure H.2-16 Contributions to the transient rock temperature at the calculation radius from the central package, adjacent point sources and adjacent line sources for new extraction-1 in salt

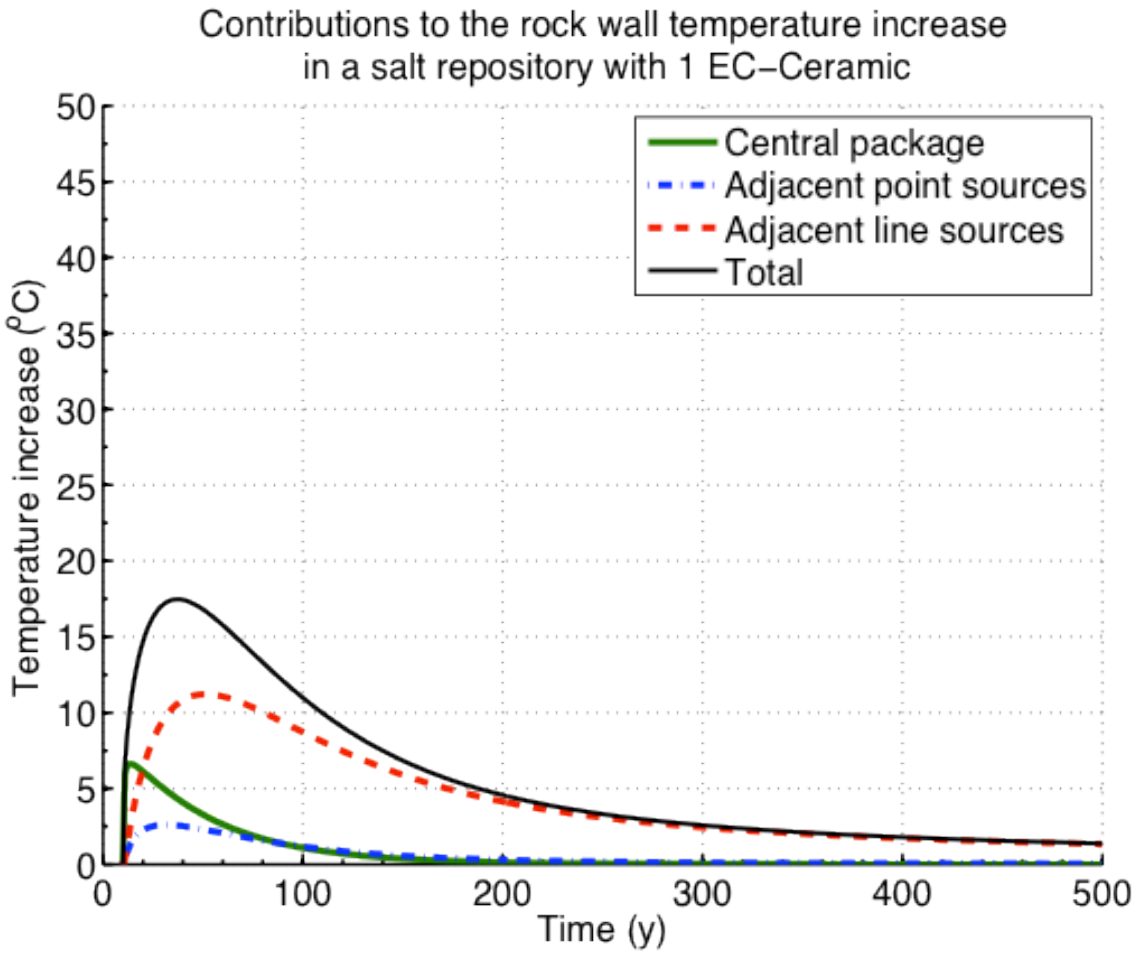

Figure H.2-17 Contributions to the transient rock temperature at the calculation radius from the central package, adjacent point sources and adjacent line sources for ECC-1 salt

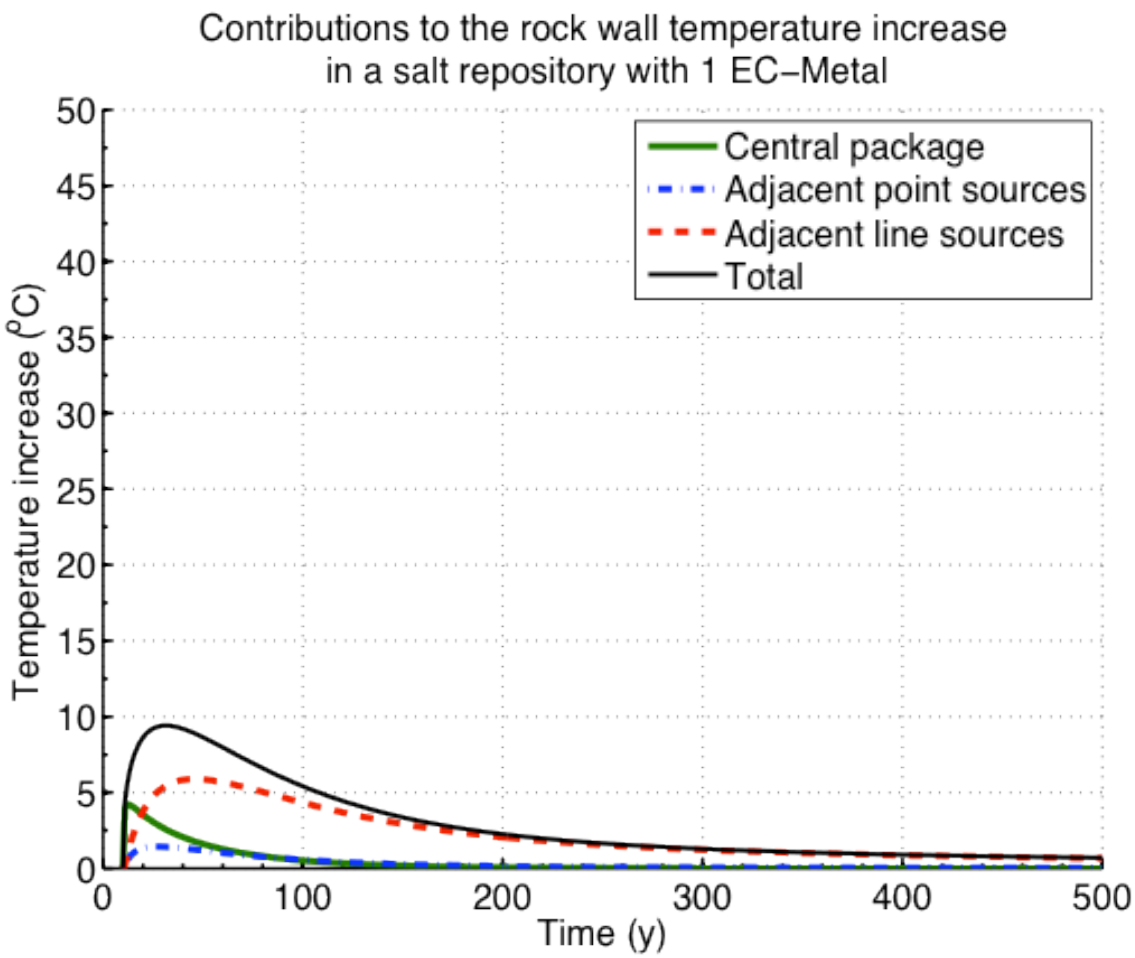

Figure H.2-18 Contributions to the transient rock temperature at the calculation radius from the central package, adjacent point sources and adjacent line sources for ECM-1 in salt

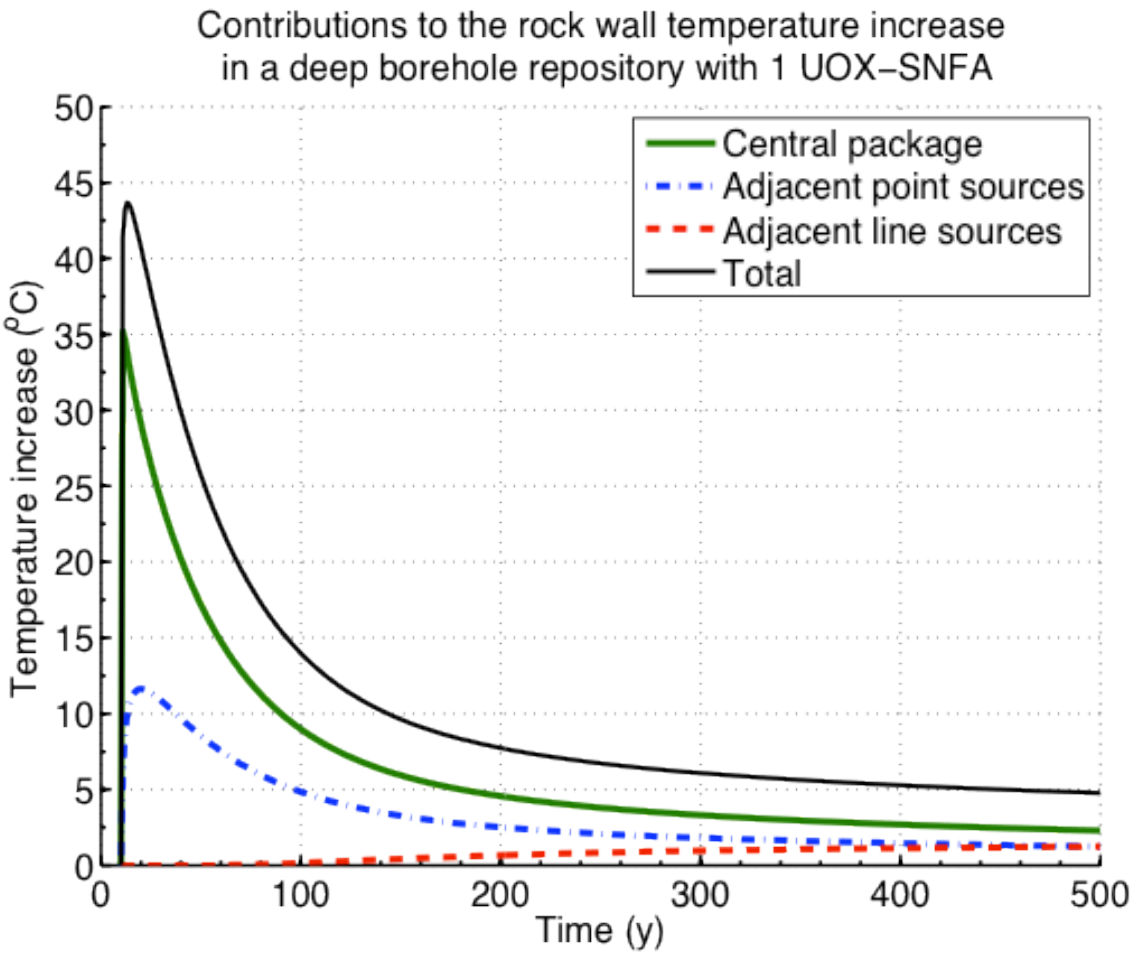

Figure H.2-19 Contributions to the transient rock temperature at the calculation radius from the central package, adjacent point sources and adjacent line sources for UOX-1 in a deep borehole

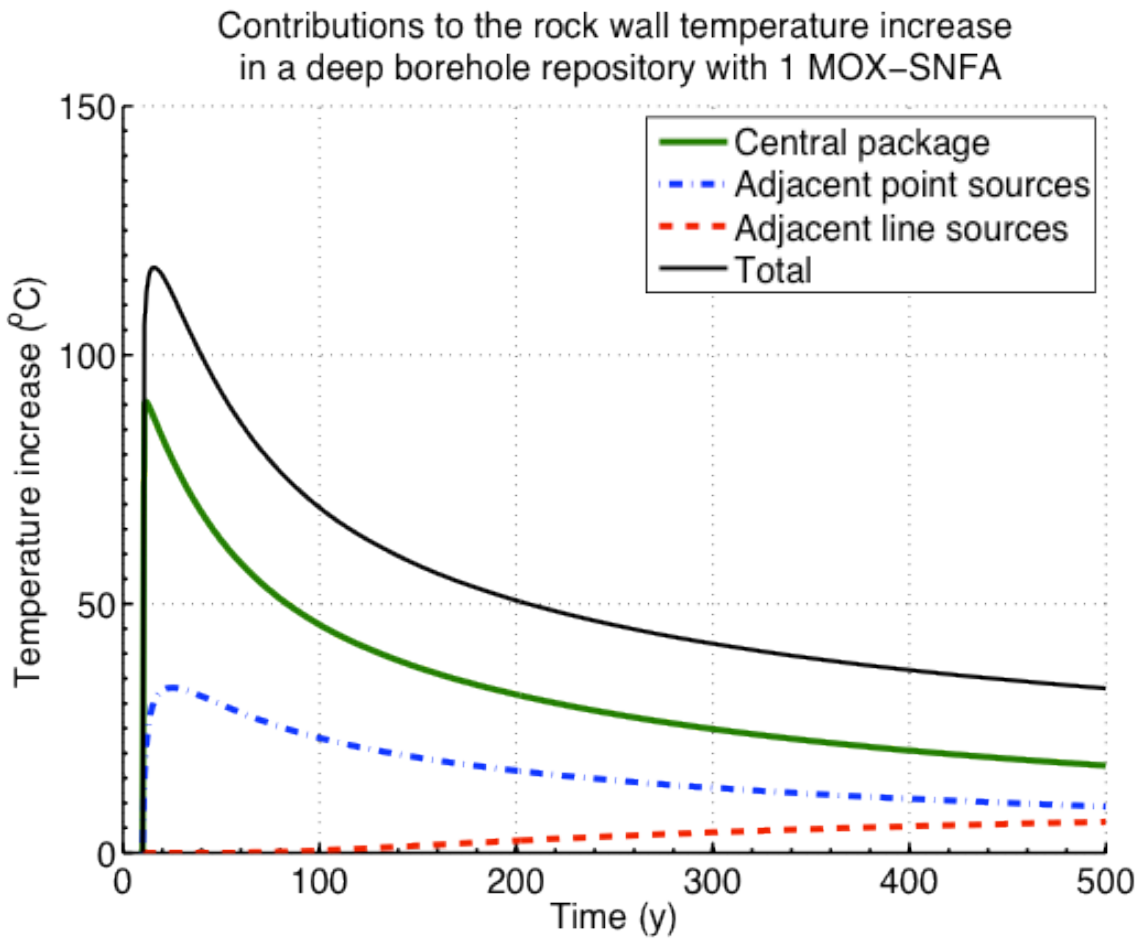

Figure H.2-20 Contributions to the transient rock temperature at the calculation radius from the central package, adjacent point sources and adjacent line sources for MOX-1 in a deep borehole

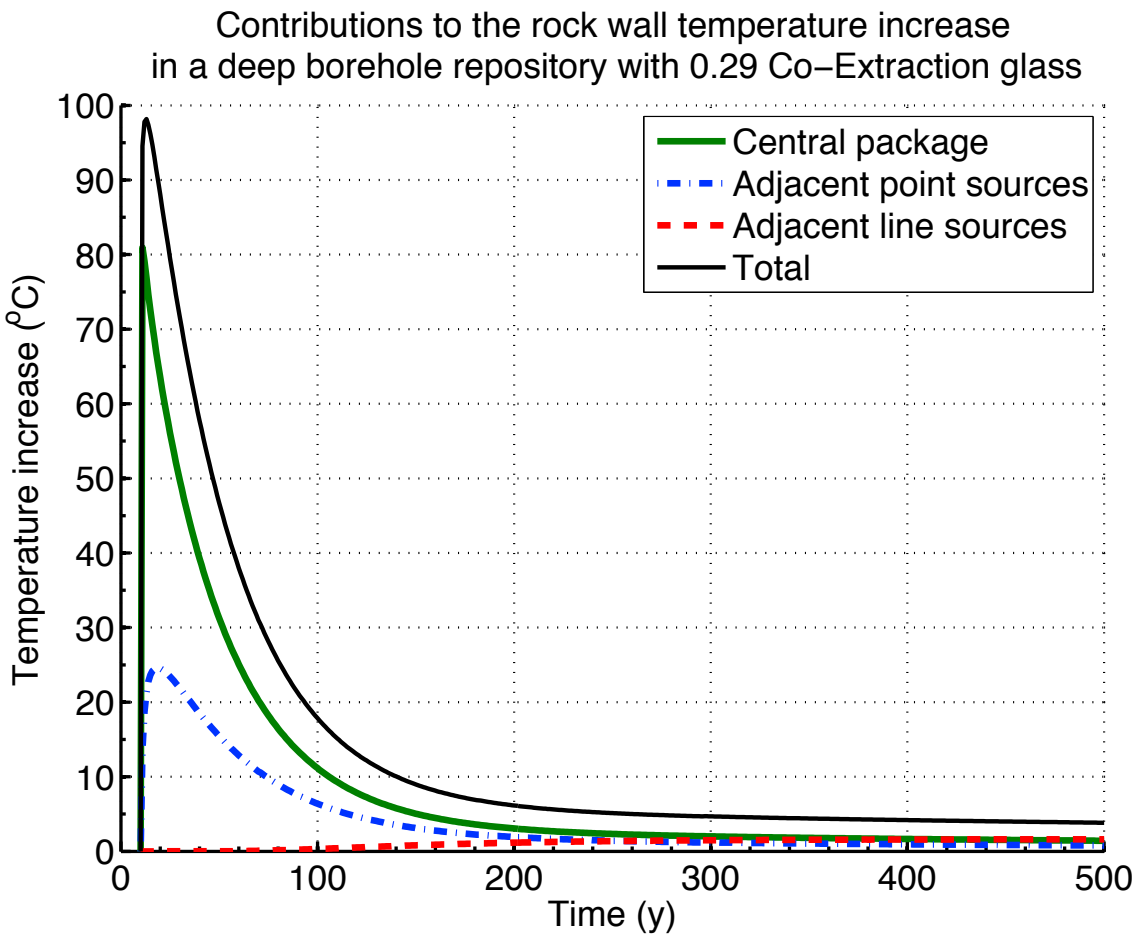

Figure H.2-21 Contributions to the transient rock temperature at the calculation radius from the central package, adjacent point sources and adjacent line sources for one narrow co-extraction (co-extraction-0.291) HLW canister per waste package in a deep borehole. The narrow canister contains 0.291 times the waste in a standard canister

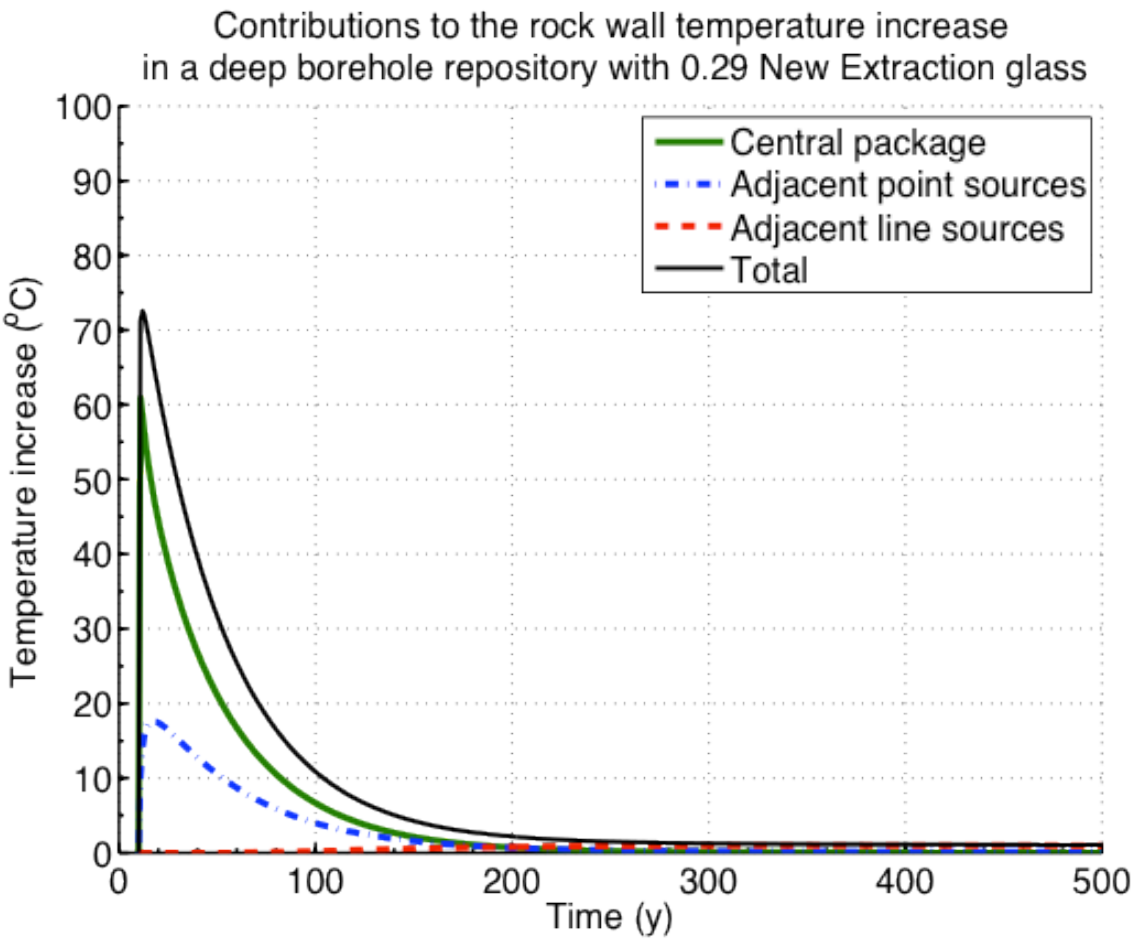

Figure H.2-22 Contributions to the transient rock temperature at the calculation radius from the central package, adjacent point sources and adjacent line sources for one narrow new extraction (new extraction-0.291) HLW canister per waste package in a deep borehole. The narrow canister contains 0.291 times the waste in a standard canister

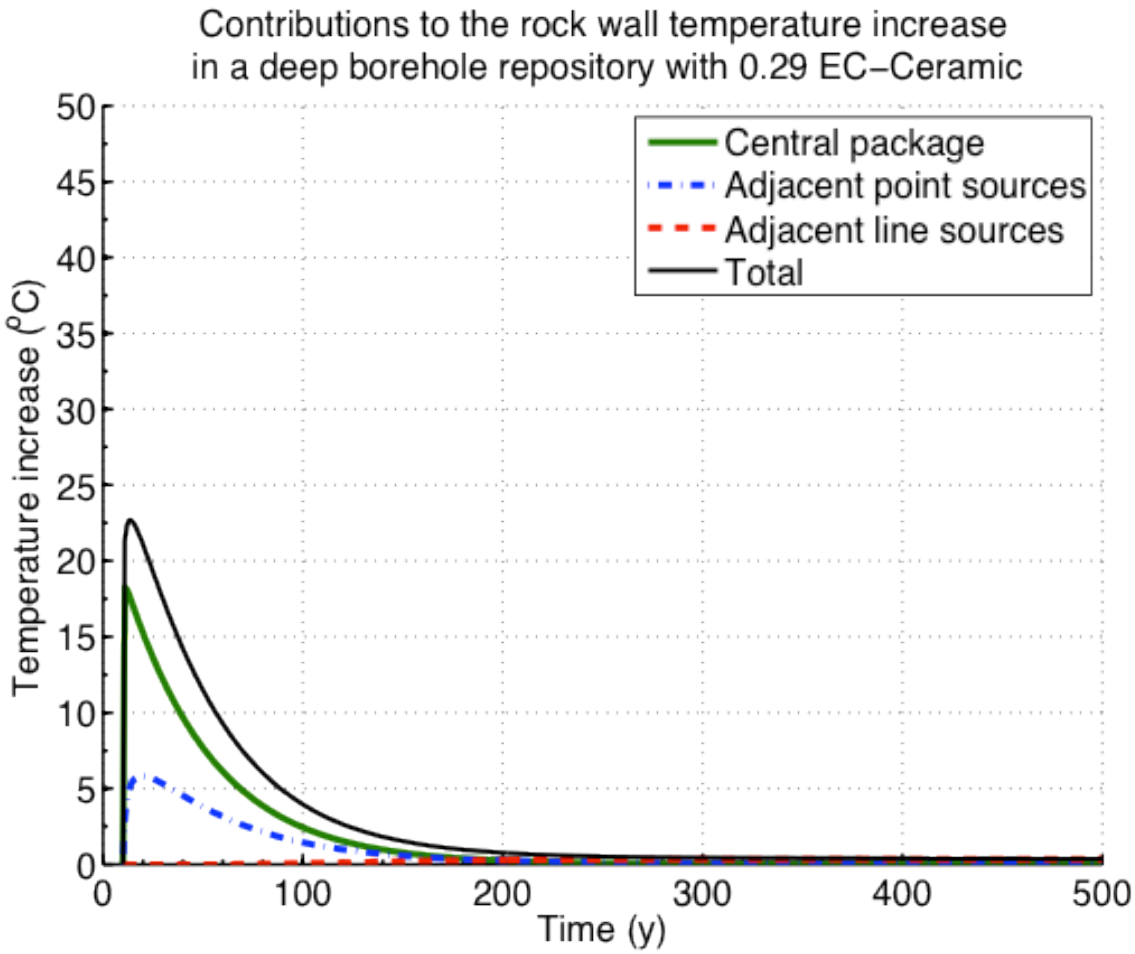

Figure H.2-23 Contributions to the transient rock temperature at the calculation radius from the central package, adjacent point sources and adjacent line sources for one narrow EC-Ceramic (ECC-0.291) HLW canister per waste package in a deep borehole. The narrow canister contains 0.291 times the waste in a standard canister

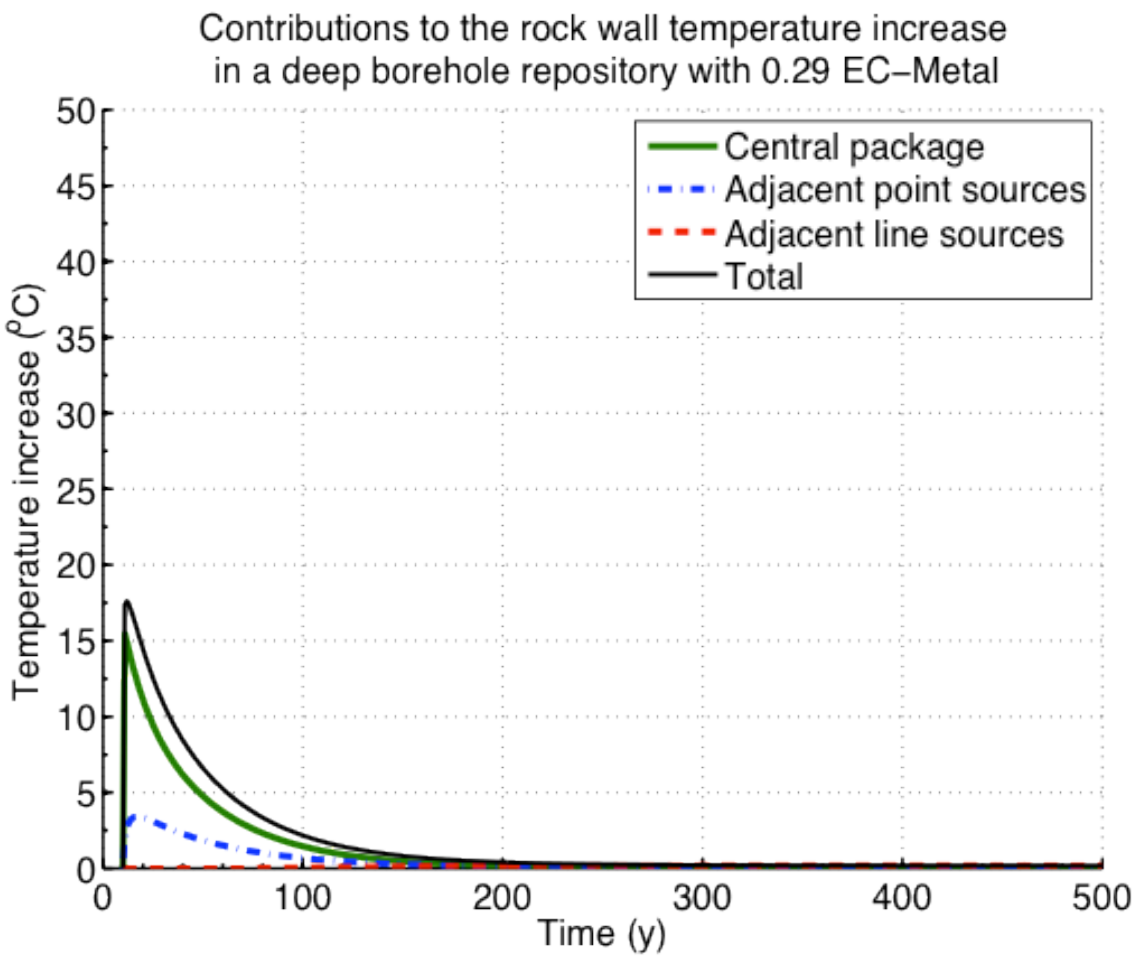

Figure H.2-24 Contributions to the transient rock temperature at the calculation radius from the central package, adjacent point sources and adjacent line sources for one narrow EC-Metal (ECM-0.291) HLW canister per waste package in a deep borehole. The narrow canister contains 0.291 times the waste in a standard canister

H.3 Transient temperature in the Host Rock

The calculation radii for the four media are as follows:

- Granite: SNF 0.83 m, HLW 0.76 m
- Clay: SNF 1.32 m, HLW 0.37 m
- Salt: SNF and HLW 4 m
- Deep borehole: SNF 0.19 m, HLW 0.20 m

The number of assemblies or canisters per waste package are as defined in Section H.2, except as indicated in the figure captions below.

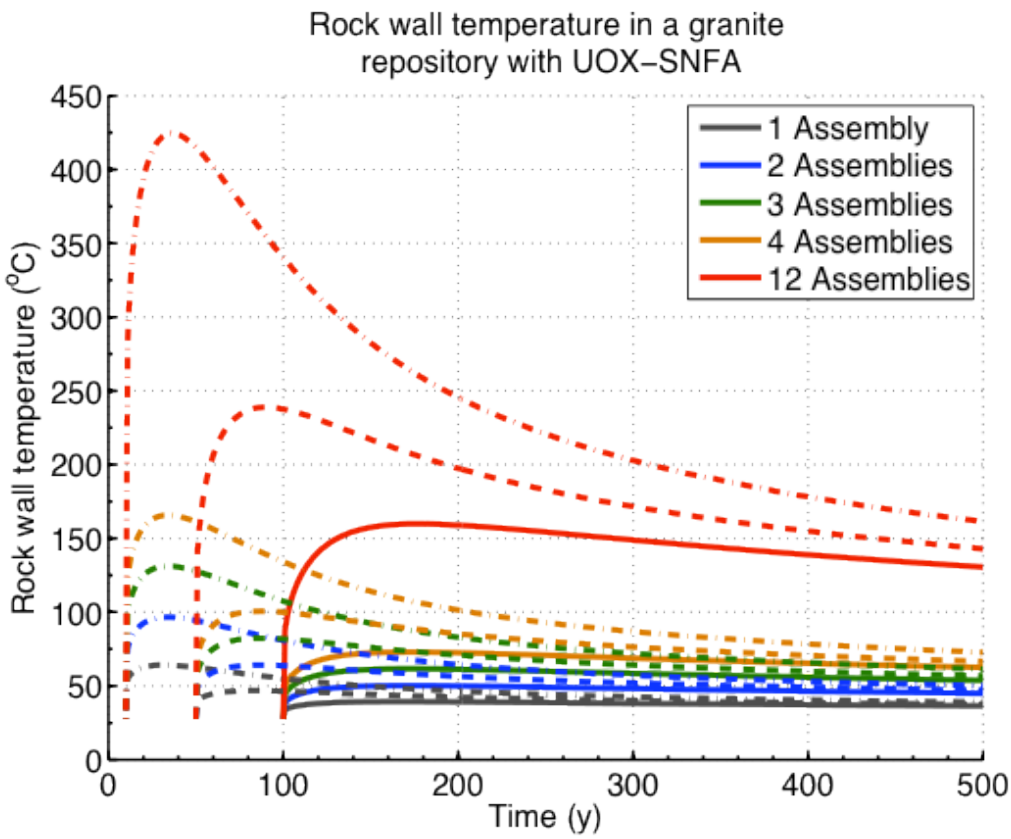

Figure H.3-1 Transient host rock temperature at the calculation radius after storage times of 10, 50 and 100 years for a waste package containing 1, 2, 3, 4 and 12 UOX assemblies in granite

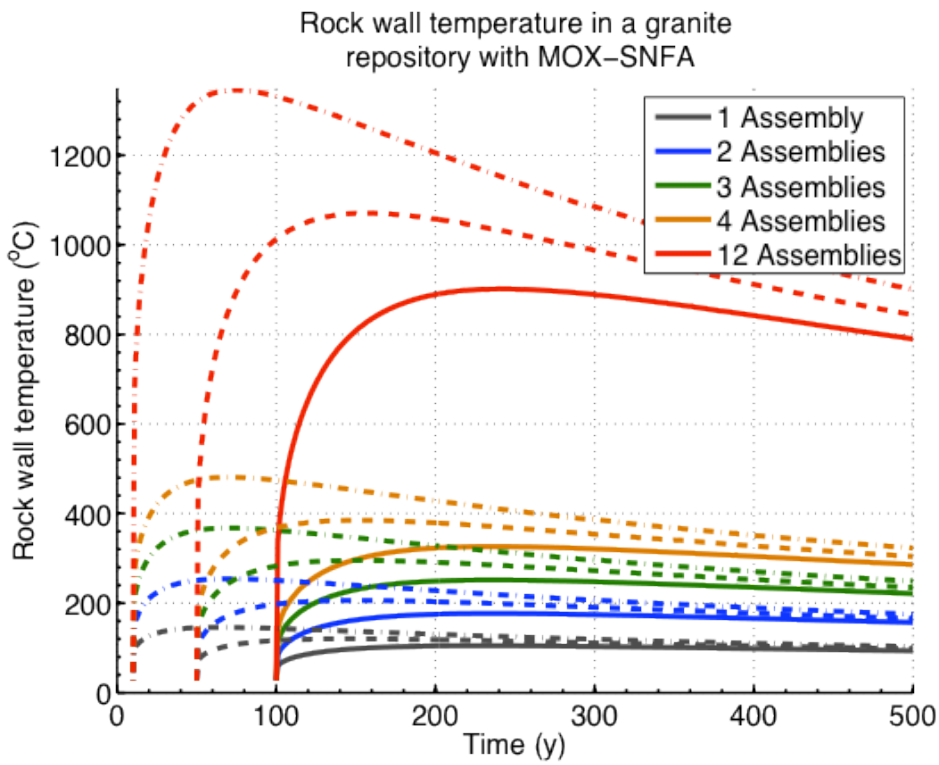

Figure H.3-2 Transient host rock temperature at the calculation radius after storage times of 10, 50 and 100 years for a waste package containing 1, 2, 3, 4 and 12 MOX assemblies in granite

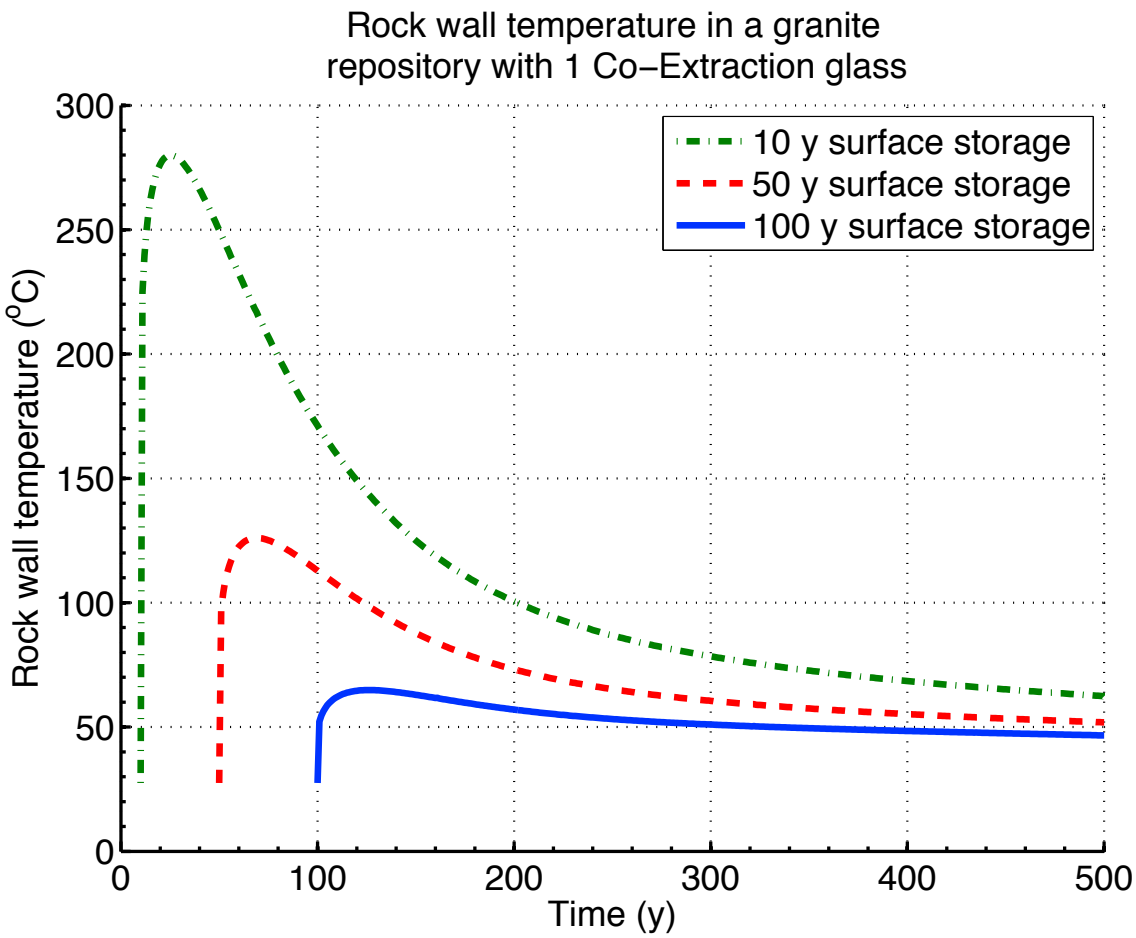

Figure H.3-3 Transient host rock temperature at the calculation radius after storage times of 10, 50 and 100 years for co-extraction-1 in granite

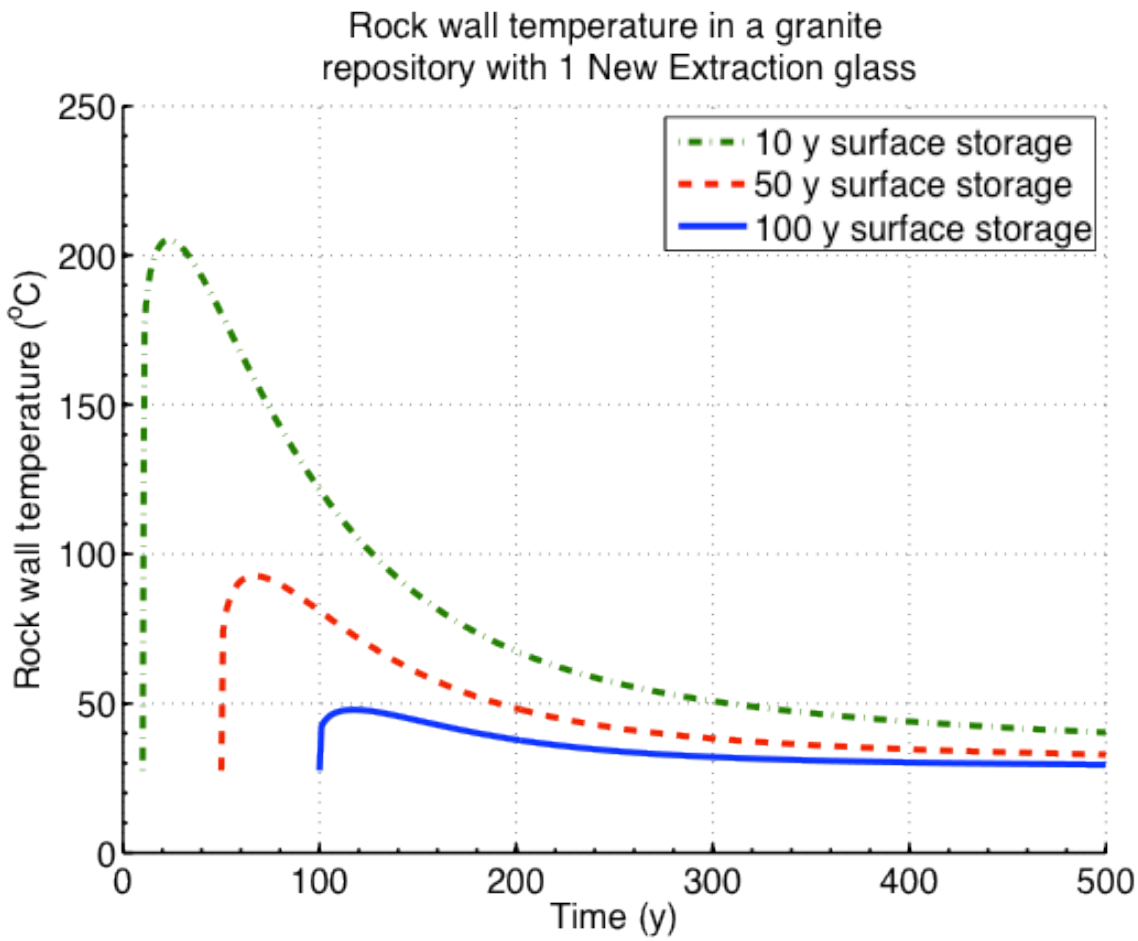

Figure H.3-4 Transient host rock temperature at the calculation radius after storage times of 10, 50 and 100 years for new extraction-1 in granite

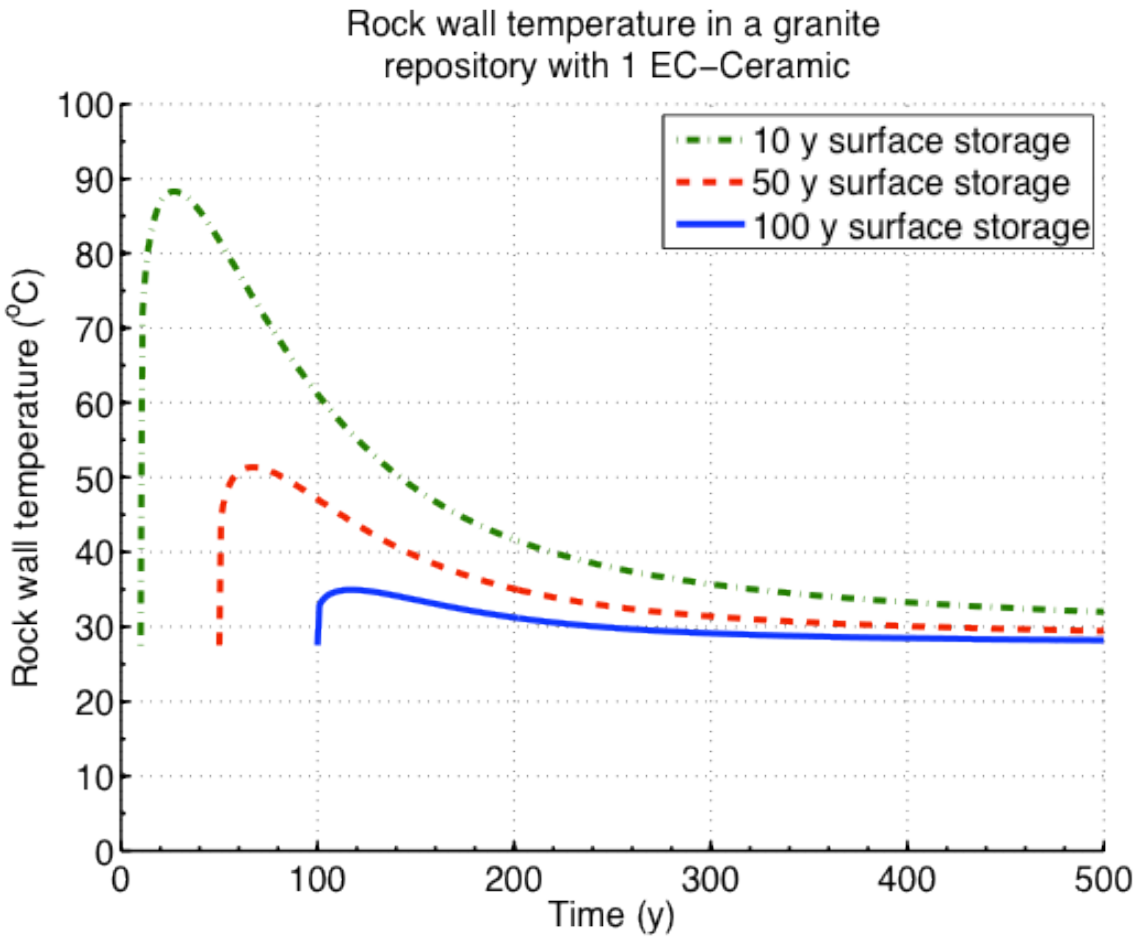

Figure H.3-5 Transient host rock temperature at the calculation radius after storage times of 10, 50 and 100 years for ECC-1 in granite

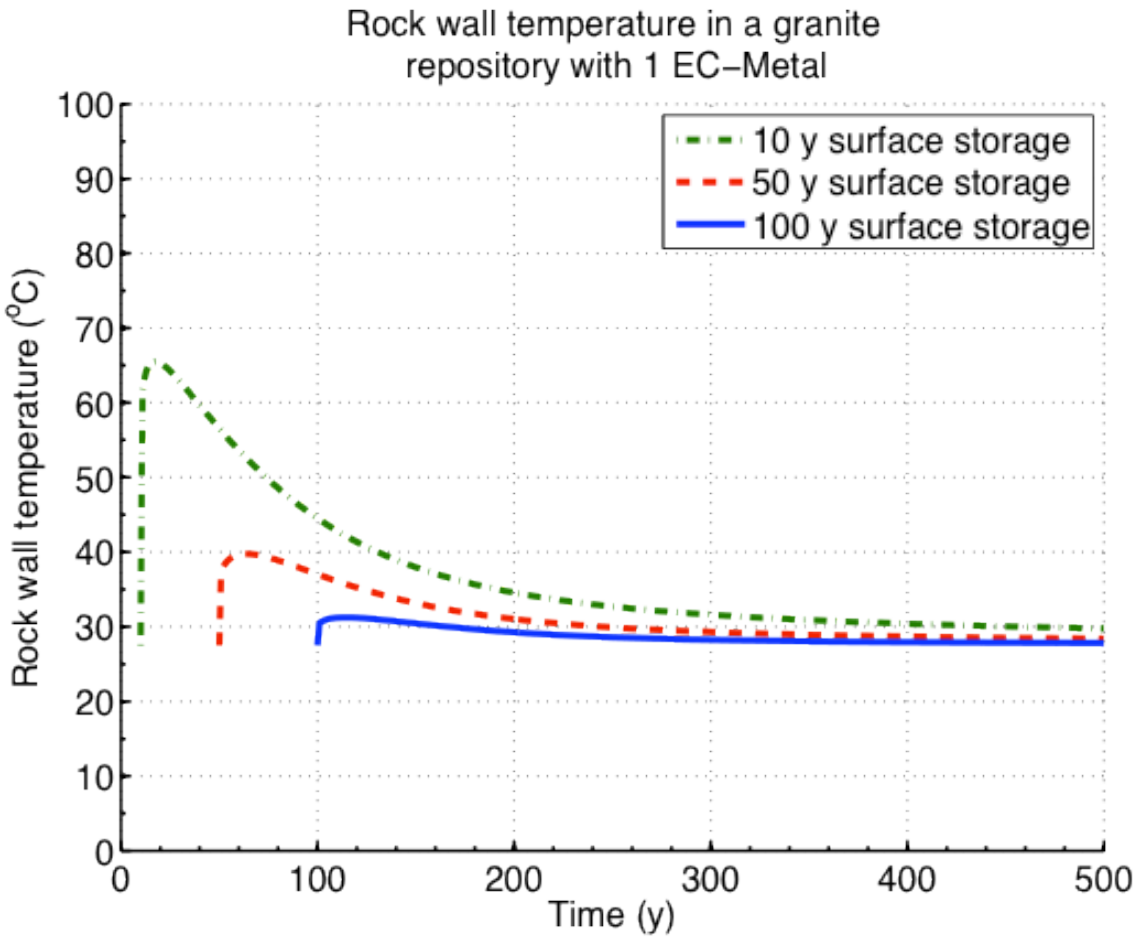

Figure H.3-6 Transient host rock temperature at the calculation radius after storage times of 10, 50 and 100 years for ECM-1 in granite

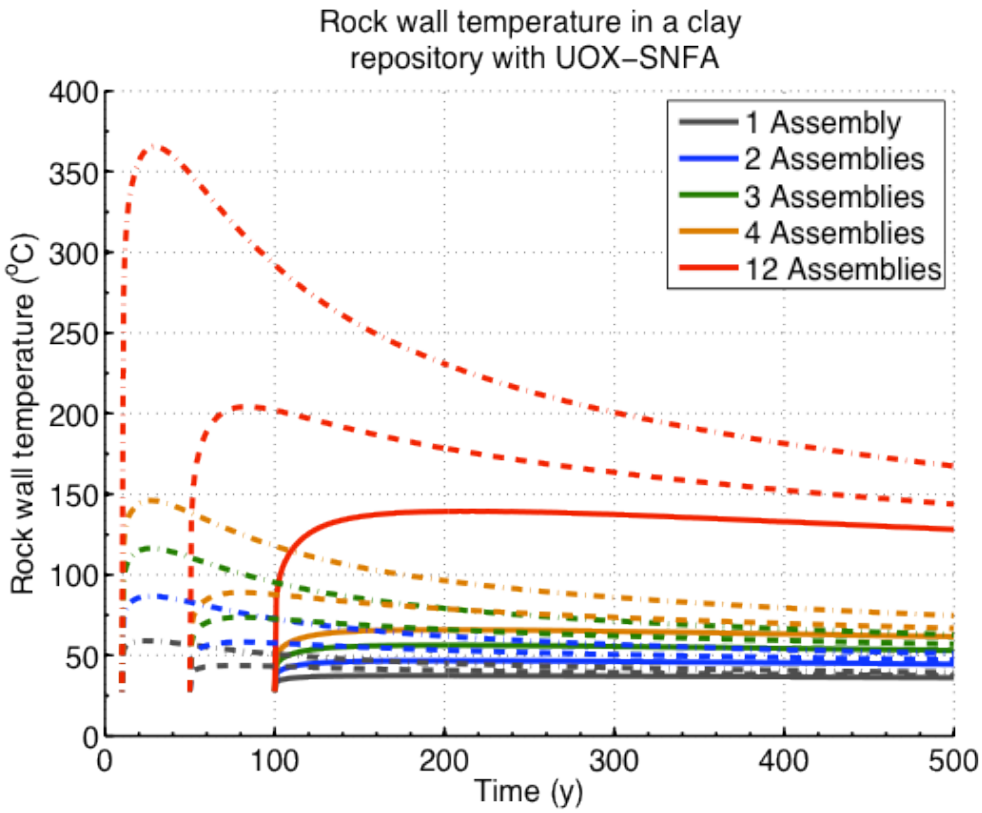

Figure H.3-7 Transient host rock temperature at the calculation radius after storage times of 10, 50 and 100 years for a waste package containing 1, 2, 3, 4 and 12 UOX assemblies in clay

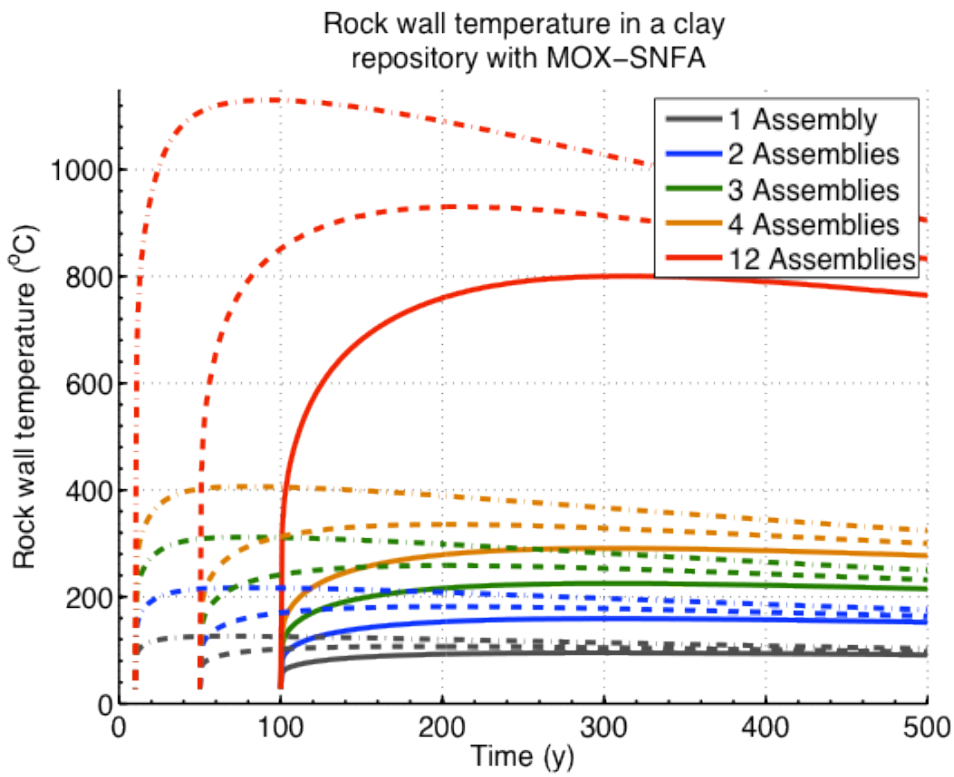

Figure H.3-8 Transient host rock temperature at the calculation radius after storage times of 10, 50 and 100 years for a waste package containing 1, 2, 3, 4 and 12 MOX assemblies in clay

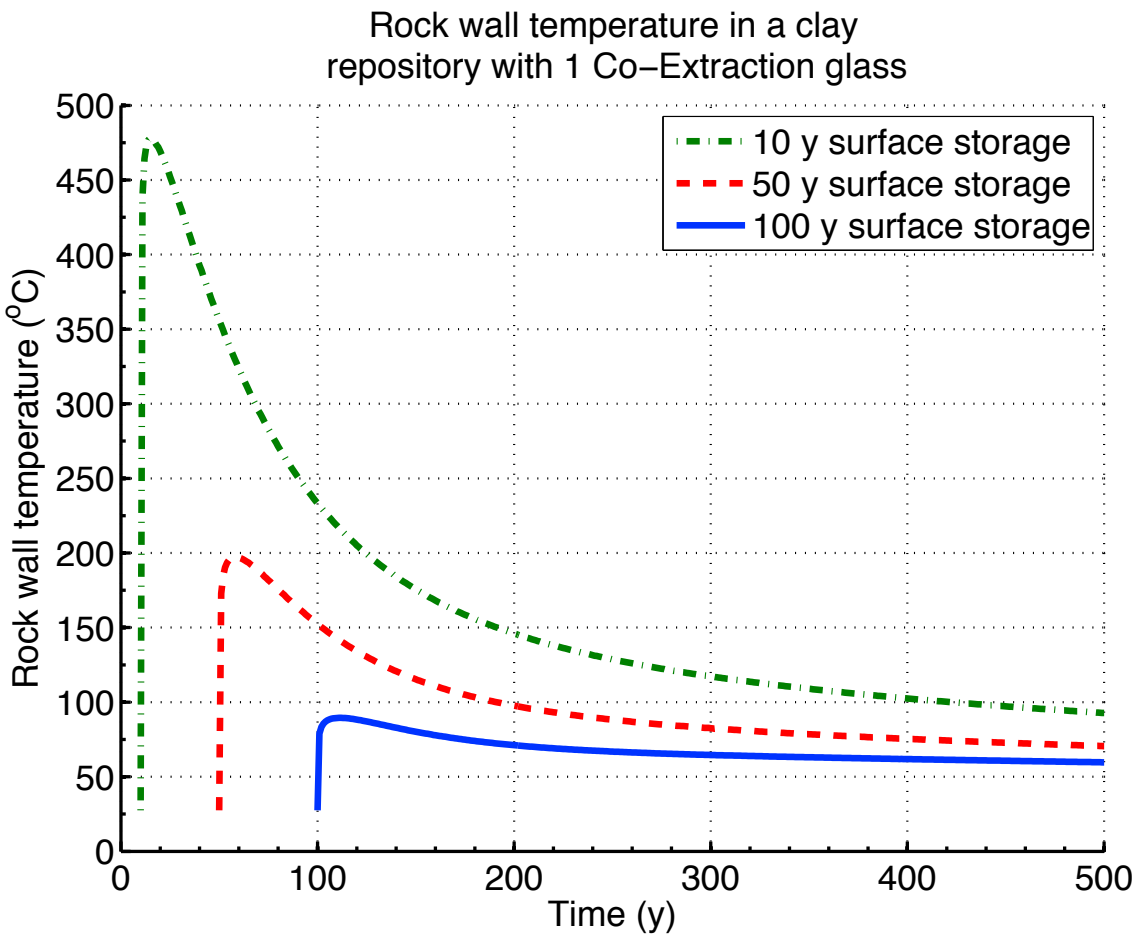

Figure H.3-9 Transient host rock temperature at the calculation radius after storage times of 10, 50 and 100 years for co-extraction-1 in clay

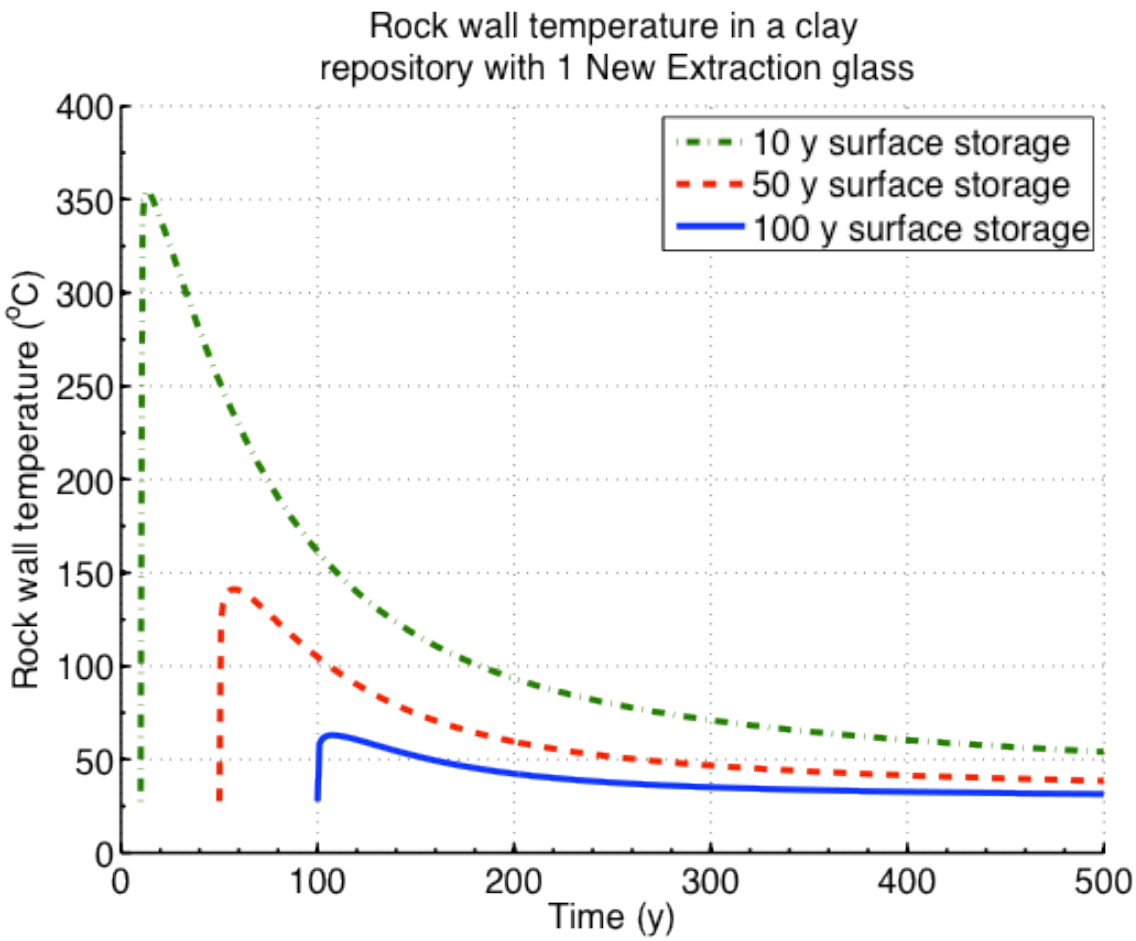

Figure H.3-10 Transient host rock temperature at the calculation radius after storage times of 10, 50 and 100 years for new extraction-1 in clay

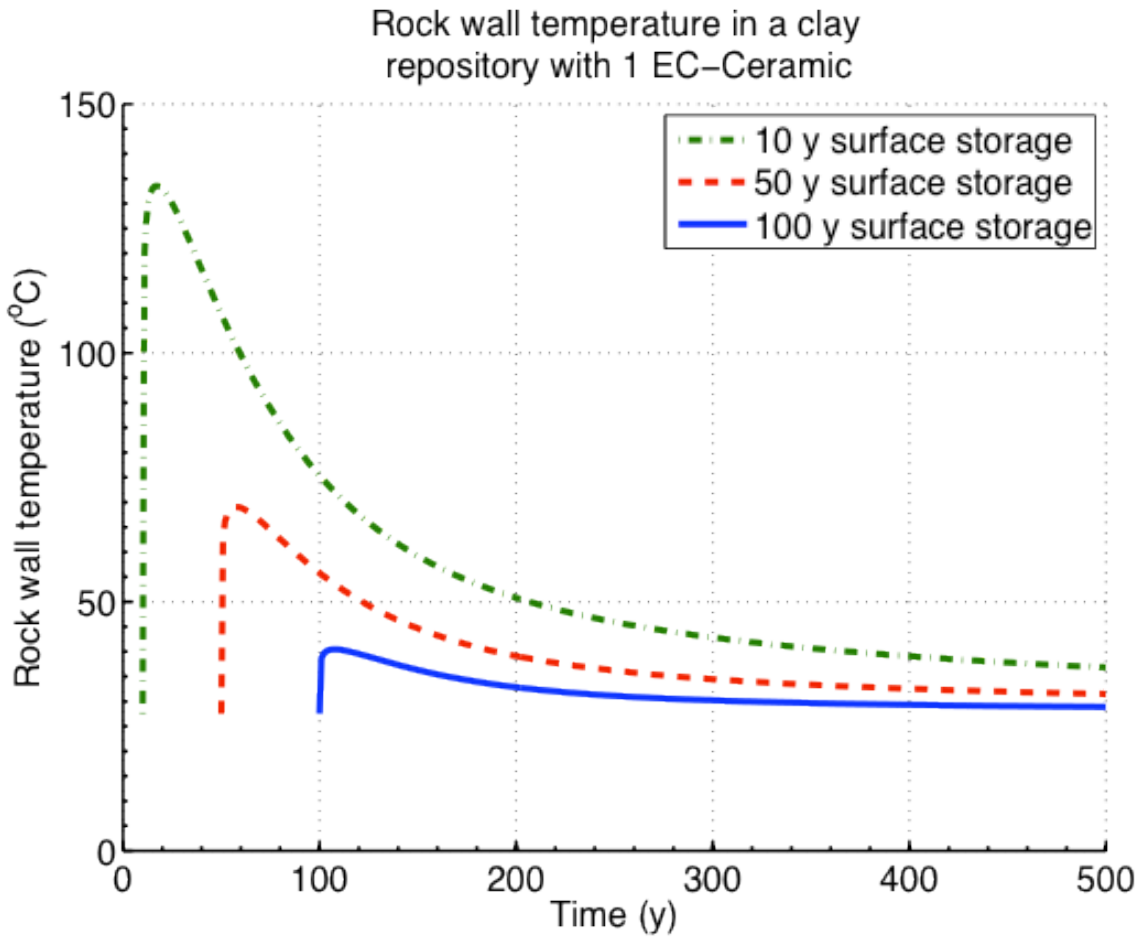

Figure H.3-11 Transient host rock temperature at the calculation radius after storage times of 10, 50 and 100 years for ECC-1 in clay

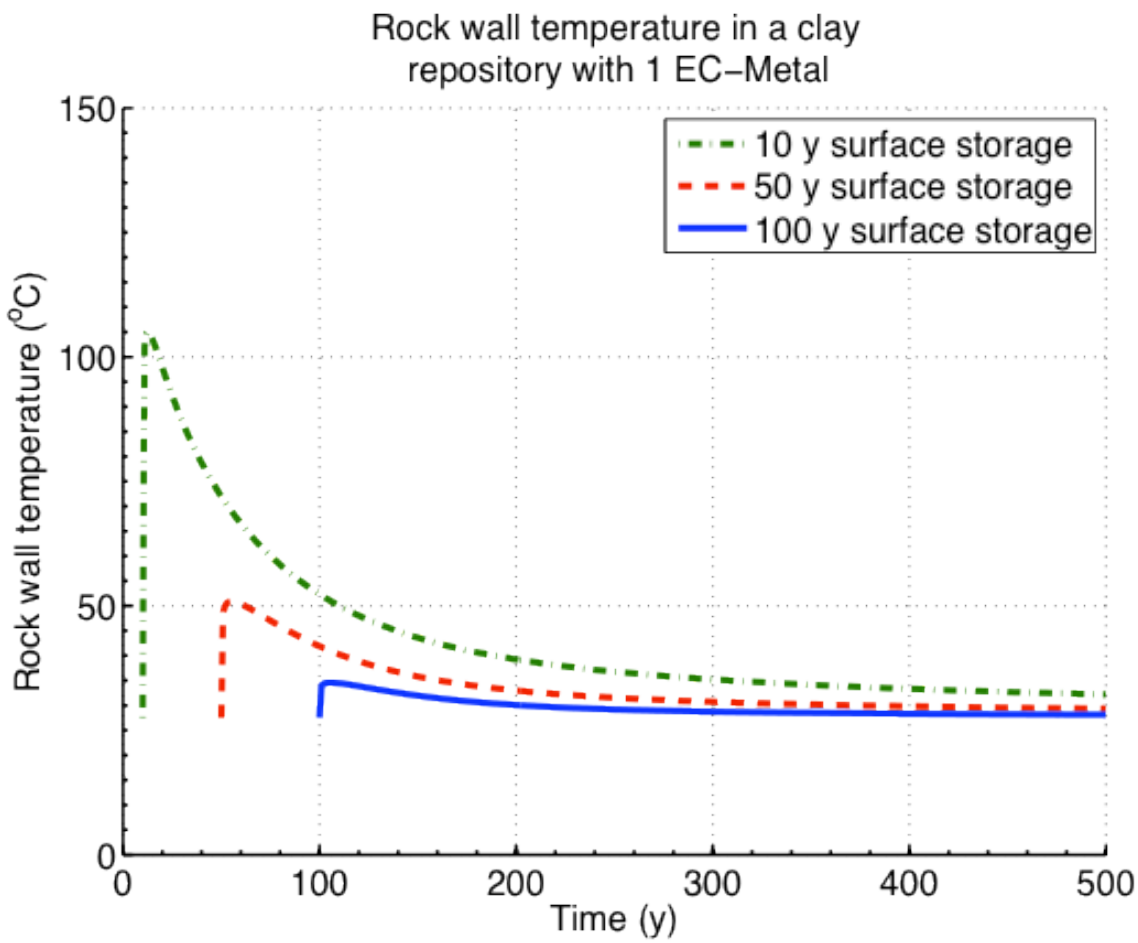

Figure H.3-12 Transient host rock temperature at the calculation radius after storage times of 10, 50 and 100 years for ECM-1 in clay

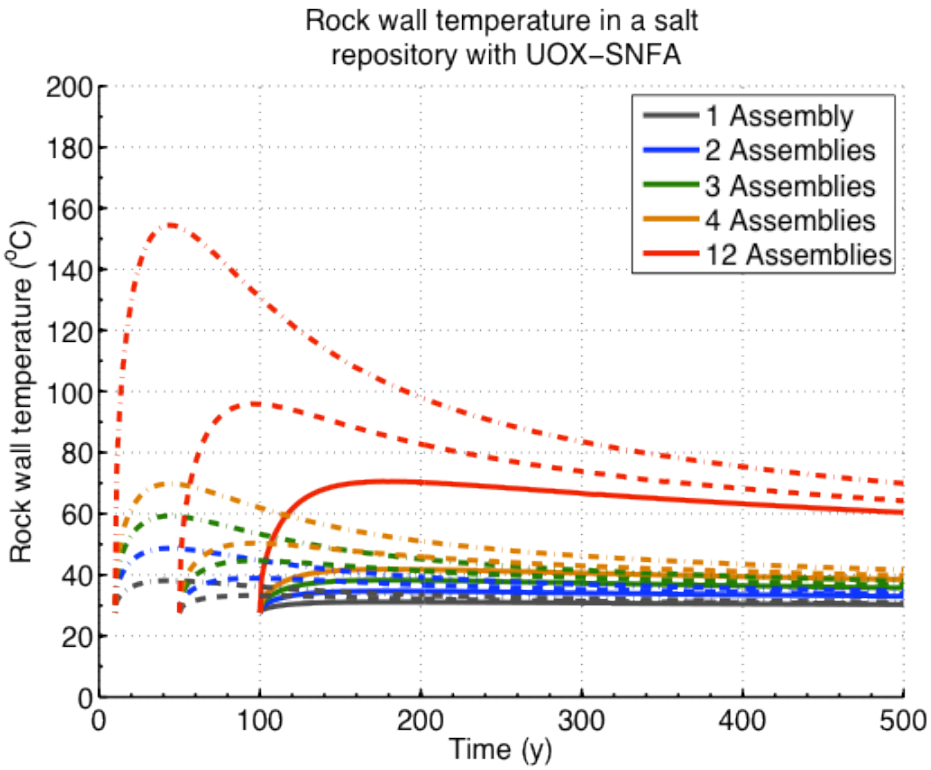

Figure H.3-13 Transient host rock temperature at the calculation radius after storage times of 10, 50 and 100 years for a waste package containing 1, 2, 3, 4 and 12 UOX assemblies in salt

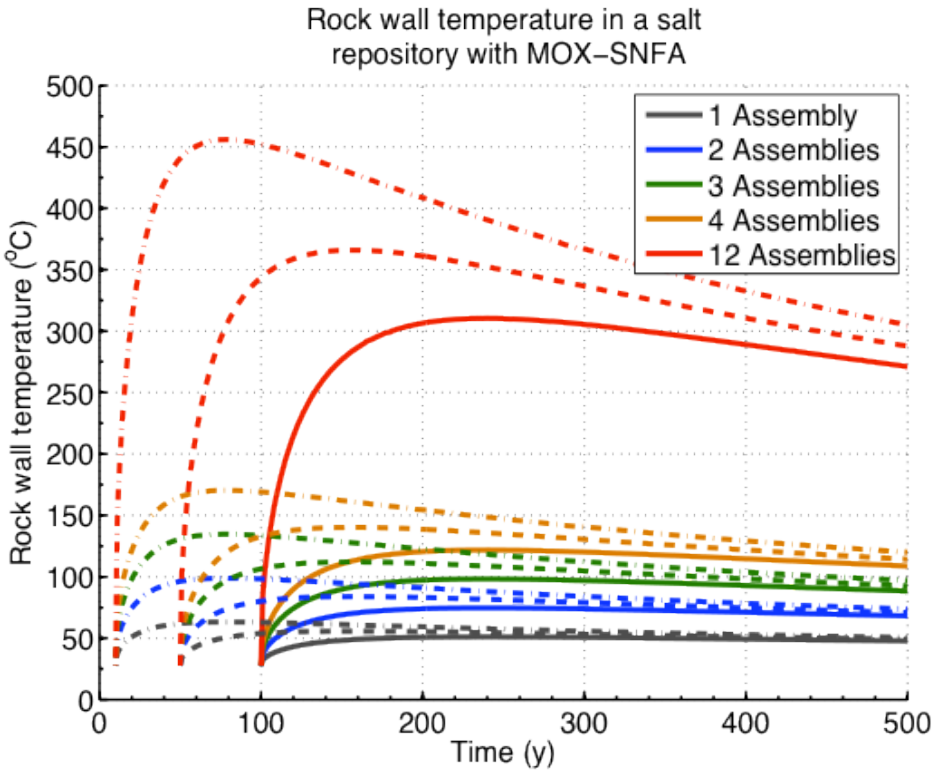

Figure H.3-14 Transient host rock temperature at the calculation radius after storage times of 10, 50 and 100 years for a waste package containing 1, 2, 3, 4 and 12 MOX assemblies in salt

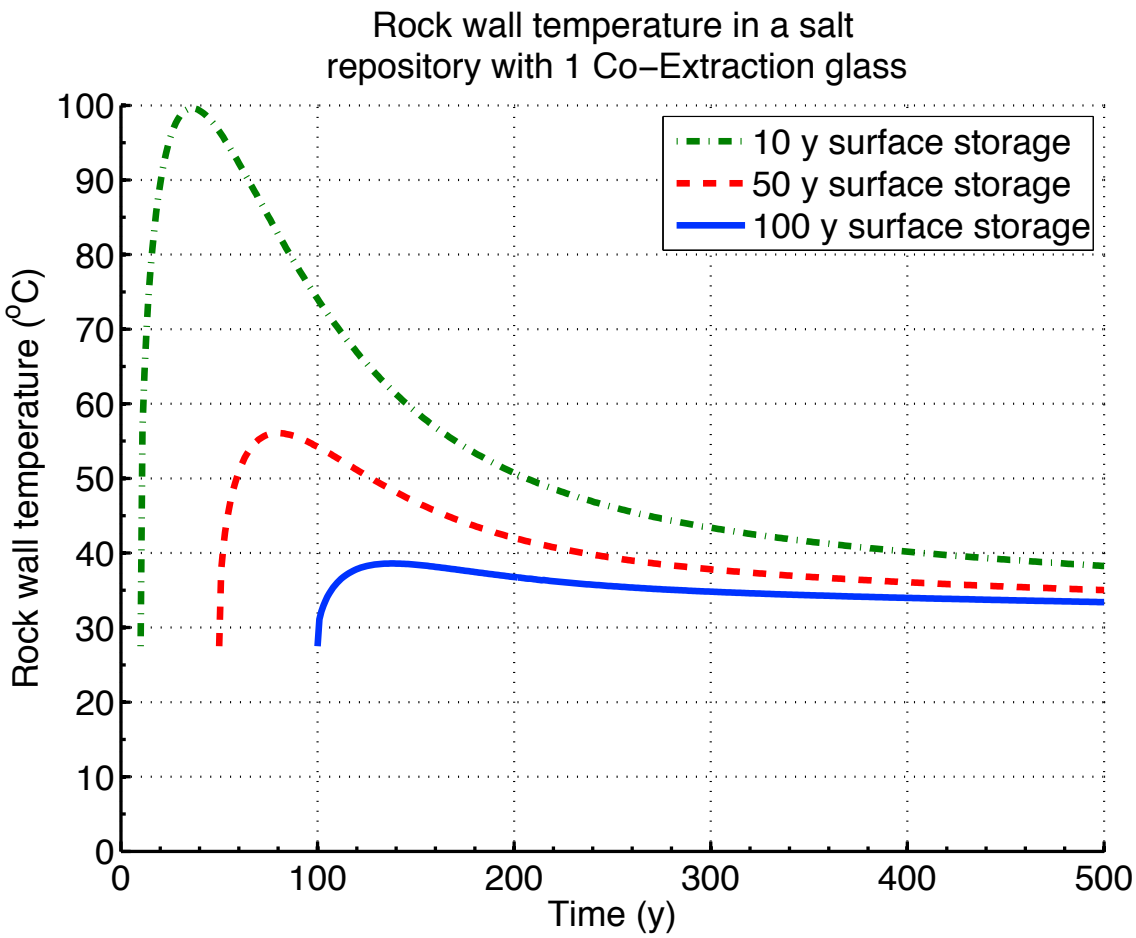

Figure H.3-15 Transient host rock temperature at the calculation radius after storage times of 10, 50 and 100 years for co-extraction-1 in salt

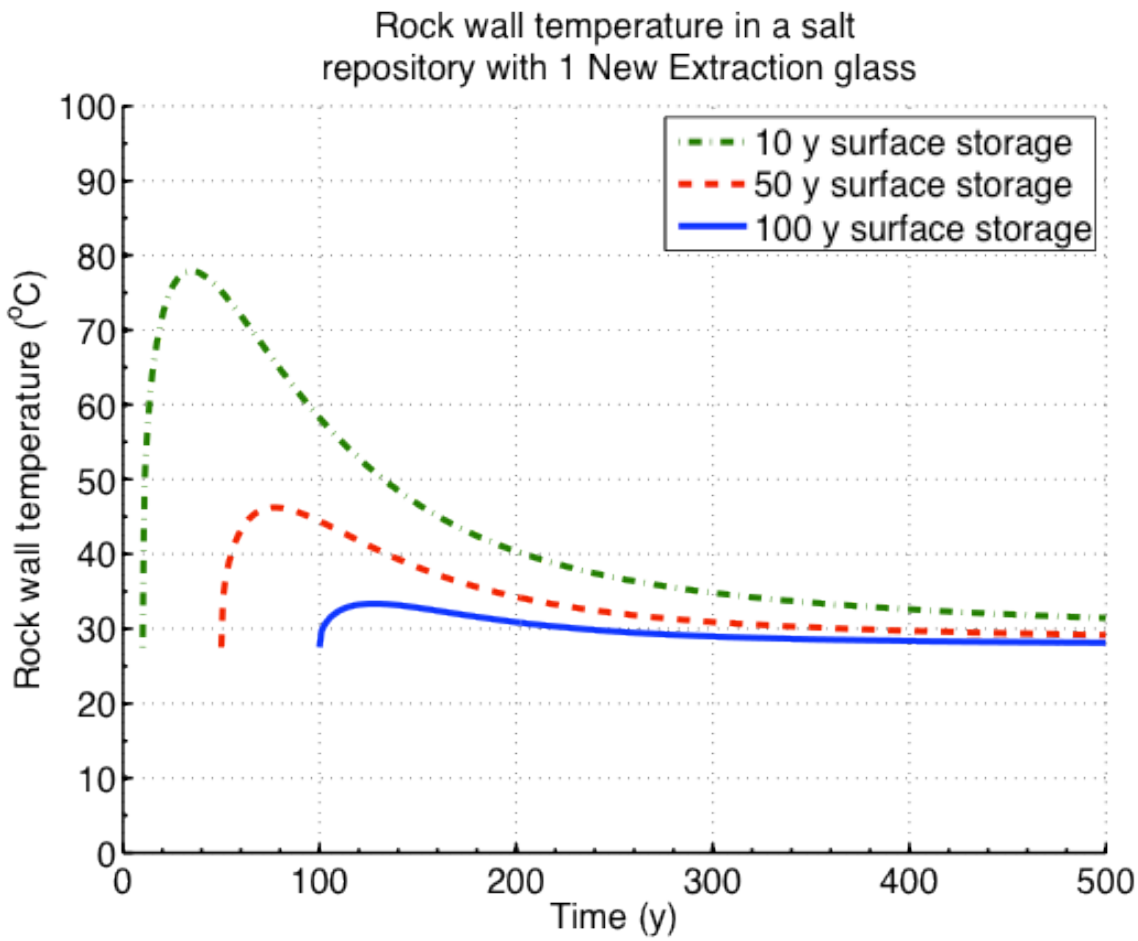

Figure H.3-16 Transient host rock temperature at the calculation radius after storage times of 10, 50 and 100 years for new extraction-1 in salt

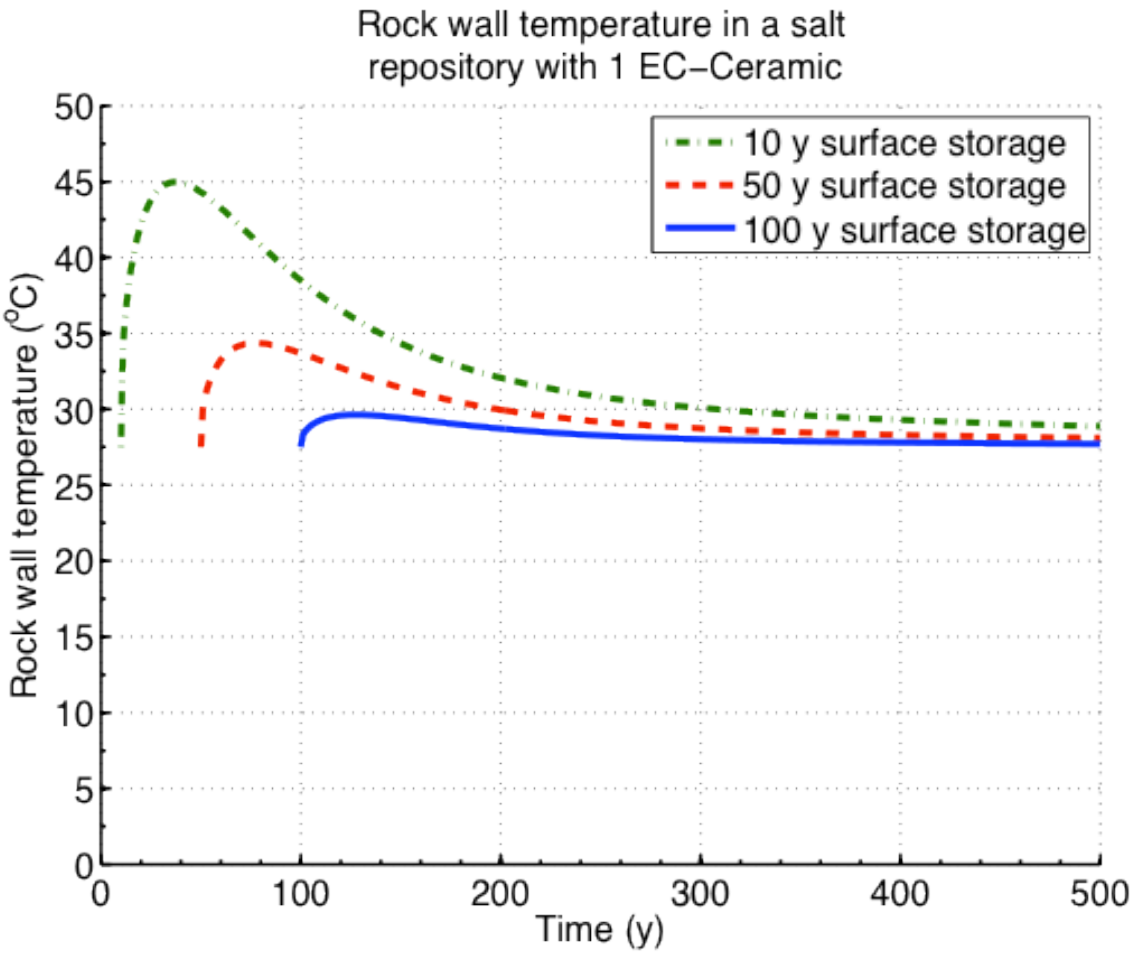

Figure H.3-17 Transient host rock temperature at the calculation radius after storage times of 10, 50 and 100 years for ECC-1 in salt

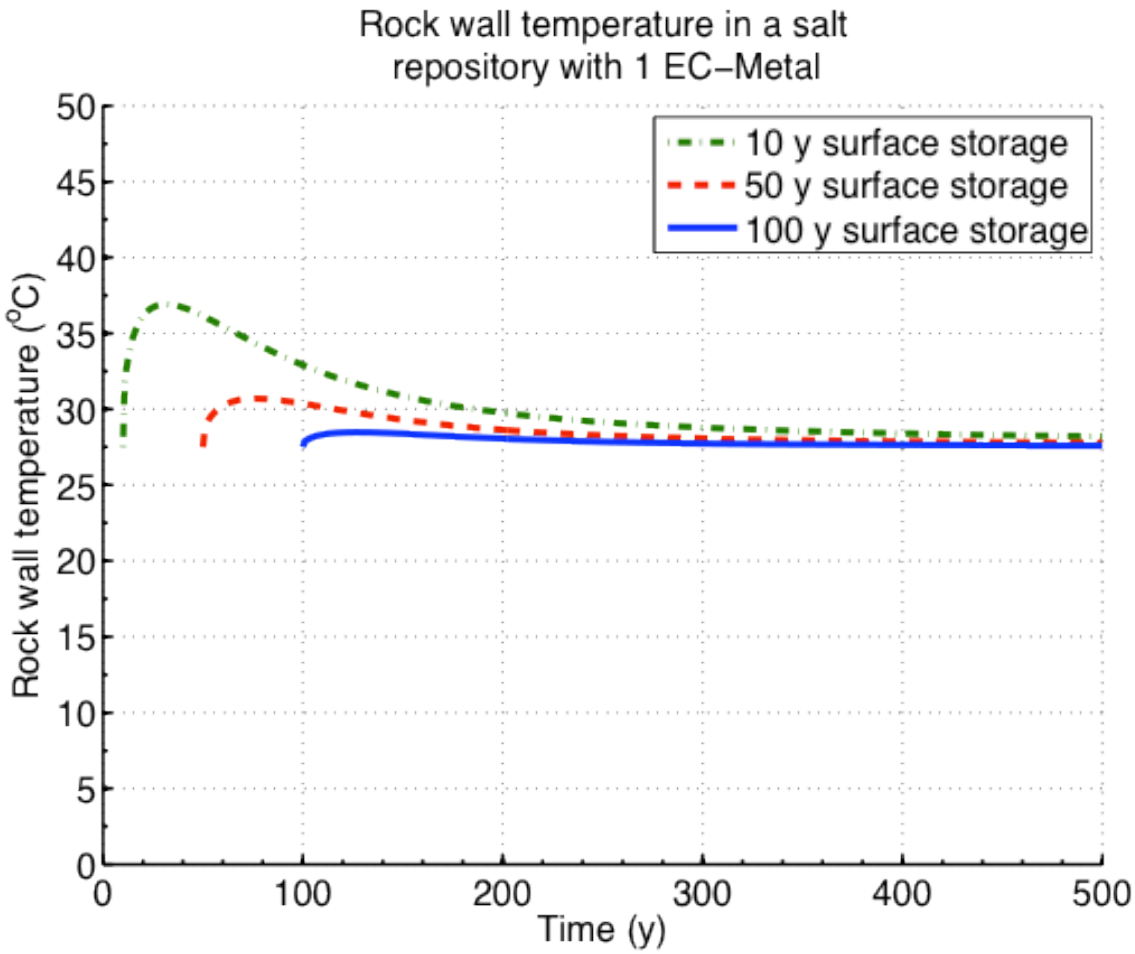

Figure H.3-18 Transient host rock temperature at the calculation radius after storage times of 10, 50 and 100 years for ECM-1 in salt

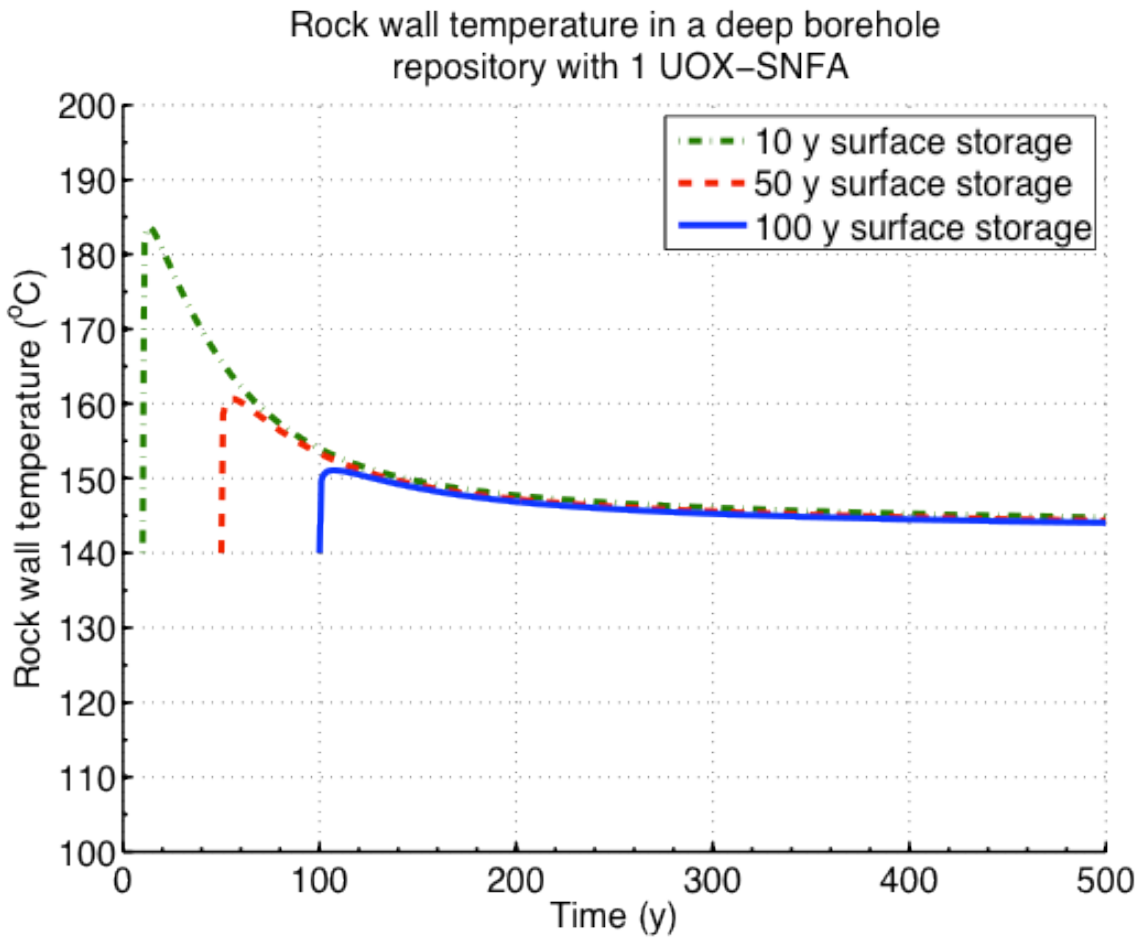

Figure H.3-19 Transient host rock temperature at the calculation radius after storage times of 10, 50 and 100 years for UOX-1 in a deep borehole

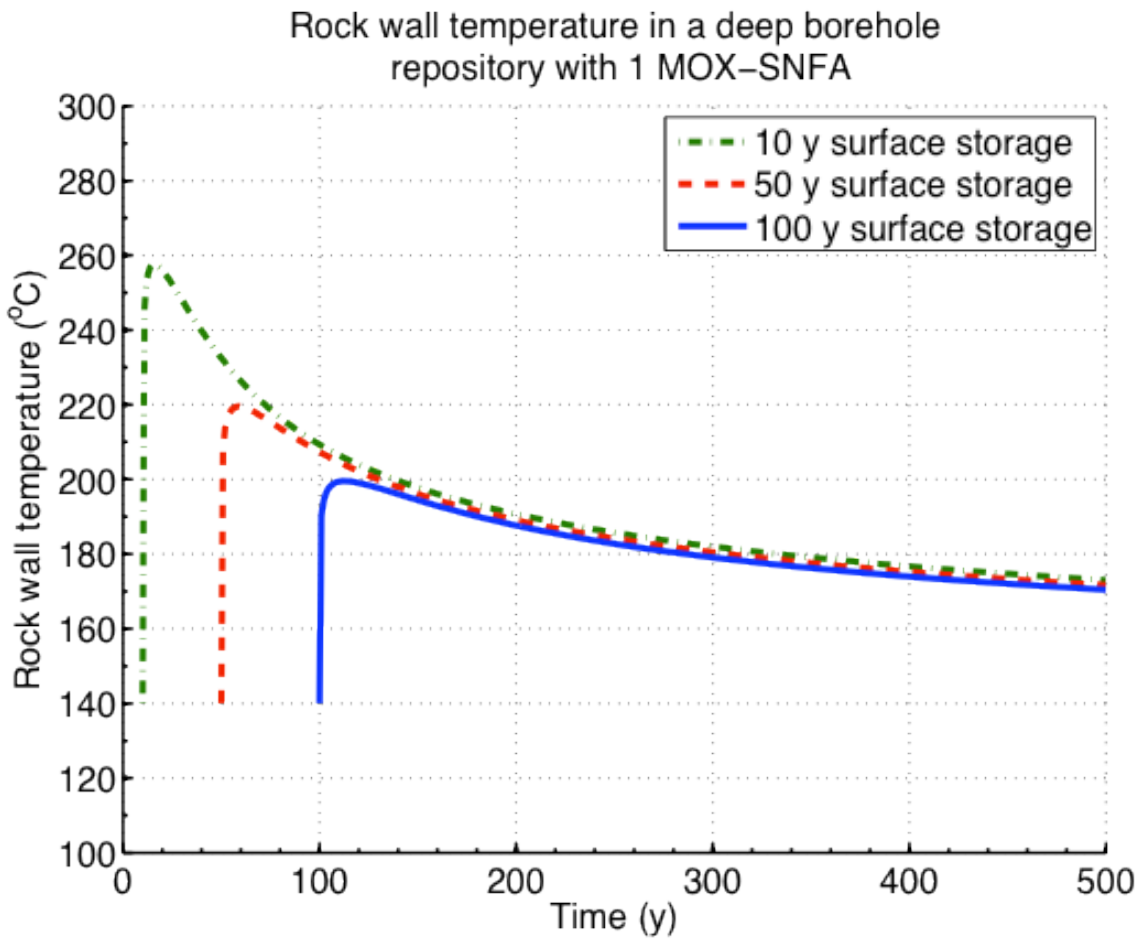

Figure H.3-20 Transient host rock temperature at the calculation radius after storage times of 10, 50 and 100 years for MOX-1 in a deep borehole

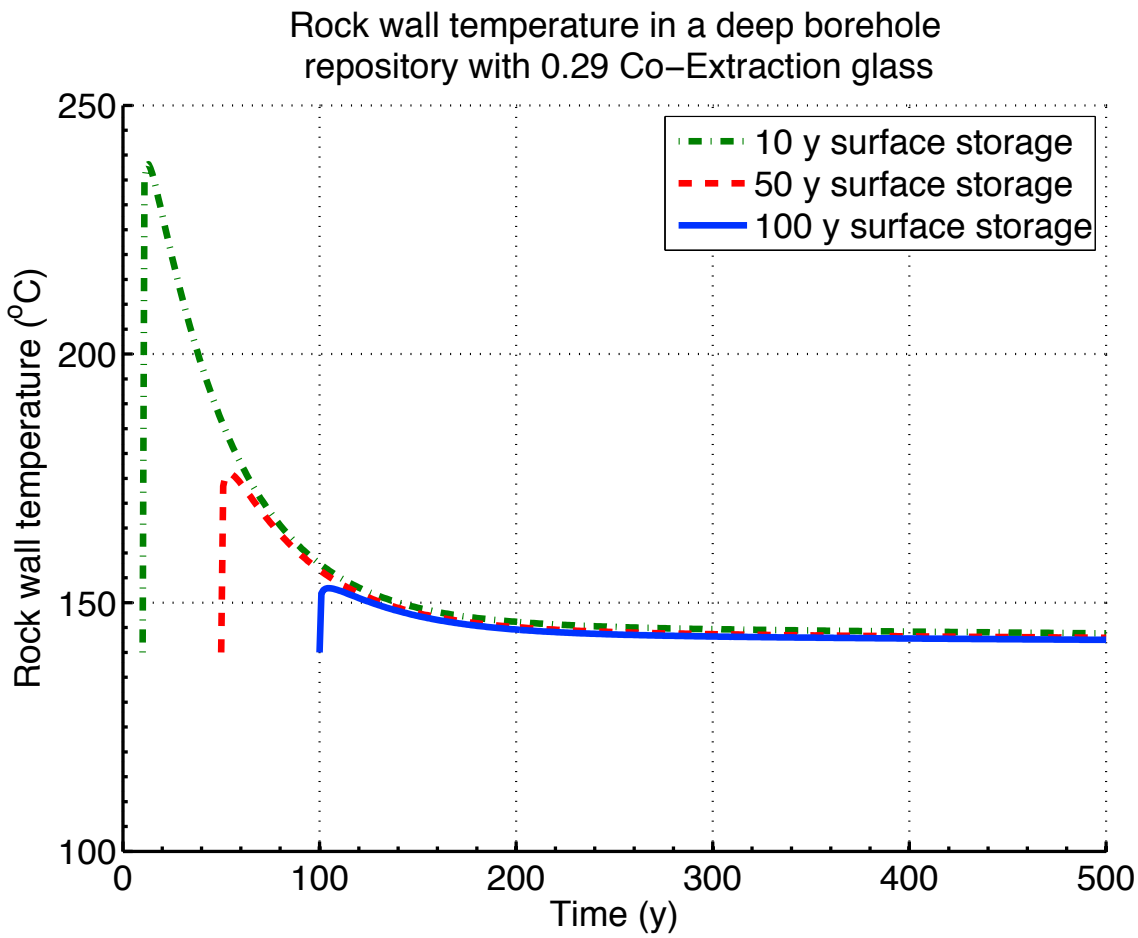

Figure H.3-21 Transient host rock temperature at the calculation radius after storage times of 10, 50 and 100 years for co-extraction-0.291 in a deep borehole

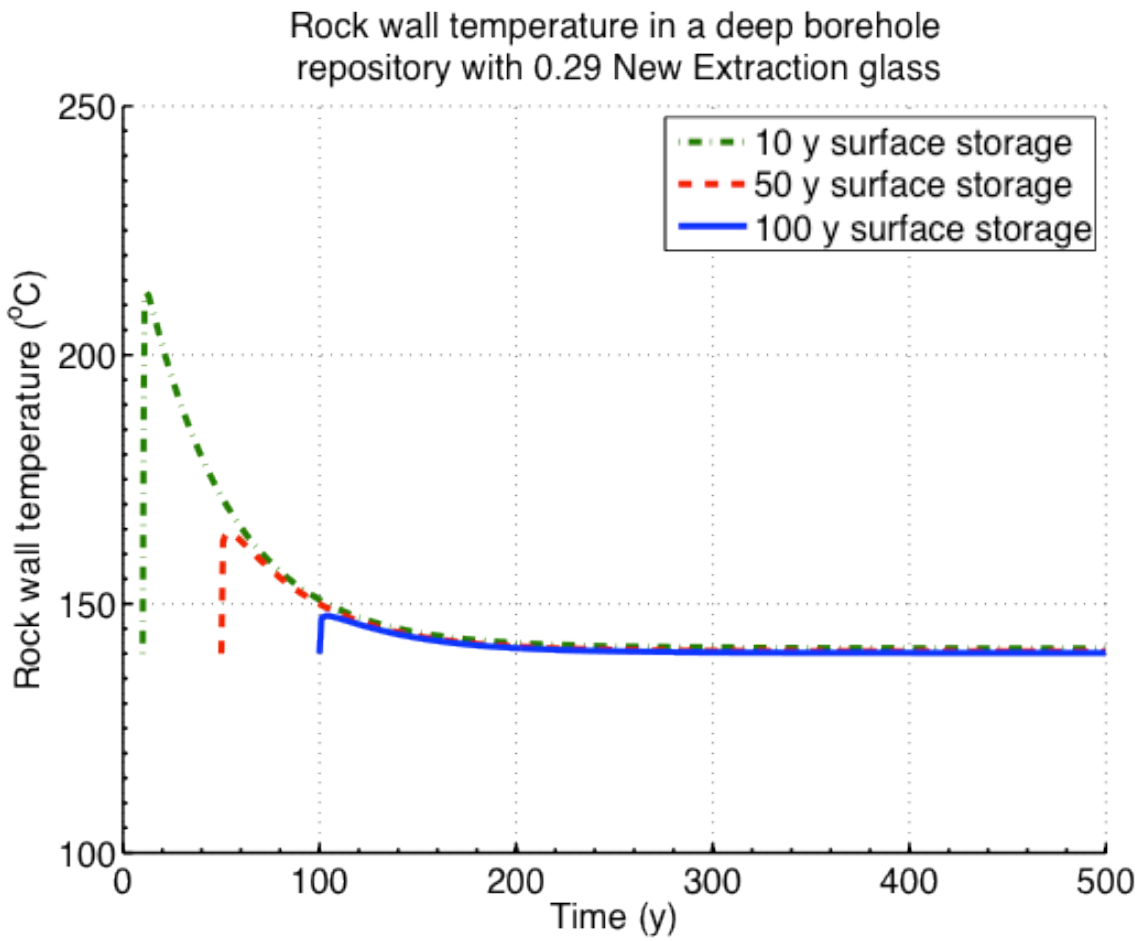

Figure H.3-22 Transient host rock temperature at the calculation radius after storage times of 10, 50 and 100 years for new extraction-0.291 in a deep borehole

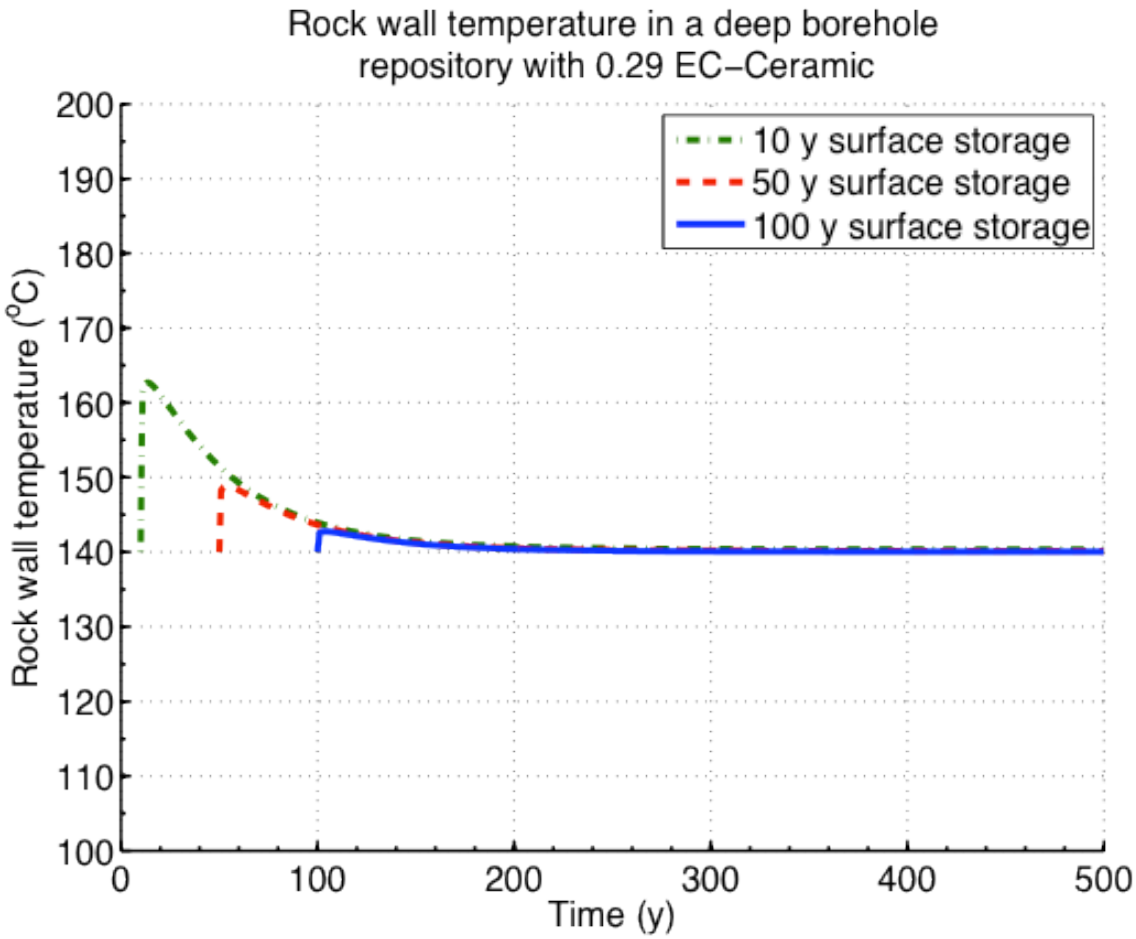

Figure H.3-23 Transient host rock temperature at the calculation radius after storage times of 10, 50 and 100 years for ECC-0.291 in a deep borehole

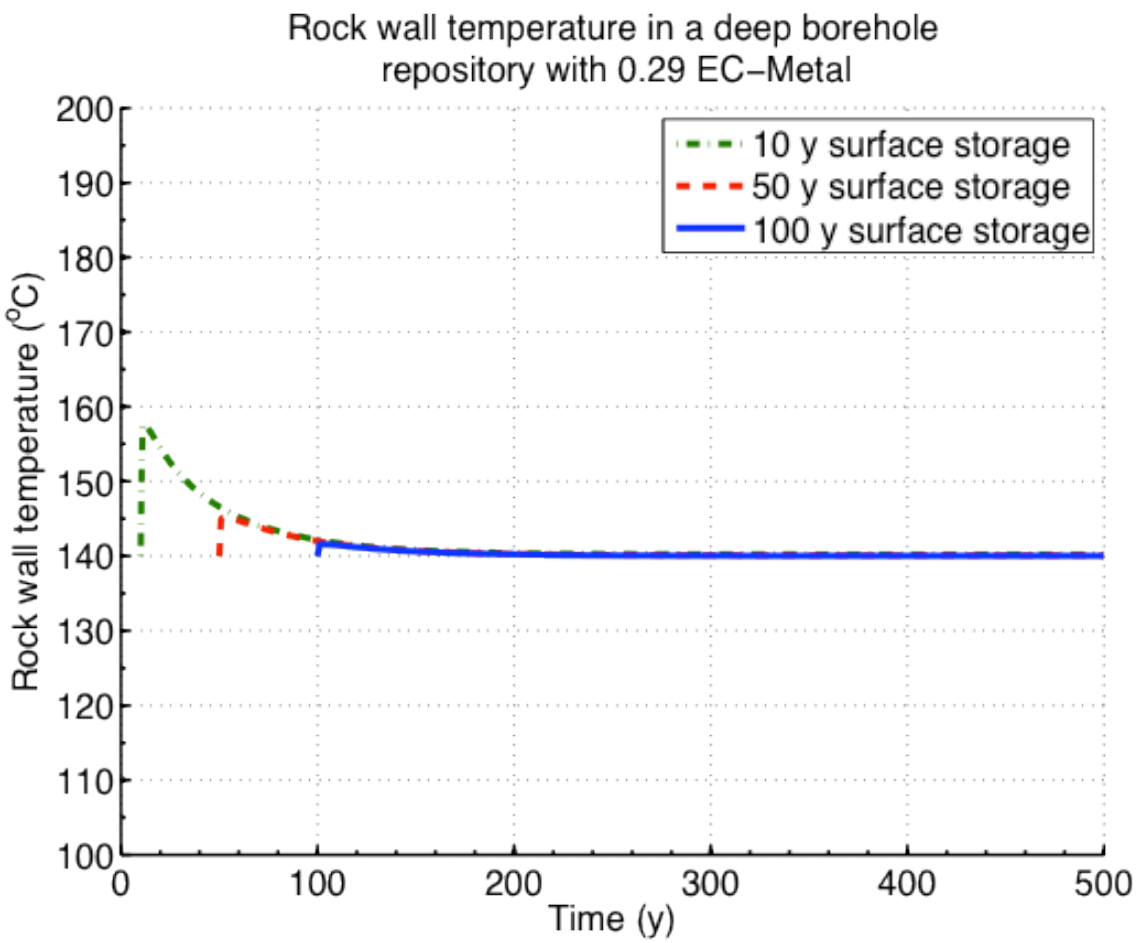

Figure H.3-24 Transient host rock temperature at the calculation radius after storage times of 10, 50 and 100 years for ECM-0.291 in a deep borehole

H.4 WASTE PACKAGE SURFACE TEMPERATURE

The calculation radii for the four media are as follows:

- Granite: SNF 0.83 m, HLW 0.76 m
- Clay: SNF 1.32 m, HLW 0.37 m
- Salt: SNF and HLW 4 m
- Deep borehole: SNF 0.19 m, HLW 0.20 m

The following temperature limits were applied at the interface between the waste package surface and the EBS (or rock wall, depending on design):

- Granite: 100°C. This is based on a bentonite layer near the waste package surface
- Clay: 100°C. This is based on the host rock for the HLW cases, and on a bentonite layer for the UOX and MOX cases
- Salt: 200°C. This is based on the bulk salt
- A limit for deep borehole remains to be determined.

These temperature limits are not final, and may be lower than the limits that will eventually be set after site investigations and in license applications.

This section shows the results of a steady state calculation at each point in time inward from the calculation radius to the outer surface of the waste package. The calculation uses the temperature result from the homogeneous calculation in Section H.3 above. The calculation assumes that the waste package heat travels through the calculation radius with no storage or heat loss within the interior layers of the EBS.

The number of assemblies or canisters per waste package are as defined in Section H.2, except as indicated in the figure captions below.

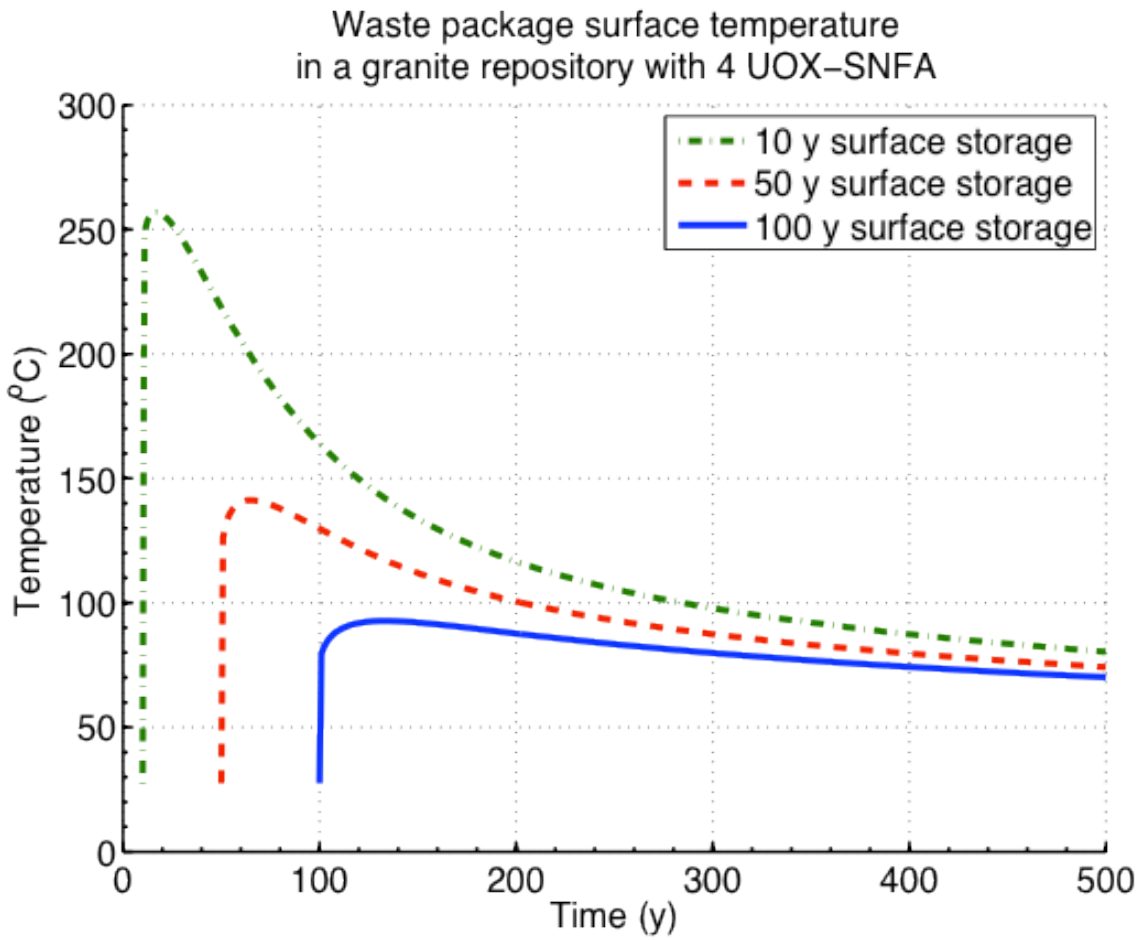

Figure H.4-1 Calculated waste package temperature after storage times of 10, 50 and 100 years for UOX-4 in granite

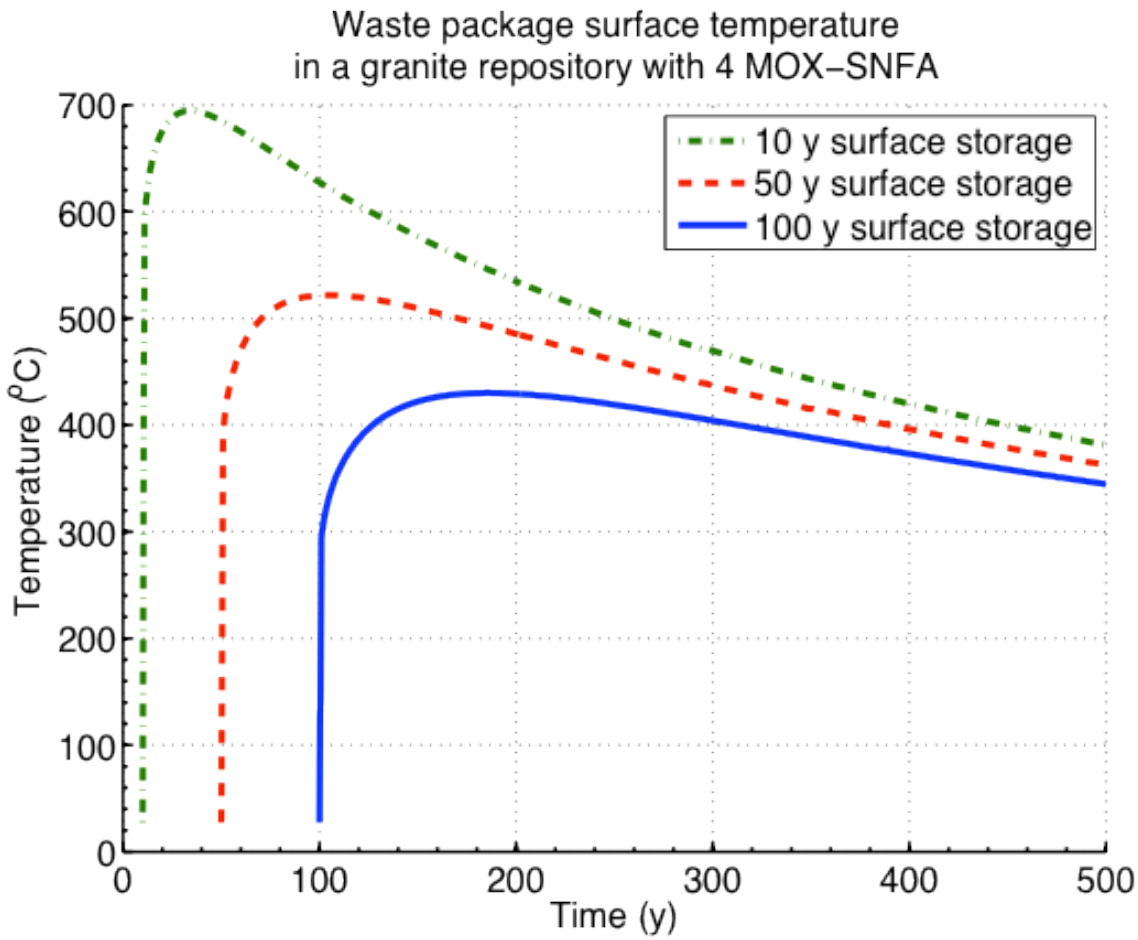

Figure H.4-2 Calculated waste package temperature after storage times of 10, 50 and 100 years for MOX-4 in granite

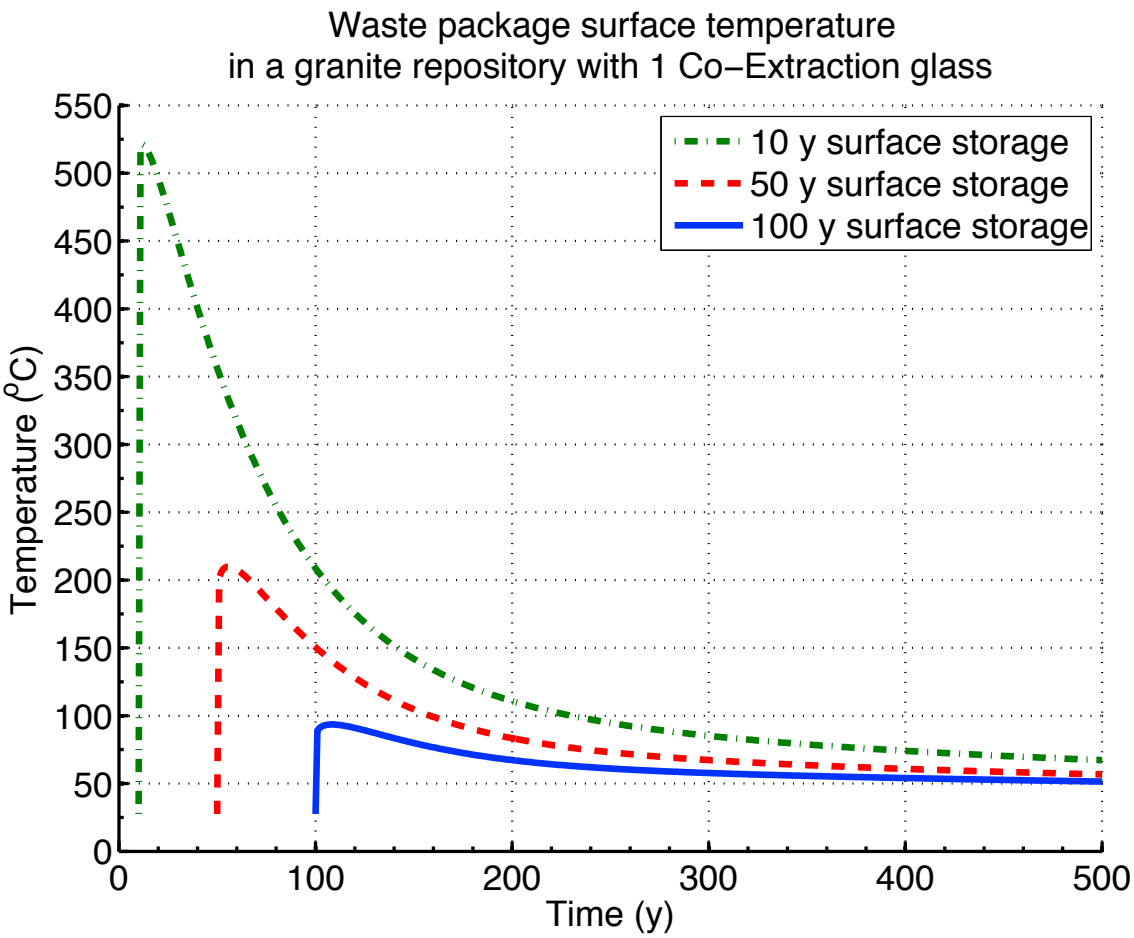

Figure H.4-3 Calculated waste package temperature after storage times of 10, 50 and 100 years for co-extraction-1 in granite

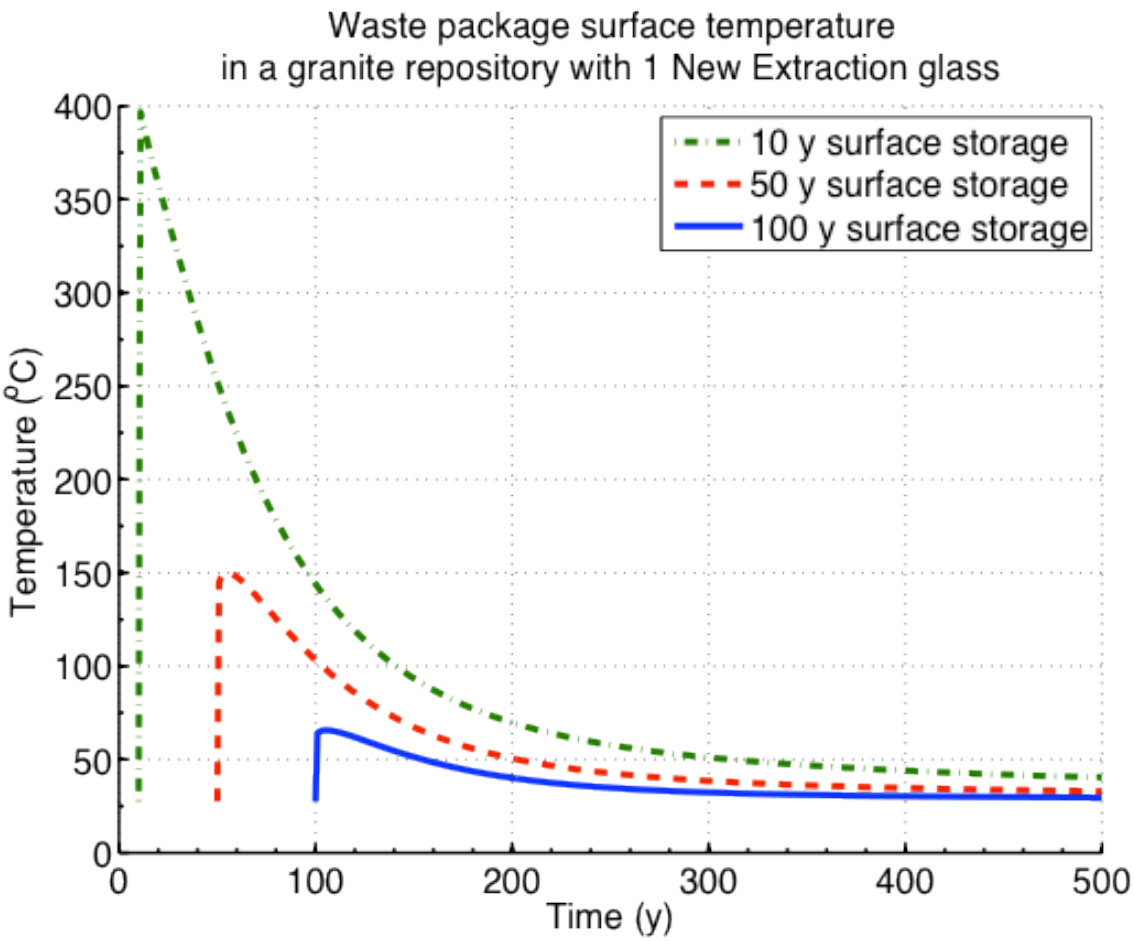

Figure H.4-4 Calculated waste package temperature after storage times of 10, 50 and 100 years for new extraction-1 in granite

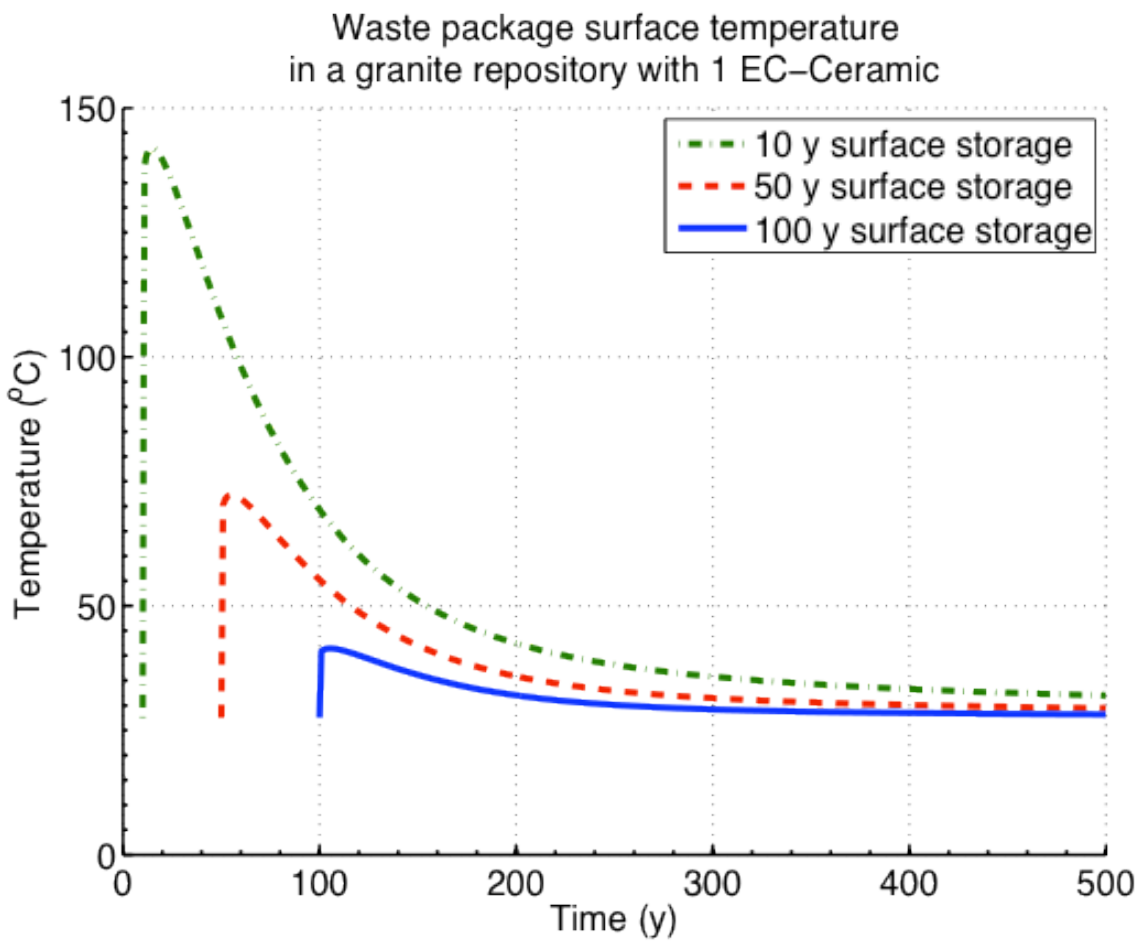

Figure H.4-5 Calculated waste package temperature after storage times of 10, 50 and 100 years for ECC-1 in granite

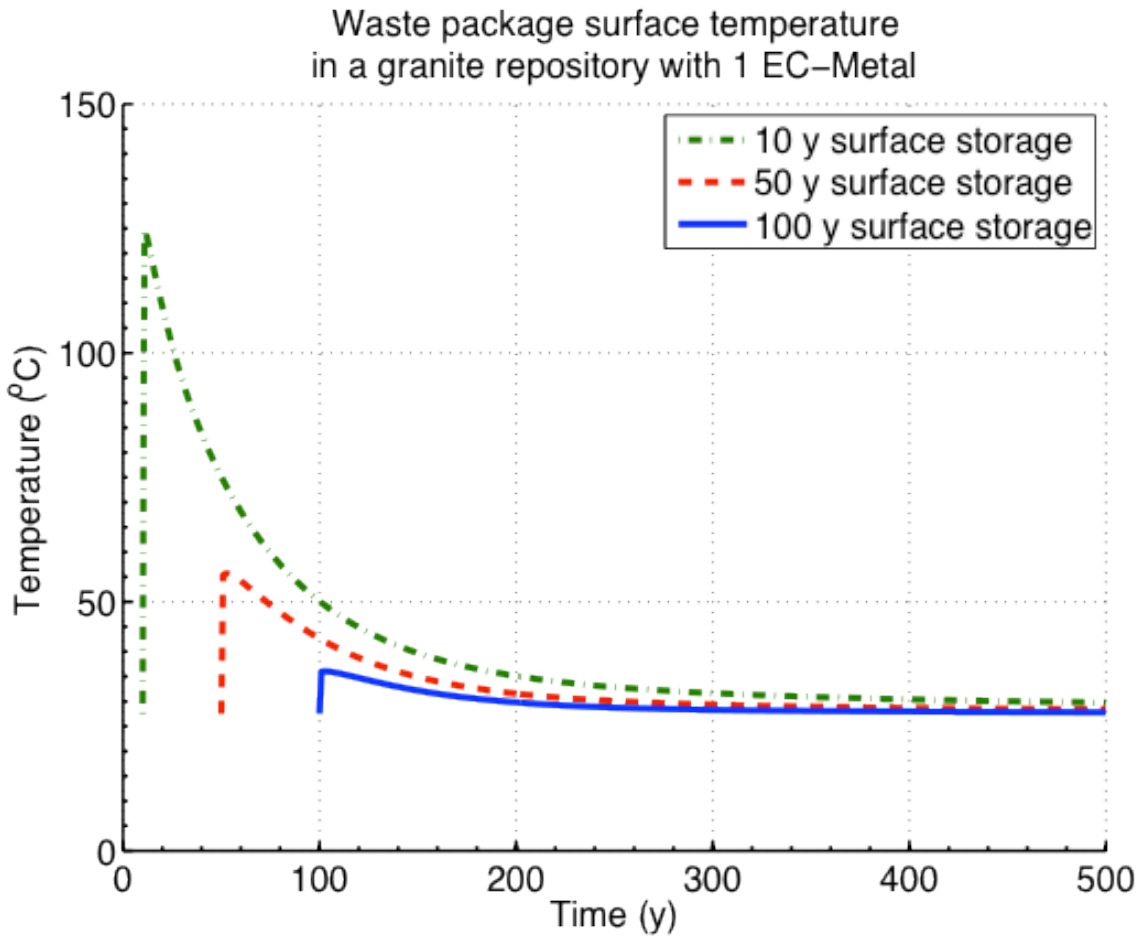

Figure H.4-6 Calculated waste package temperature after storage times of 10, 50 and 100 years for ECM-1 in granite

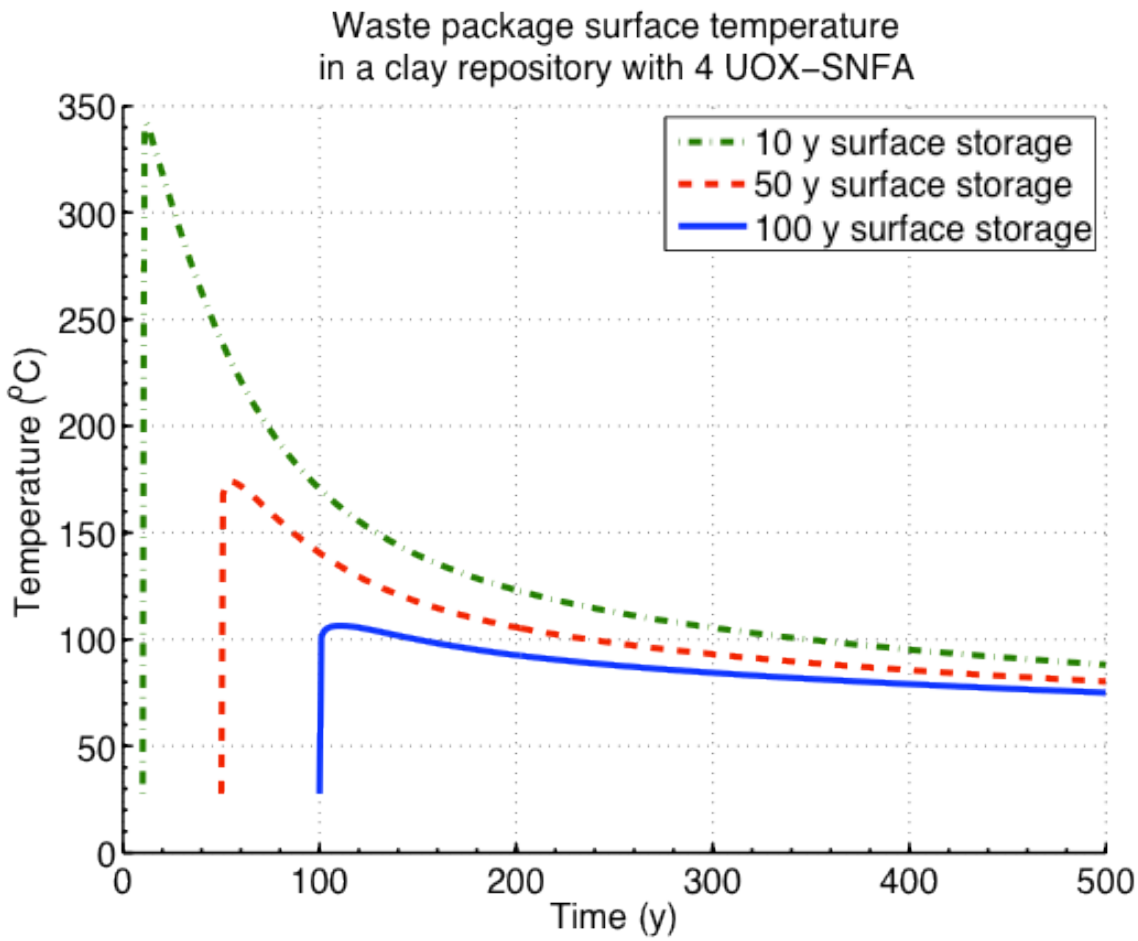

Figure H.4-7 Calculated waste package temperature after storage times of 10, 50 and 100 years for UOX-4 in clay

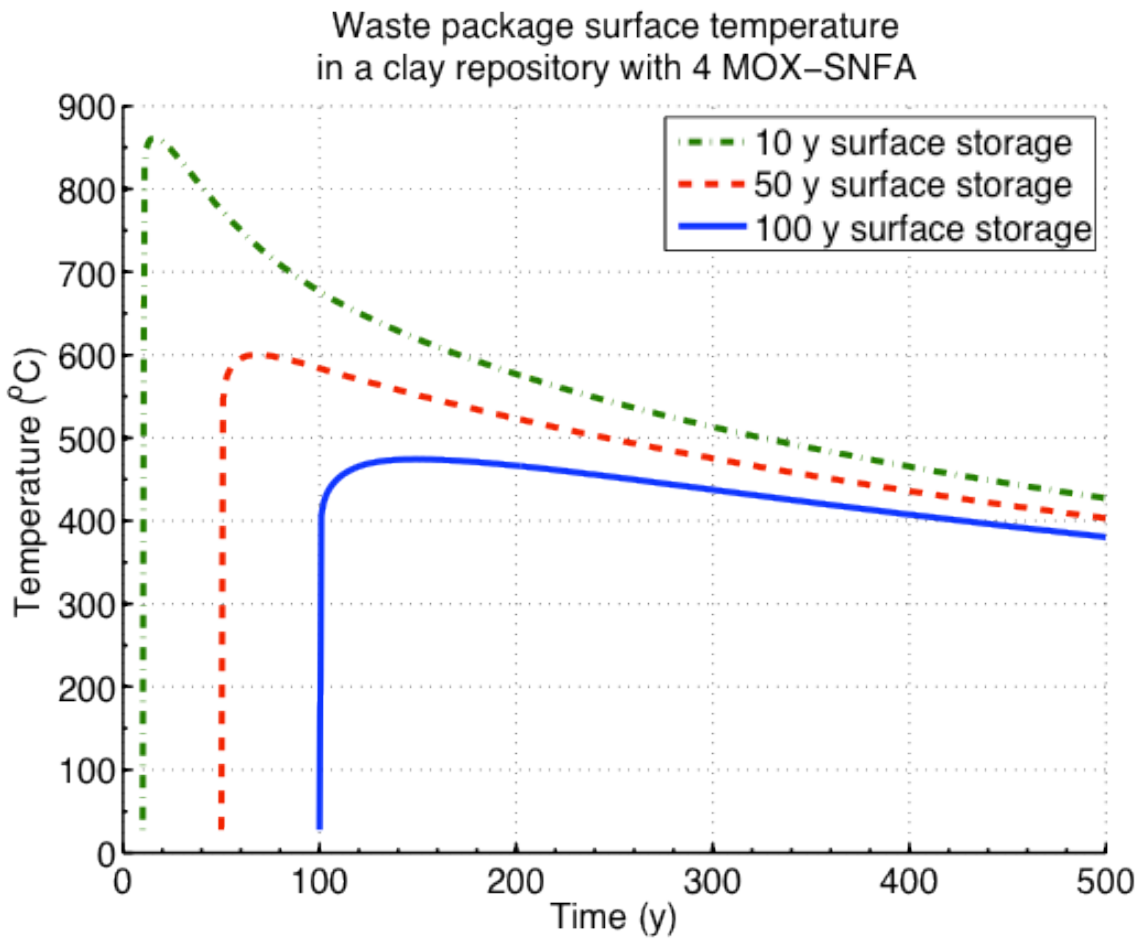

Figure H.4-8 Calculated waste package temperature after storage times of 10, 50 and 100 years for MOX-4 in clay

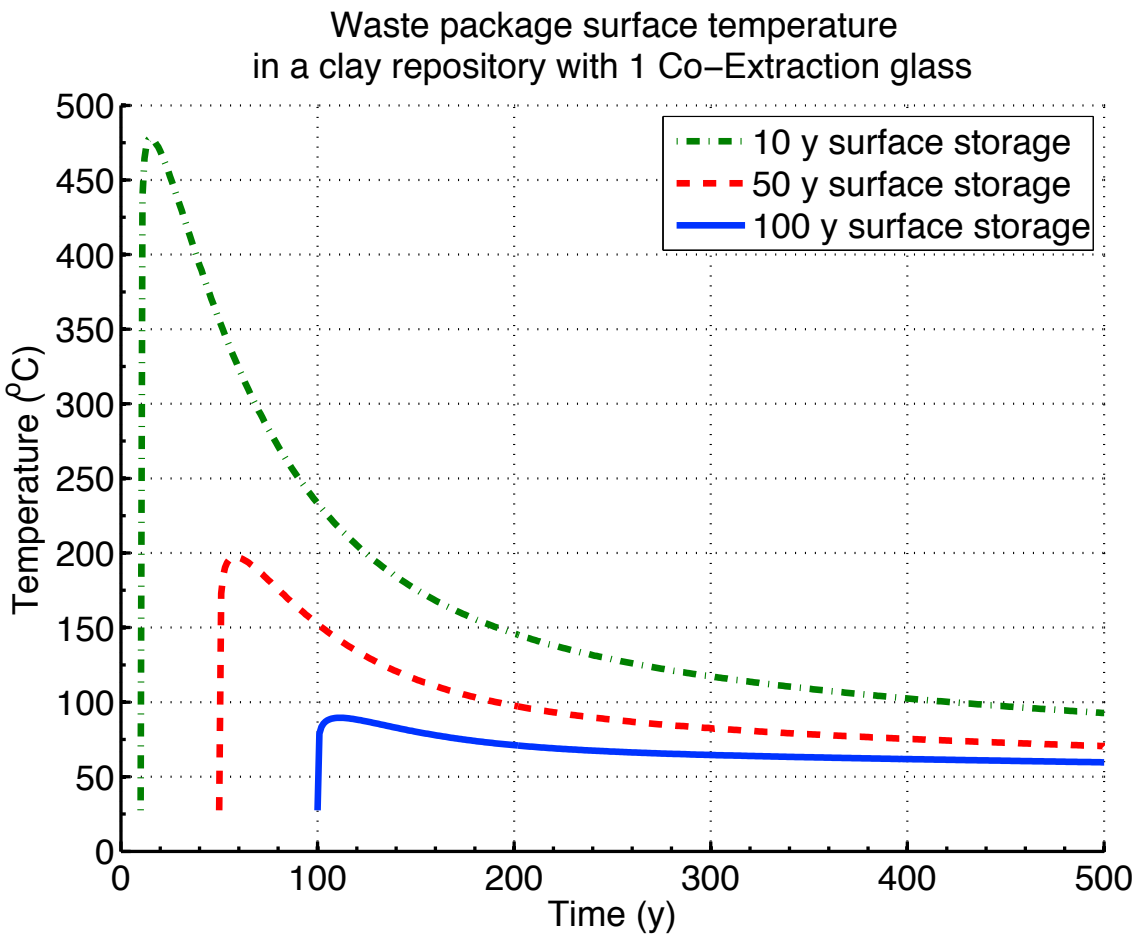

Figure H.4-9 Calculated waste package temperature after storage times of 10, 50 and 100 years for co-extraction-1 in clay

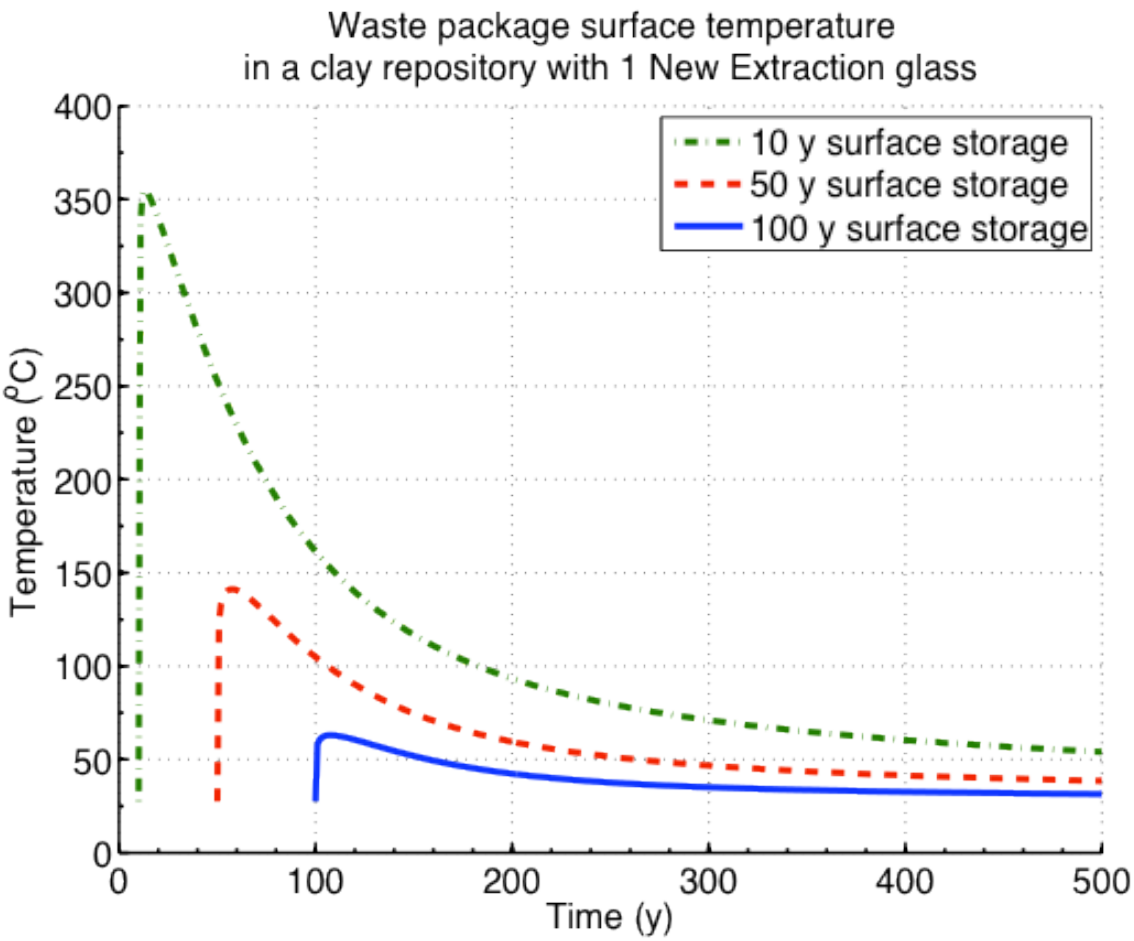

Figure H.4-10 Calculated waste package temperature after storage times of 10, 50 and 100 years for new extraction-1 in clay

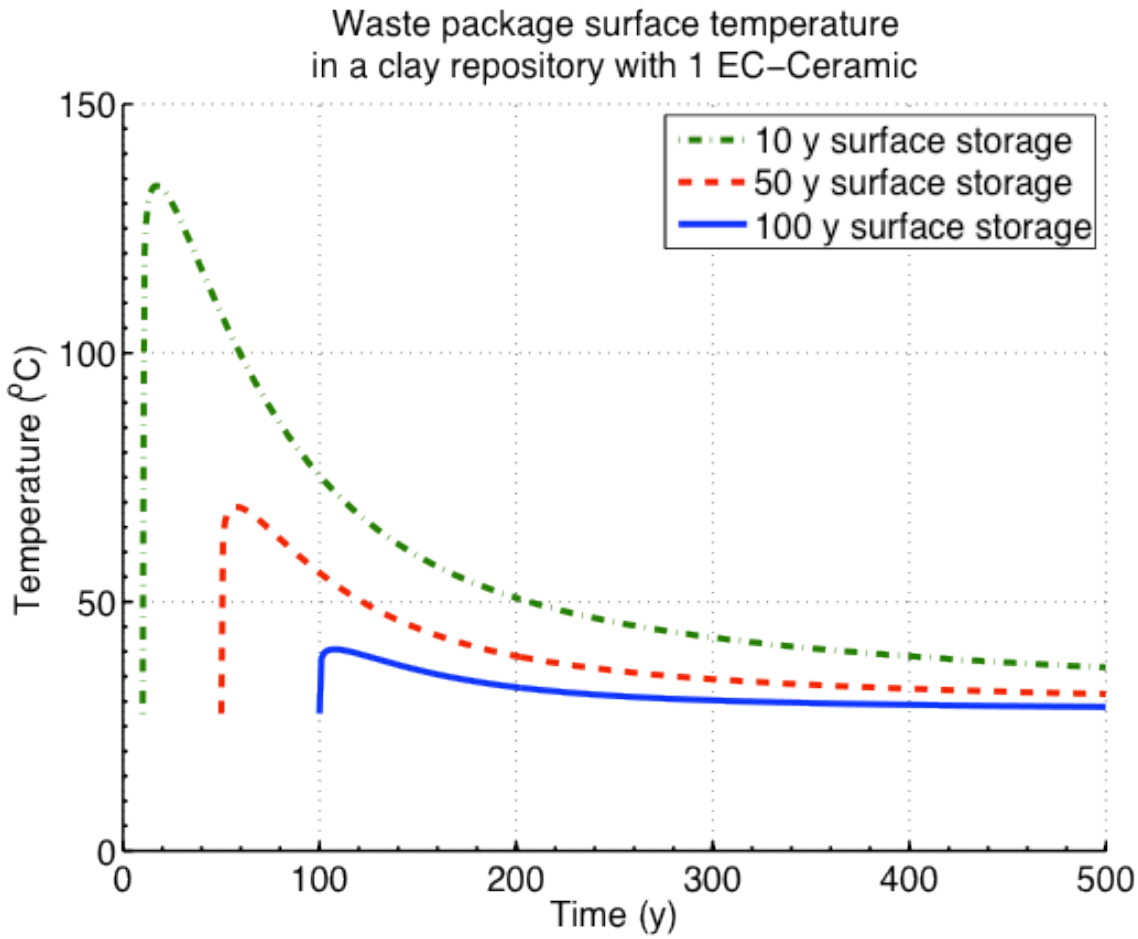

Figure H.4-11 Calculated waste package temperature after storage times of 10, 50 and 100 years for ECC-1 in clay

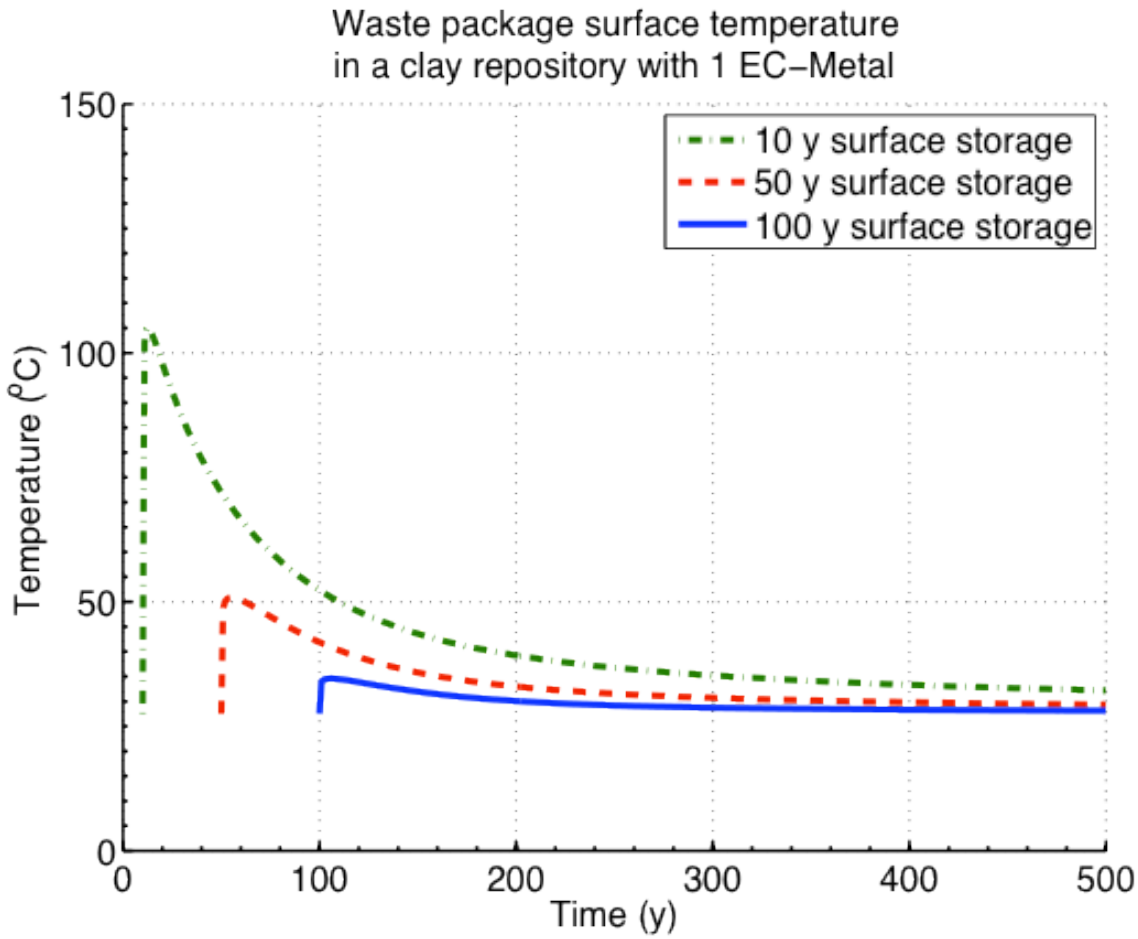

Figure H.4-12 Calculated waste package temperature after storage times of 10, 50 and 100 years for ECM-1 in clay

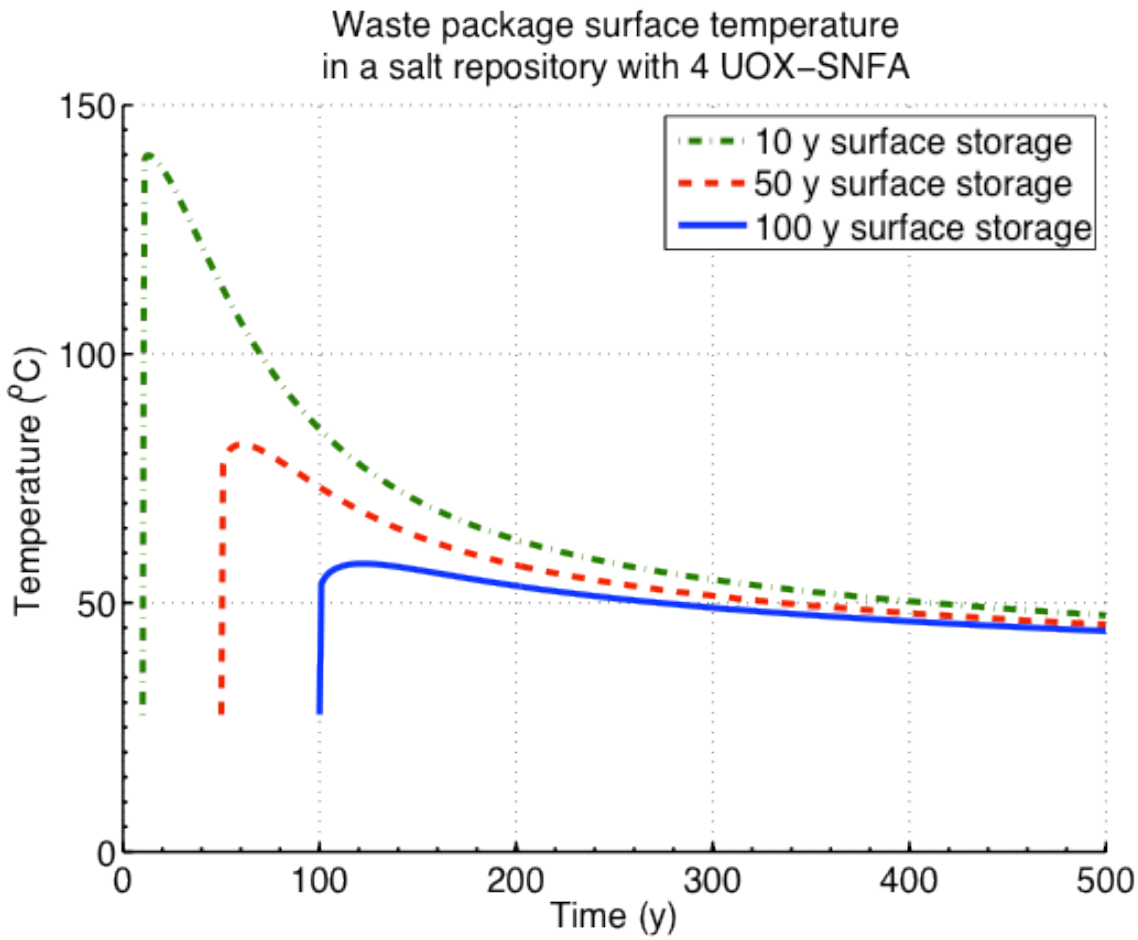

Figure H.4-13 Calculated waste package temperature after storage times of 10, 50 and 100 years for UOX-4 in salt, with 75% of the waste package surface contacting intact salt

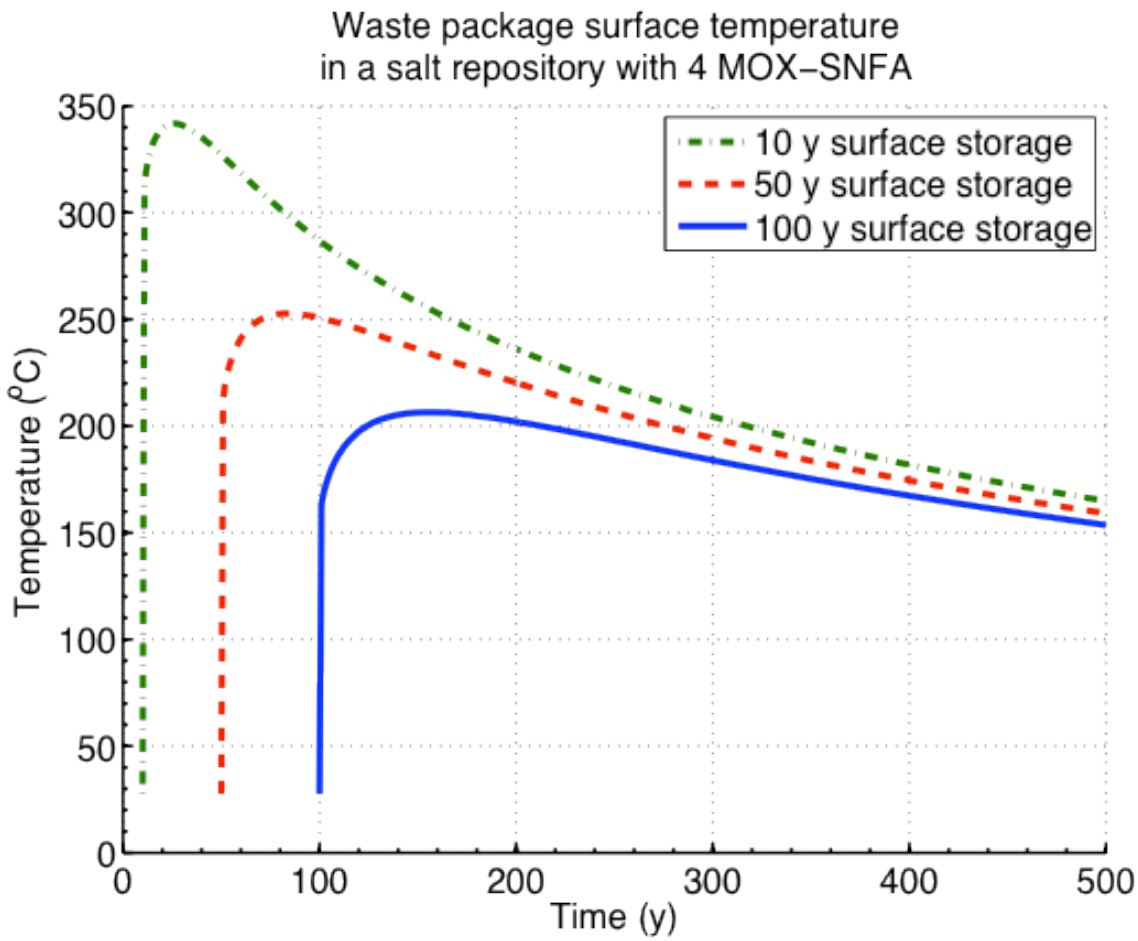

Figure H.4-14 Calculated waste package temperature after storage times of 10, 50 and 100 years for MOX-4 in salt, with 75% of the waste package surface contacting intact salt

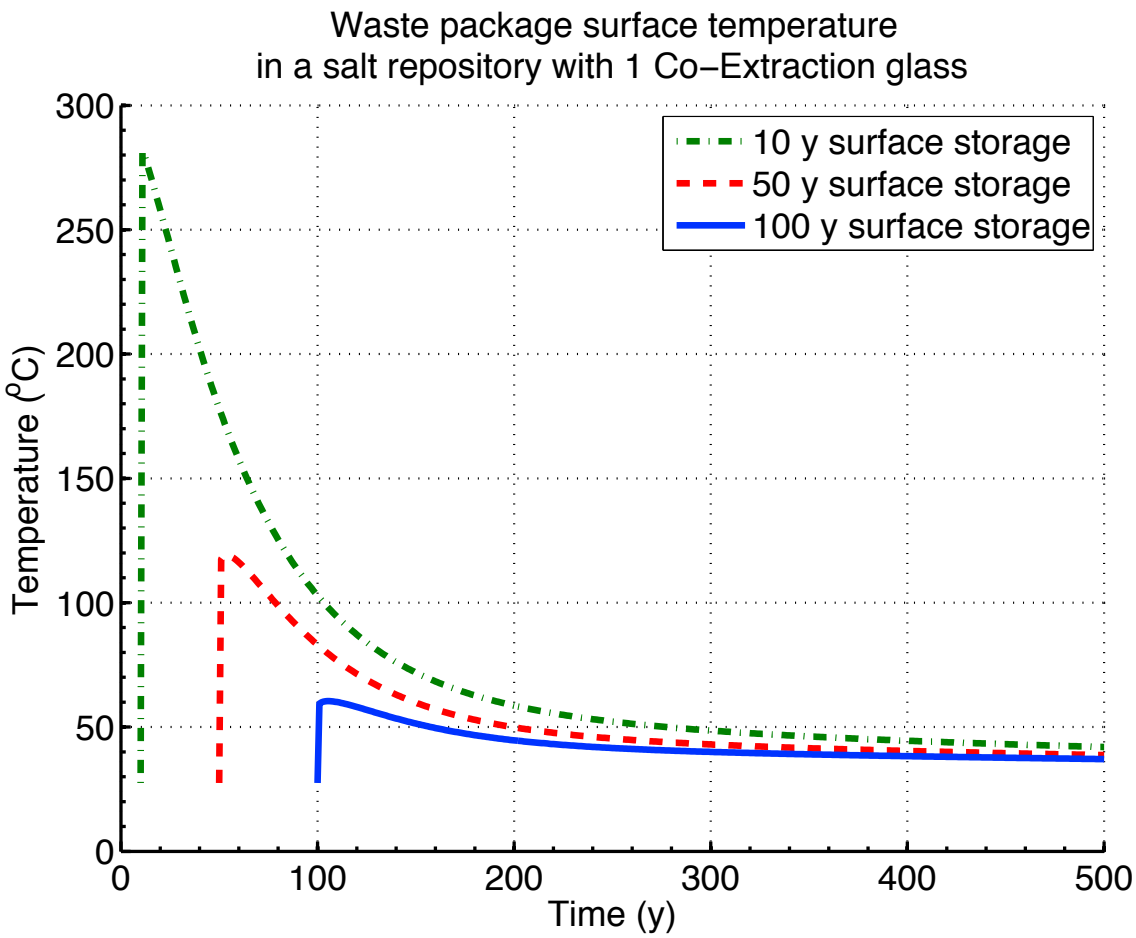

Figure H.4-15 Calculated waste package temperature after storage times of 10, 50 and 100 years for co-extraction-1 in salt, with 75% of the waste package surface contacting intact salt

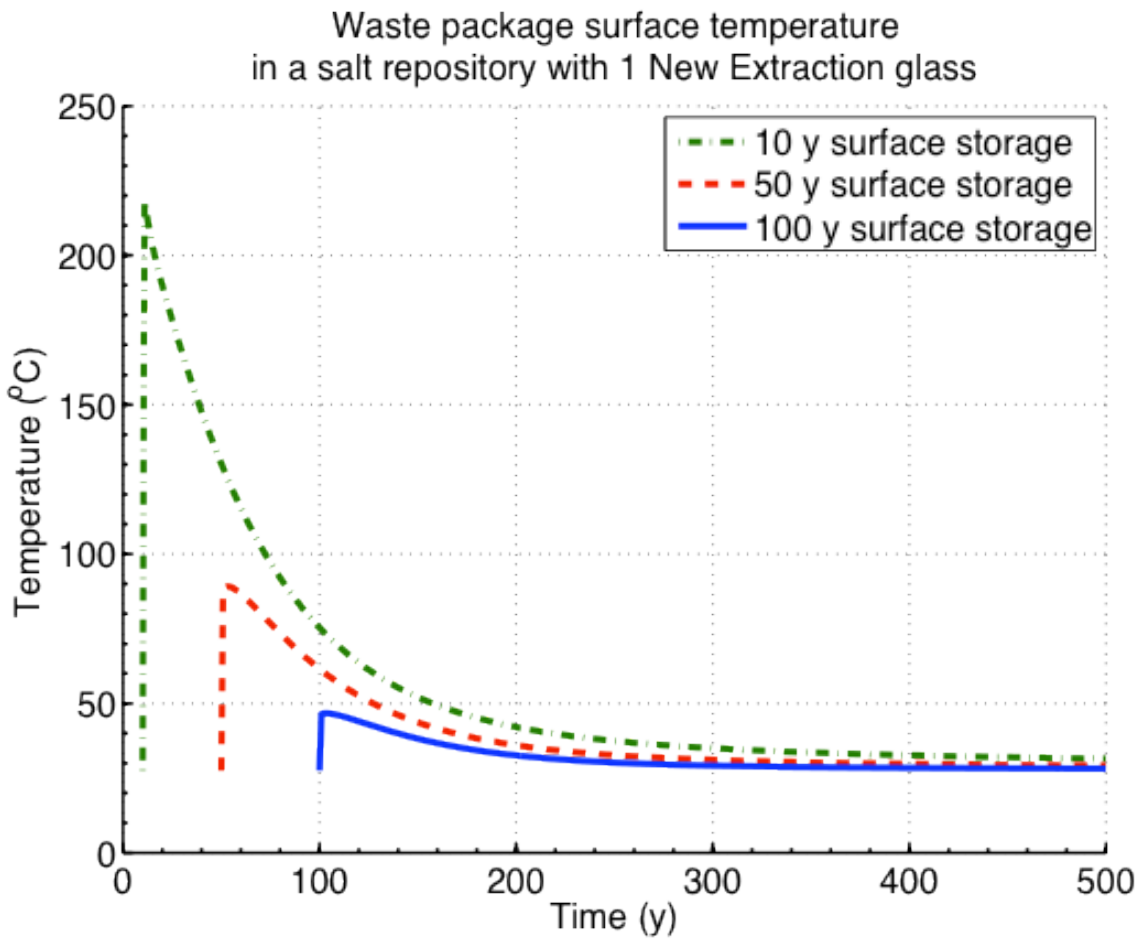

Figure H.4-16 Calculated waste package temperature after storage times of 10, 50 and 100 years for new extraction-1in salt, with 75% of the waste package surface contacting intact salt

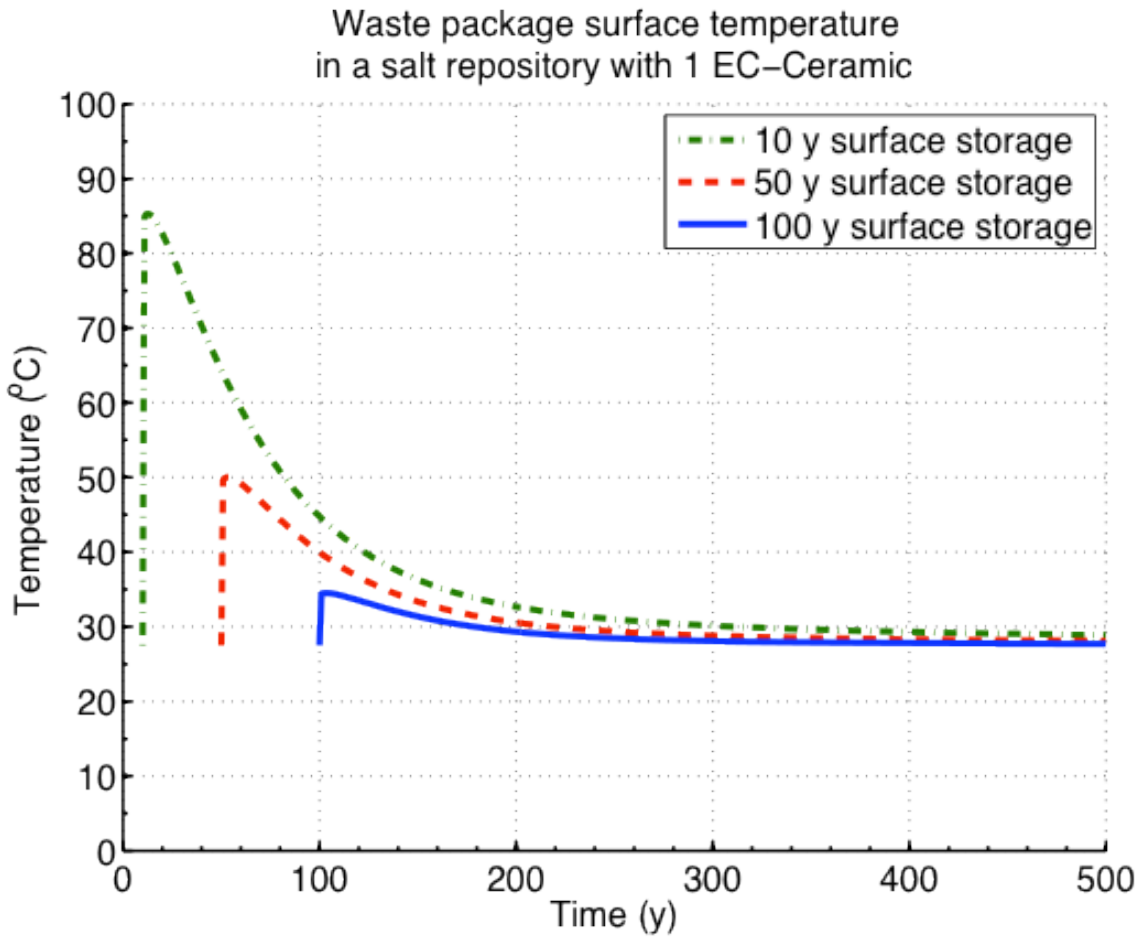

Figure H.4-17 Calculated waste package temperature after storage times of 10, 50 and 100 years for ECC-1 in salt, with 75% of the waste package surface contacting intact salt

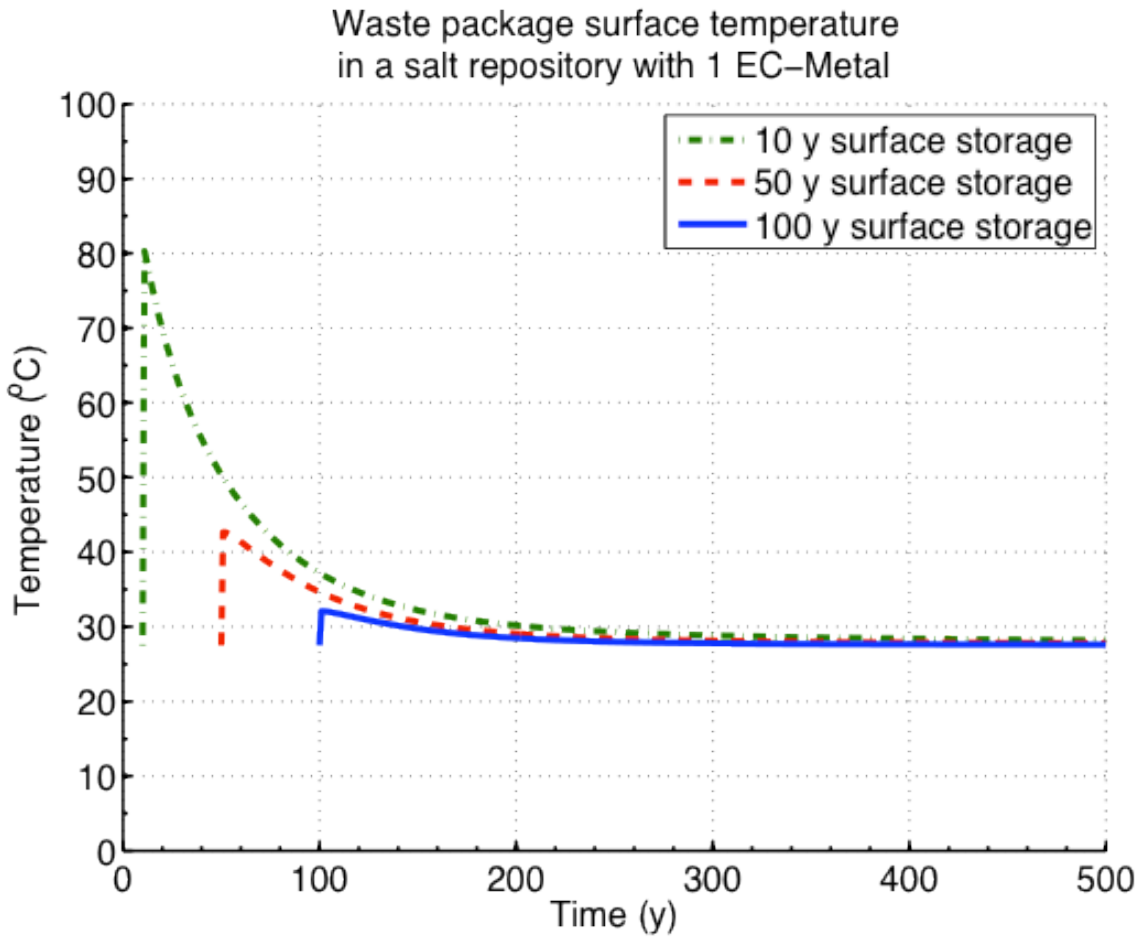

Figure H.4-18 Calculated waste package temperature after storage times of 10, 50 and 100 years for ECM-1 in salt, with 75% of the waste package surface contacting intact salt

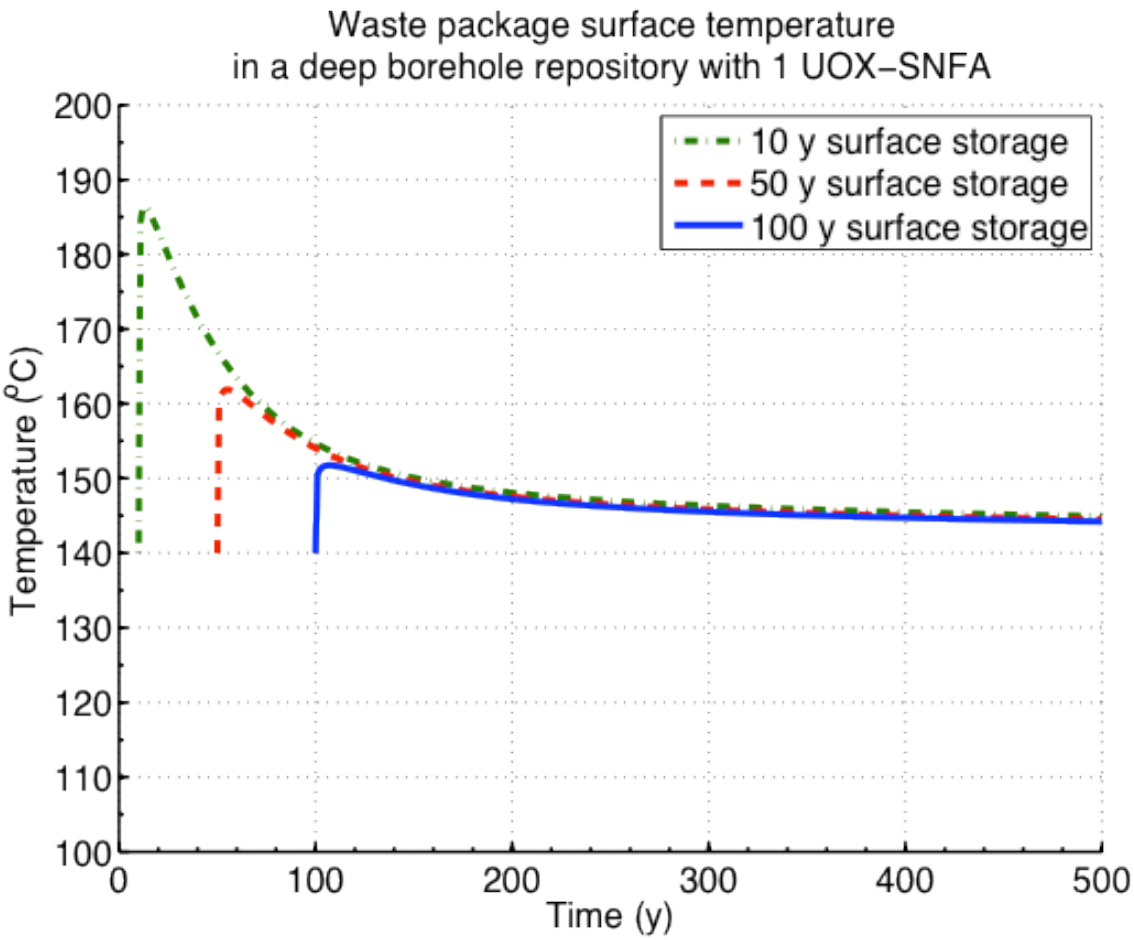

Figure H.4-19 Calculated waste package temperature after storage times of 10, 50 and 100 years for UOX-1 in a deep borehole

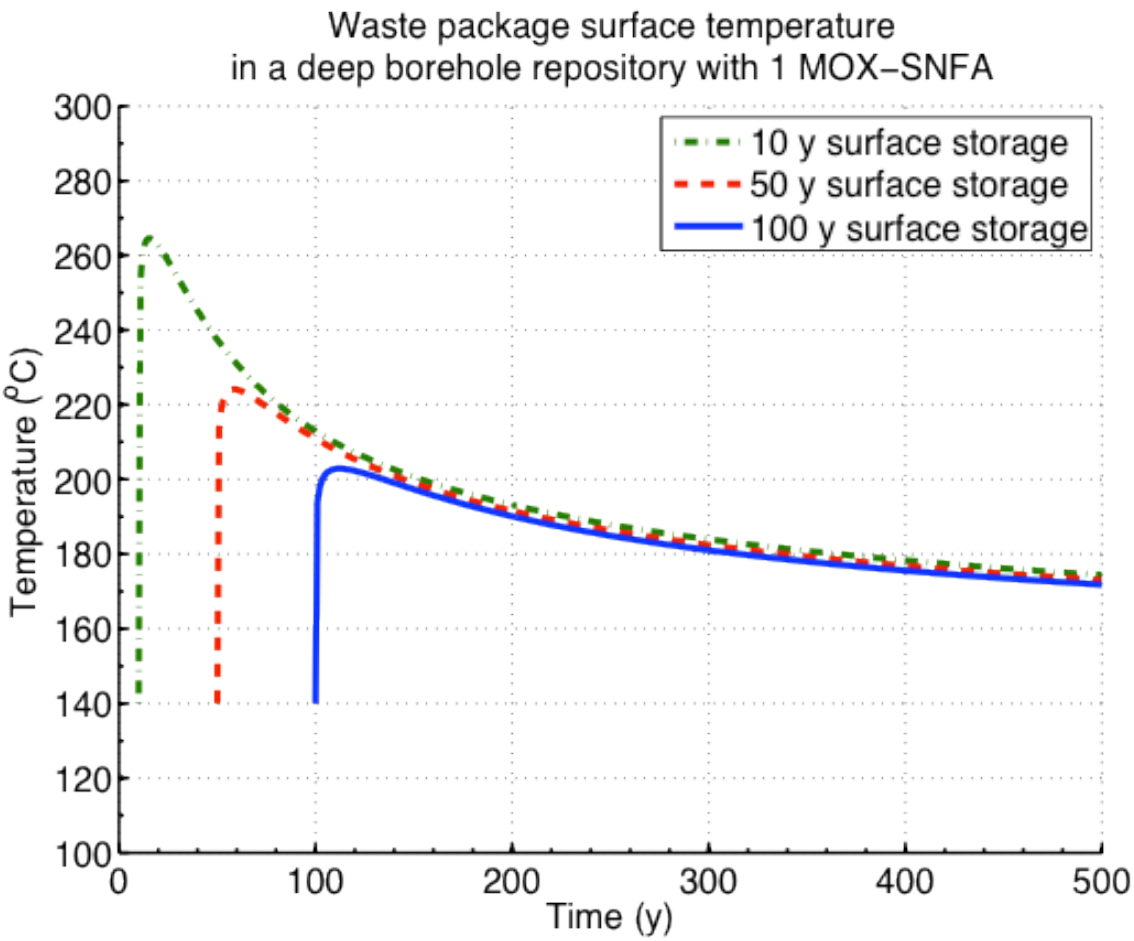

Figure H.4-20 Calculated waste package temperature after storage times of 10, 50 and 100 years for MOX-1 in a deep borehole

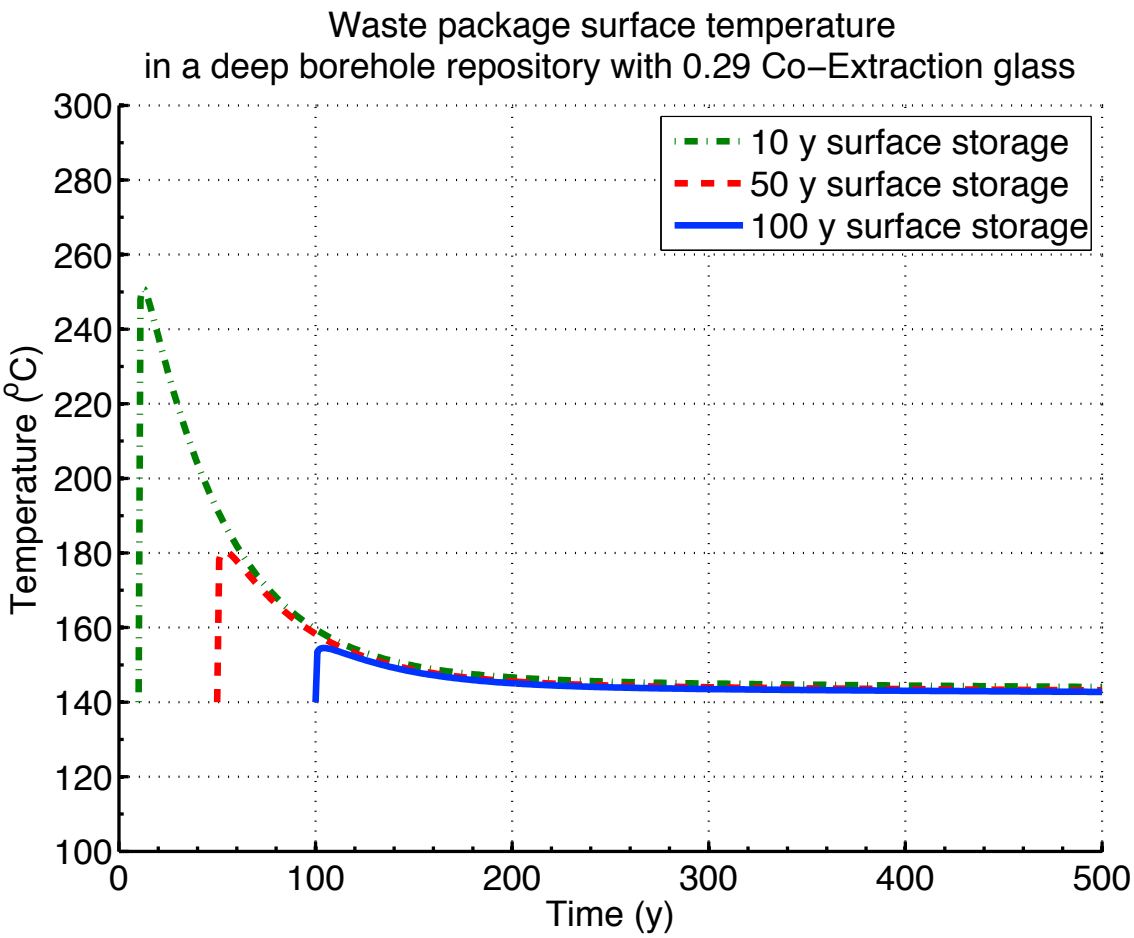

Figure H.4-21 Calculated waste package temperature after storage times of 10, 50 and 100 years for co-extraction-0.291 in a deep borehole

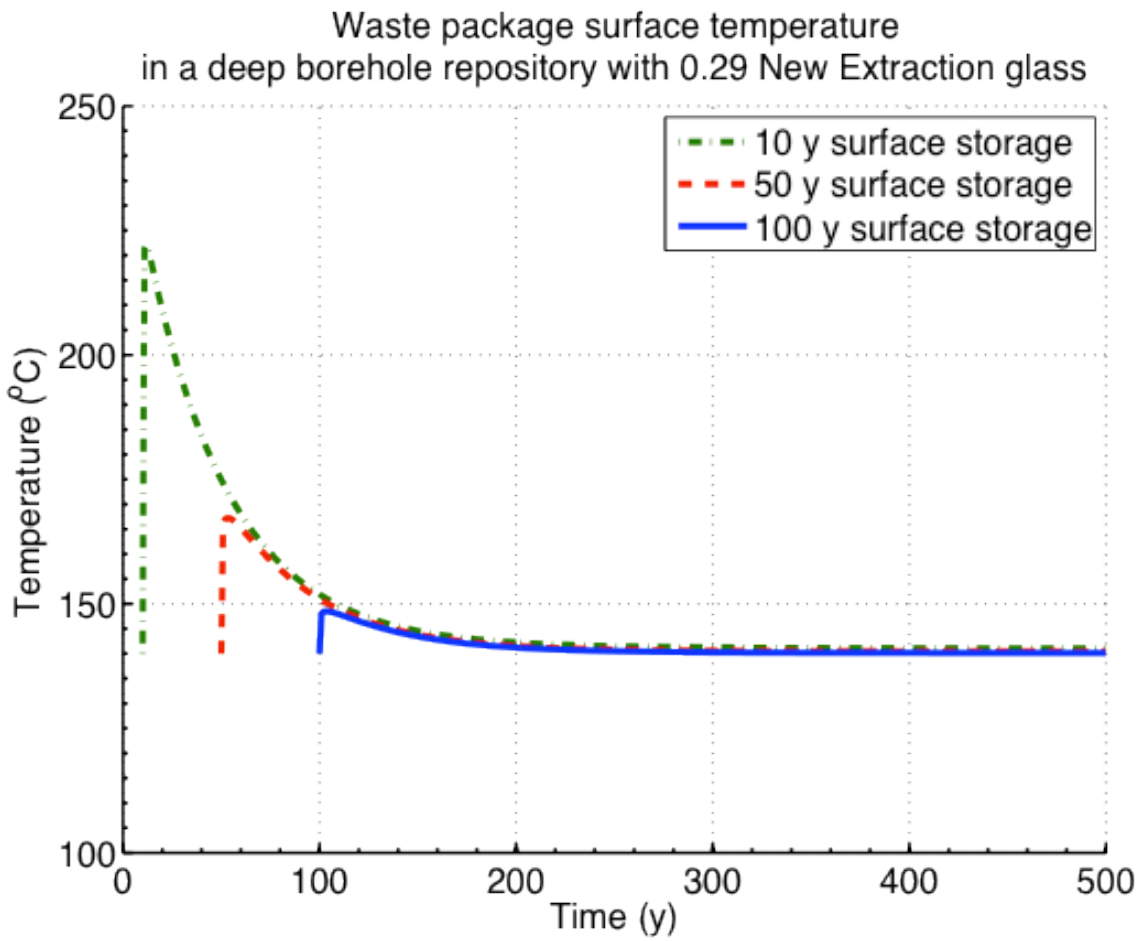

Figure H.4-22 Calculated waste package temperature after storage times of 10, 50 and 100 years for new extraction-0.291in a deep borehole

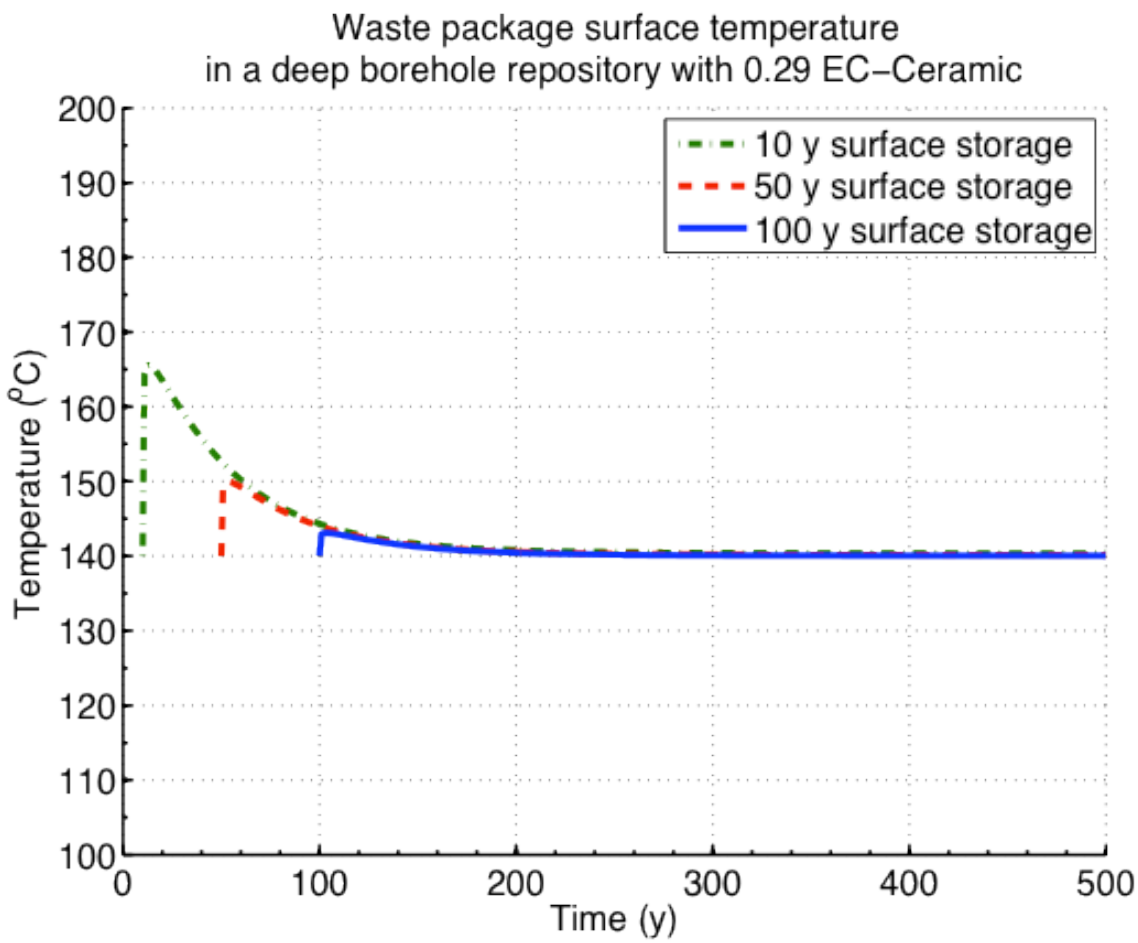

Figure H.4-23 Calculated waste package temperature after storage times of 10, 50 and 100 years for ECC-0.291 in a deep borehole

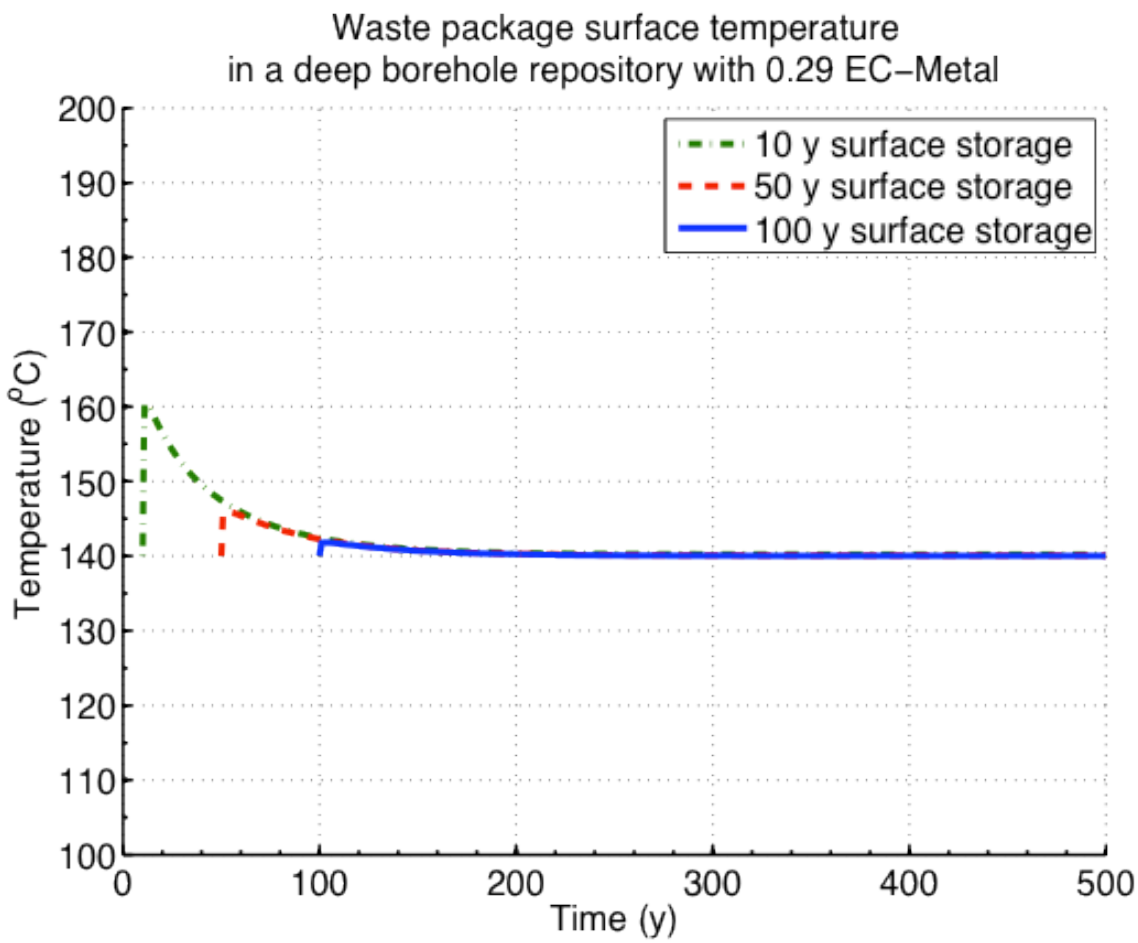

Figure H.4-24 Calculated waste package temperature after storage times of 10, 50 and 100 years for ECM-0.291 in a deep borehole

H.5 Waste Package Peak Temperature as a Function of Storage Time and Number of Assemblies

For granite, clay and salt media, the peak temperature was calculated for storage times ranging from 10 years to 1400 years, for 1, 2, 3, 4 and 12 UOX or MOX assemblies per waste package. The long storage time range is not intended to imply that a repository would be designed for such a long storage period; this allows interpolation, rather than extrapolation, when constructing the trade curves in the following Section H.6. The figures in this section are displayed out to 300 years to show the detail for storage periods of 100 years or less.

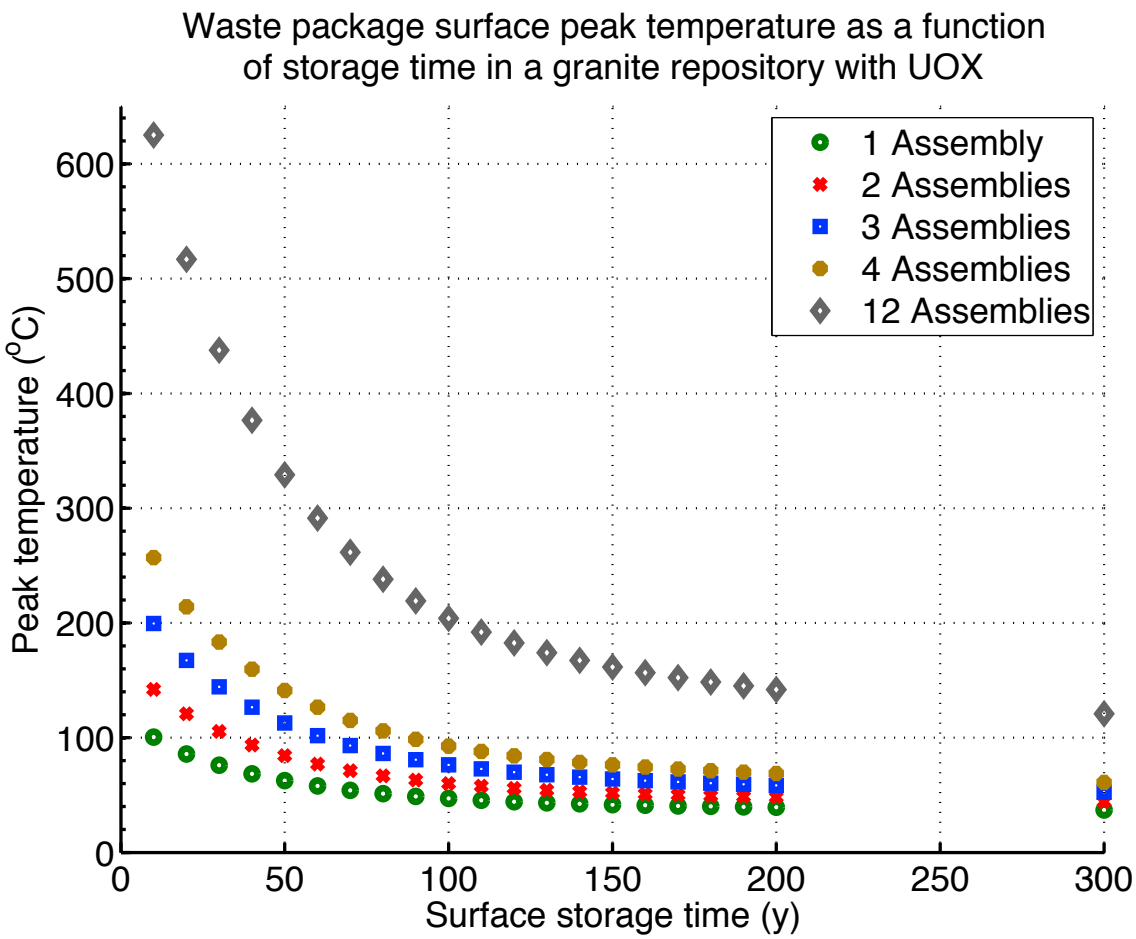

Figure H.5-1 Waste package surface peak temperature as a function of surface storage time for UOX in a granite repository

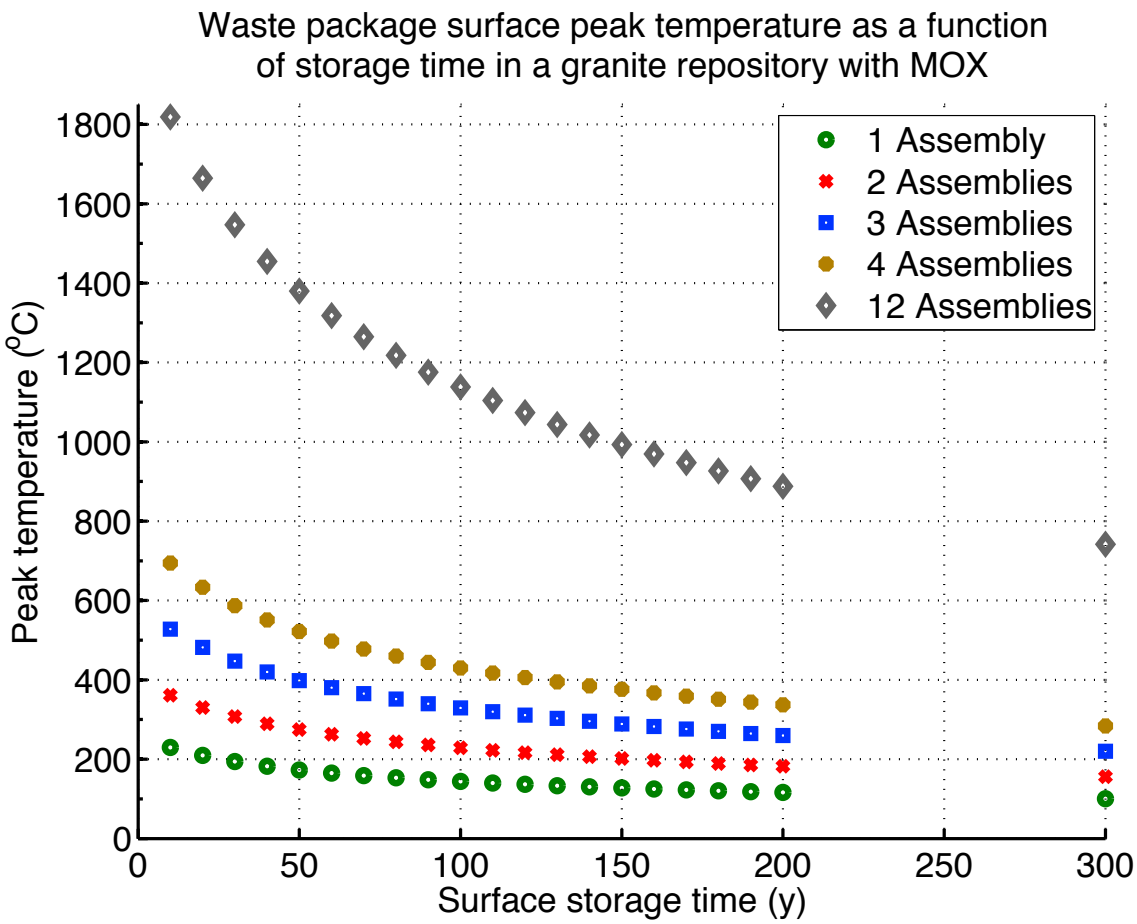

Figure H.5-2 Waste package surface peak temperature as a function of surface storage time for MOX in a granite repository

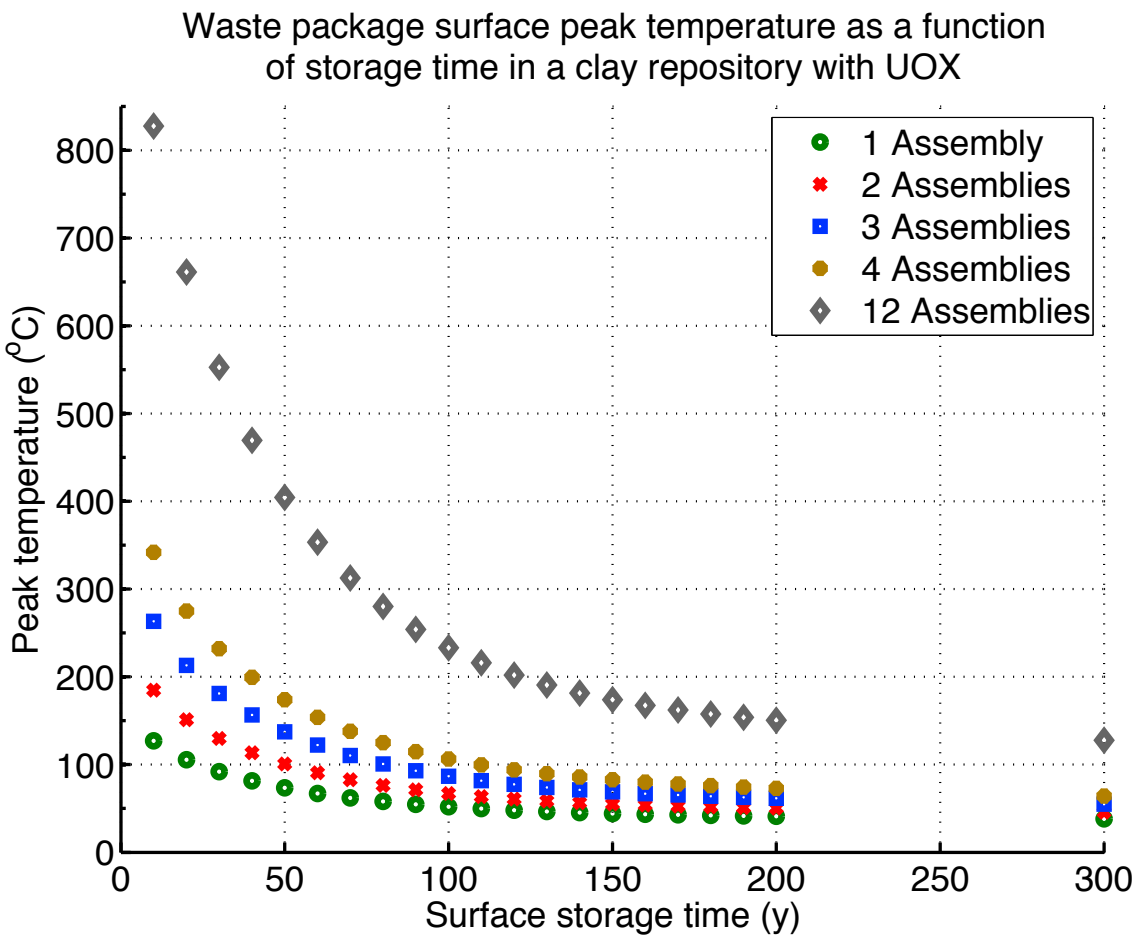

Figure H.5-3 Waste package surface peak temperature as a function of surface storage time for UOX in a clay repository

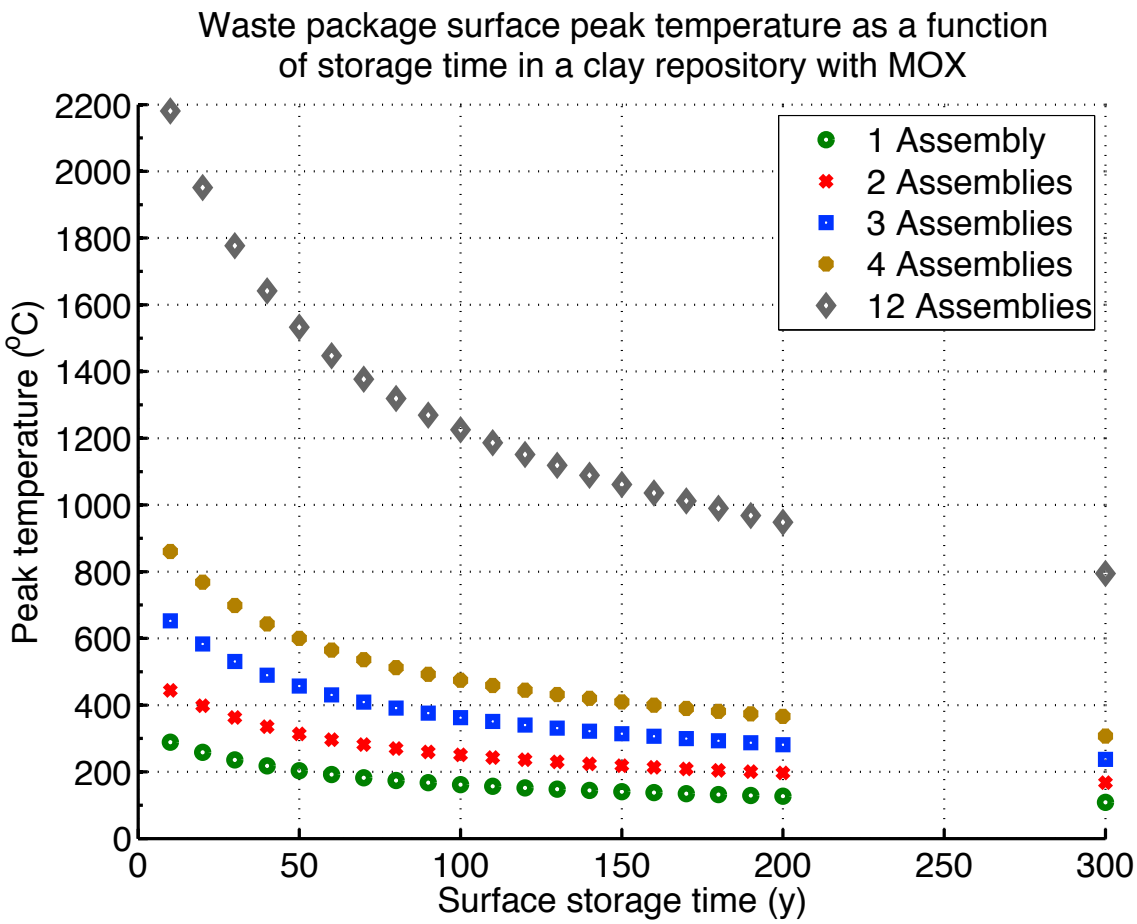

Figure H.5-4 Waste package surface peak temperature as a function of surface storage time for MOX in a clay repository

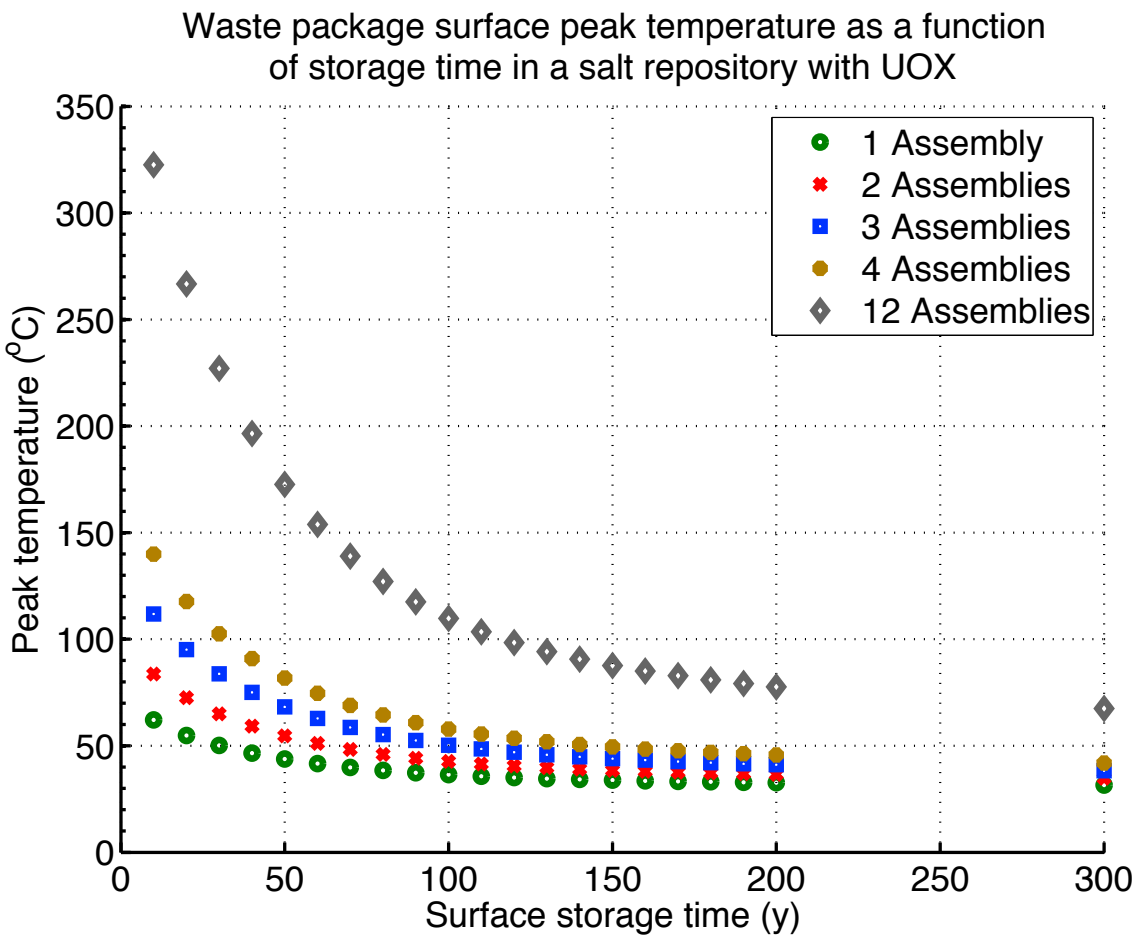

Figure H.5-5 Waste package surface peak temperature as a function of surface storage time for UOX in a salt repository with 75% of the waste package surface contacting intact salt

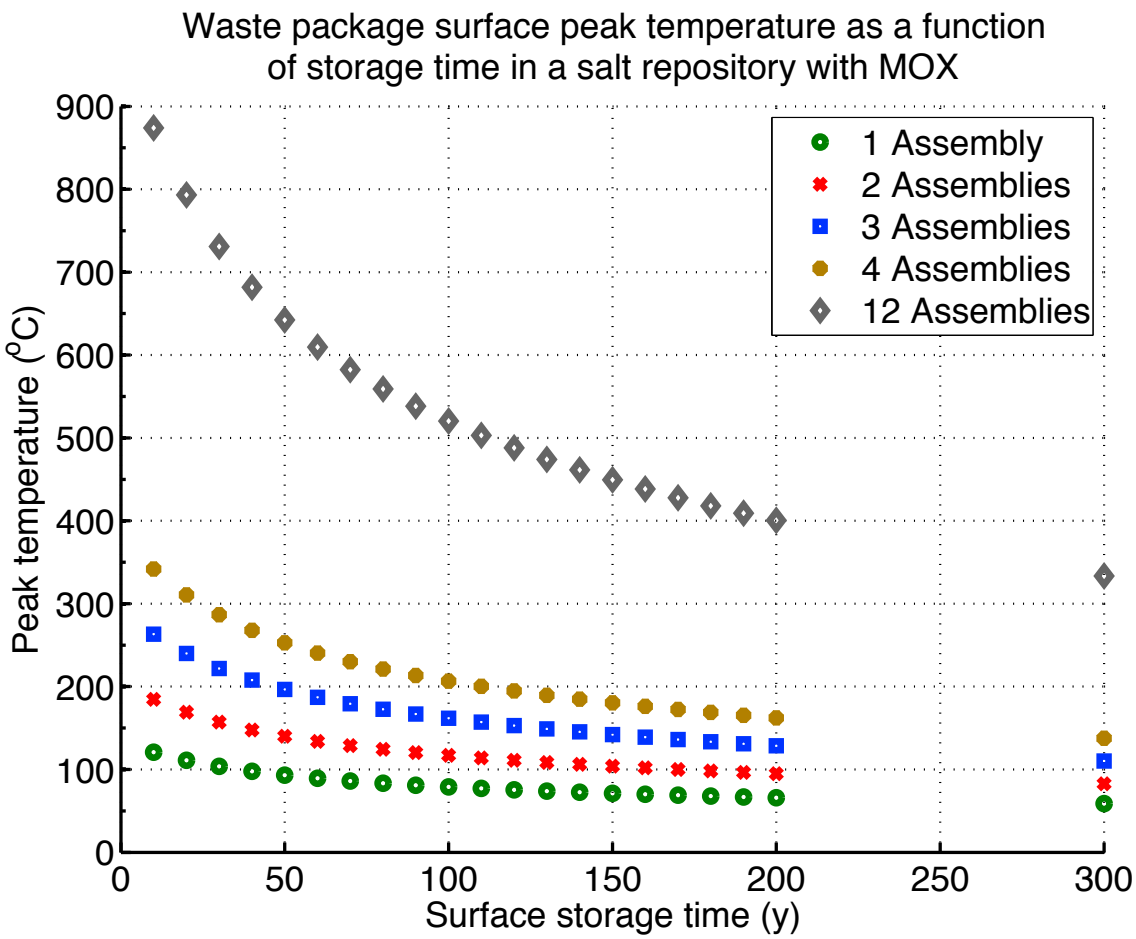

Figure H.5-6 Waste package surface peak temperature as a function of surface storage time for MOX in a salt repository with 75% of the waste package surface contacting intact salt

H.6 Trade-off of Storage Time and Waste Package Capacity

This section documents calculation of the minimum surface storage time required to maintain a temperature at interface between the waste package and the nearest EBS component (or rock wall depending on design) below the prescribed thermal constraint at all times. This storage time was determined by interpolating the peak temperature data (illustrated in Section H.5 for times up to 300 years). Decay heat values were available starting from 5 years; therefore, storage times less than 5 years have not been considered.

The temperature limit at the waste package surface for the three media is as follows:

- Granite: 100°C
- Clay: 100°C
- Salt: 200°C

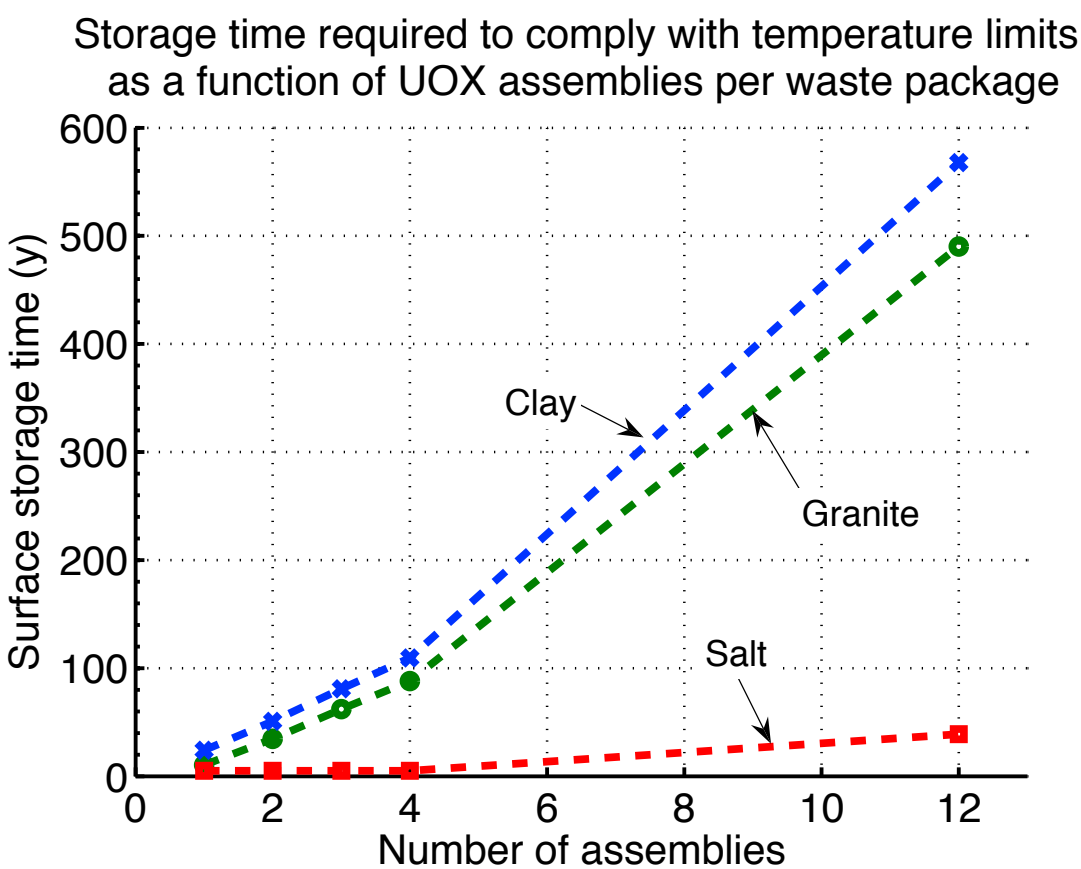

Figure H.6-1 Minimum surface storage time necessary to comply with waste package surface temperature limit as function of UOX assemblies per waste package in a granite, clay, and salt (with 75% of the waste package surface contacting intact salt) repository

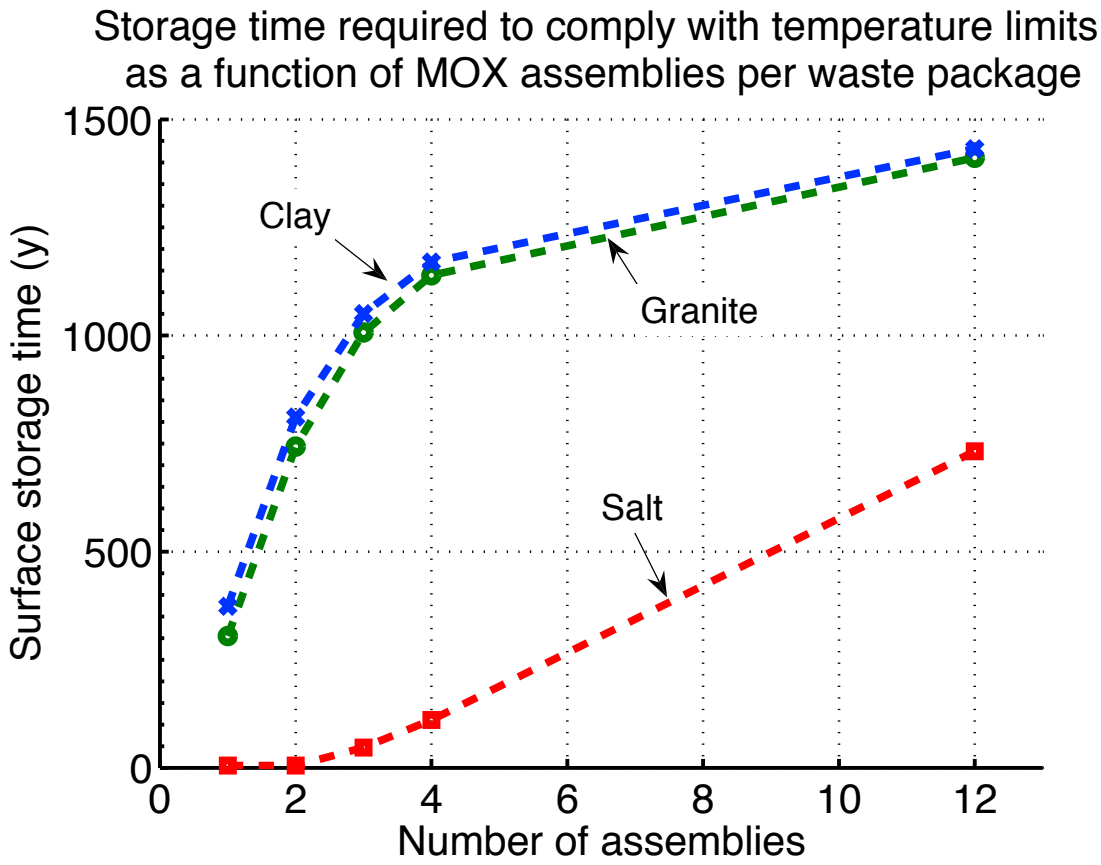

Figure H.6-2 Minimum surface storage time necessary to comply with waste package surface temperature limit as function of MOX assemblies per waste package in a granite, clay, and salt (with 75% of the waste package surface contacting intact salt) repository